The mechanism of chromate reduction by *Thermus scotoductus* SA−01

by

Diederik Johannes Opperman

Submitted in fulfillment of the requirements
for the degree

Philosophiae Doctor

In the Faculty of Natural and Agricultural Sciences
Department of Microbial, Biochemical and Food Biotechnology
University of the Free State
Bloemfontein
South Africa

February 2008

Promoter: Prof E van Heerden

ACKNOWLEDGEMENTS

This research was supported by the NRF (National Research Foundation, South Africa), the Ernst, Ethel Erickson Trust and the Oppenheimer Memorial Trust.

I would like to express my sincere gratitude to my promoter, Prof. Esta van Heerden, for her support and the freedom she gave me, the opportunities she made possible, and not only teaching me science but also about life.

I also thank Dr. LA Piater, Prof. D Litthauer, Prof. J Berenguer, Dr. F Cava, Dr. V Parro García, Dr LA Rivas Mena, Prof. T Kieft, Prof. TC Onstott and Prof. D Cowan for all their helpful advice during my studies and the preparation of this manuscript.

To my parents for their unconditional support and understanding and allowing me this opportunity I am for ever grateful.

To all my friends and members of the Extreme Biochemistry Group who have become like family, thank you for your support, kindness, sharing my (and your) successes and failures as well as interesting and unusual (sometimes disturbing) quad discussions.

Deo gratias, optimo maximo.

INDEX

CHAPTER 1

LITERATURE REVIEW

CHAPTER 2

Cr(VI) REDUCTION BY *THERMUS SCOTODUCTUS* STRAIN SA–01

CHAPTER 3

PURIFICATION AND CHARACTERIZATION OF THE SOLUBLE Cr(VI) REDUCTASE

CHAPTER 4

PURIFICATION AND CHARACTERIZATION OF THE MEMBRANE-ASSOCIATED Cr(VI) REDUCTASE

CHAPTER 5

IDENTIFICATION OF THE GENE SEQUENCES CODING THE CHROMATE REDUCTASES

CHAPTER 6

HETEROLOGOUS EXPRESSION OF THE CHROMATE REDUCTASES IN *E. COLI* AND *T. THERMOPHILUS*

LIST OF TABLES

LIST OF FIGURES

Figure 5.5: Double restriction digests of positive clones identified in genomic library screening for the peripherally bound membrane (lanes 2 – 5, A) and cytoplasmic (lanes 2 and 3, B) chromate reductase with *Eco*RI and *Sal*I to evaluate insert size. Lanes 1, molecular weight marker.

Figure 5.6: Nucleotide sequence of the chromate reductase of *Thermus scotoductus* SA-01 and deduced amino acid sequence. The putative -35 and -10 promoter regions and ribosome binding site (rbs) are boxed with the putative inverted termination sequences underlined.

Figure 5.7: Multiple alignment (Clustal W) of the chromate reductase with the predicted NADH:flavin oxidoreductase from *Thermus thermophilus* (NCBI:YP 143423) and from *Geobacter metallireducens* (NCBI:YP 385521), with the xenobiotic reductase from *Pseudomonas putida* 86 (PDB:2H8X) and YqjM of *Bacillus subtilis* (PDB:1Z41A). Predicted secondary structure elements are indicated by α (helix) or β (sheet). Symbols indicate identical residues (*/purple), conserved substitutions (:) and semi-conserved substitutions (.).

Figure 5.8: Substrate binding sites of the flavoproteins XenA from *Pseudomonas putida* (A; Kitzing *et al.*, 2005) and YqjM from *Bacillus subtilis* (B; Griese *et al.*, 2006) complexed with sulphate. An asterisk denotes a residue from the adjacent monomer extending into the catalytic site.

Figure 5.9: Multiple alignment (Clustal W) of the deduced amino acid sequence of the dihydrolipoamide dehydrogenase (LPD) from *Thermus scotoductus* SA-01 with the LPD counterparts in *Thermus thermophilus* HB27 (YP005722 & YP005669), *Deinococcus radiodurans* R1 (NP296246), *Pseudomonas putida* PpG2 (AAA65618), *Escherichia coli* CFT073 (NP752095), *Shewanella oneidensis* MR-1 (NP 716063) and *Geobacillus stearothermophilus* NCA 1503 (CAA37631). Boxed sequences show the FAD-binding, disulphide from the active site, NADH-binding and His-Glu active site diad domains. Sequence determined by Edman degradation shown in italics. Symbols indicate identical residues (*/purple), conserved substitutions (:) and semi-conserved substitutions (.).

Figure 6.1: Agarose gel electrophoresis of the PCR amplified chromate reductases. Lane 1, Molecular weight marker; lane 2, cytoplasmic chromate reductase; lane 3, membrane-associated chromate reductase from 1st start codon; lane 4, membrane-associated chromate reductase from 2nd start codon.

NON-SI ABBREVIATIONS

A	Absorbance
AP	Alkaline phosphatase
ATCC	American Type Culture Collection
BCA	Bicinchoninic acid
BCIP	5-bromo-4-chloro-3-indolyl phosphate
Bicine	N,N-bis(2-hydroxyethyl)-glycine
BLAST	Basic Logical Alignment Search Tool
bp	Base pairs
BSA	Bovine serum albumin
CD	Circular Dichroism
CDS	Coding sequences
chr	chromate resistance genes
Chr	Chromate resistance proteins
CHR	Chromate resistance mechanisms
ChrR	Chromate reductase
ChrM	Chromate reductase (membrane-associated) DNA probe
ChrS	Chromate reductase (cytoplasmic) DNA probe
CrM	Chromate reductase (membrane-associated)
CrS	Chromate reductase (cytoplasmic)
Da	Daltons
DEAE	Diethylaminoethyl
DIG	Digoxigenin
DNA	Deoxyribonucleic acid
DNase	Deoxyribonuclease
dNTPs	Deoxyribonucleoside triphosphates
DTT	Dithiothreitol
E_a	Activation energy
EDTA	Ethylenediaminetetraacetate
EH_2/EH_4	Reduced enzyme

E_{ox}	Oxidized enzyme
FAD	Flavin adenine dinucleotide
FerB	Iron(III) reductase
FMN	Riboflavin 5'-monophosphate
Fre	Flavin reductase
gDNA	Genomic DNA
GlcNAc	N-acetylglucosamine
IMAC	Immobilized metal-affinity chromatography
IPTG	Isopropyl β-D-thiogalactoside
K_{cat}	Catalytic constant
K_m	Michaelis constant
LB	Luria-Bertani broth
LPD	Dehydrolipoamide dehydrogenase
PCR	Polymerase chain reaction
MES	2-(N-morpholino)ethanesulfonic acid
MIC	Minimal inhibitory concentration
MOPS	3-(N-morpholino)propanesulfonic acid
M_r	Molecular weight
MurNAc	N-acetylmuramic acid
NADH	Nicotinamide adenine dinucleotide (reduced)
NADPH	Nicotinamide adenine dinucleotide phosphate (reduced)
NBT	4-nitro blue tetrazolium chloride
NfsA	Nitroreductase
NMCO	Nominal molecular weight cut-off
NMWL	Nominal molecular weight limit
nt	nucleotides
NTA	Nitrilotriacetic acid
OD	Optical density
ORF	Open reading frame
ORP	Oxidation-reduction potential
OYE	Old Yellow Enzyme
PAGE	Polyacrylamide gel electrophoresis
PDH	Pyruvate dehydrogenase complex

RBS	Ribosome binding site
rDNA	Ribosomal DNA
RNA	Ribonucleic acid
RNase	Ribonuclease
ROS	Reactive oxygen species
rpm	Revolutions per minute
SD	Standard deviation
SDS	Sodium dodecyl sulphate
SMCC	Subsurface Microbial Culture Collection
SOD	Super oxide dismutase
TAE	Tris, Acetic acid, EDTA
TB	Tryptone, yeast extract, NaCl medium
TE	Tris, EDTA
TLC	Thin layer chromatography
TYG	Tryptone, Yeast Extract and Glucose
U	Units
UV-vis	Ultraviolet-visible
V_e	Elution volume
V_o	Void volume
V_{max}	Maximum initial velocity
XenA	Xenobiotic reductase
x g	Gravitation force
X-Gal	5-bromo-4-chloro-3-indolyl β-D-galactoside
YieF	Chromate/quinone reductase from *Pseudomonas*
YgjM	Old Yellow Enzyme homologue from *Bacillus*

PUBLICATIONS

Opperman, D.J. and van Heerden, E. (2007) Aerobic Cr(VI) reduction by *Thermus scotoductus* strain SA-01. *Journal of Applied Microbiolology* **103**:1097-1913.

Opperman, D.J. and van Heerden, E. (2008) A membrane-associated protein with Cr(VI)-reducting activity from *Thermus scotoductus* SA-01. *FEMS Microbiology Letters* **280**:210-218.

Opperman, D.J., Piater, L.A. and van Heerden, E. (2008) A novel chromate reductase from *Thermus scotoductus* SA-01 related to Old Yellow Enzyme. *Journal of Bacteriology* **190**:3076-3082.

ABSTRACT

Thermus scotoductus SA-01, isolate from a South African deep gold mine, has the ability to tolerate up to 0.5 mM Cr(VI) during growth in a complex organic medium and reduce Cr(VI) under growth and non-growth conditions. The rate of chromate reduction is dependent on pH, temperature and Cr(VI) concentration. Cell-free extracts were shown to be able to reduce Cr(VI) using NADH as an electron donor.

A novel cytoplasmic chromate reductase was purified to homogeneity and shown to couple the oxidation of NAD(P)H to the reduction of Cr(VI). This homodimeric protein consisted of monomers of approximately 36 kDa with a non-covalently bound FMN and required the divalent metal Ca^{2+} for activity. The enzyme was optimally active at 65°C and a pH of 6.3, reducing 2 mol of NAD(P)H per mol Cr(VI), suggesting a mixed one- and two-electron transfer mechanism. The cytoplasmic chromate reductase is encoded by an ORF of 1050 bp under the regulation of an *E. coli* σ^{70}-like promoter. Sequence analysis showed the chromate reductase to be related to the Old Yellow Enzyme (OYE) family and in particular some xenobiotic reductases.

A membrane-associated associated Cr(VI) reductase was purified to homogeneity and shown to be distinct from the above mentioned cytoplasmic chromate reductase. The reductase appears to be peripherally-associated with the membrane of *T. scotoductus* and consists of two identical subunits of approximately 48 kDa. The chromate reductase contained a non-covalently bound FAD co-factor and was optimally active at 65°C and a pH of 6.5. Through N-terminal sequencing and screening of a genomic library, the membrane-associated chromate reductase was identified as homologous to the dihydrolipoamide dehydrogenase gene, encoded for by a 1386 bp ORF and located within a probable pyruvate dehydrogenase operon.

Although neither of these enzymes are dedicated physiological chromate reductases, their catalytic efficiency toward Cr(VI) as substrate proved to be superior than that found for

other chromate reductases described in literature, which include the nitroreductases and quinone reductases isolated from *Pseudomonas putida* and *Escherichia coli.*

Heterologous expression of the cytoplasmic and membrane-associated chromate reductases in *E. coli* and *T. thermophilus* yielded active, soluble enzymes. Kinetic studies of the recombinant proteins showed that the recombinant chromate reductases expressed in *T. thermophilus* were more catalytic efficient than their *E. coli*-expressed counterparts. The *T. thermophilus*-expressed recombinant cytoplasmic chromate reductase proved to be more stable under extreme chemical and thermal conditions.

The mechanisms of chromate reduction employed by *Thermus scotoductus* SA-01 is herein discussed and we propose that neither enzymatic Cr(VI) reduction mechanisms found is dedicated to Cr(VI) reduction but rather the fortuitous action of metabolically unrelated enzymes.

CHAPTER 1

LITERATURE REVIEW

1.1 INTRODUCTION

Anthropocentrically, environments hostile to man were designated as extreme (Stetter, 1999) and are usually defined by at least one physical or chemical “extreme” parameter such as temperature, radiation, pH or NaCl concentration that act nonspecifically on a broad range of cellular targets (Nies, 2000). Since the understanding of bacteria started with *Escherichia coli* microbiologists easily distinguishes “extreme” from “not extreme” through the parameters tolerated by *E. coli* (Nies, 2000).

Some of these environments were originally considered too harsh to support even microbial life but through improvement of culture conditions, thriving communities of microorganisms were found in these extreme environments and were subsequently termed extremophiles (Stetter, 1999). Extremophiles have evolved to exist in a variety of extreme environments and can be grouped into different classes (Table 1.1) where certain extremophiles exists in niches characterized by more than one extreme environmental parameter (Adams *et al*., 1995).

Some environments naturally contain high concentrations of toxic heavy metals and microorganisms have co-existed with metals long before industrial activities mobilized and increased localized concentrations (Williams & Silver, 1984; Valls & Lorenzo, 2002). Microorganisms have thus evolved elaborate metal resistance and reduction systems as well as the ability to exploit some of these metals for catalysis and protein structure. However, some metals seem to serve no biologically relevant functions (Valls & Lorenzo, 2002).

Table 1.1: Extreme environments (adapted from Adams *et al*., 1995, Demirjian *et al.*, 2001).

Extremophile	Extreme Condition	Habitat	Example Microorganism	Growth Conditions
Thermophiles and Hyperthermophiles	High temperatures	Geothermal marine sediments	*Pyrococcus furiosus*	100°C
Psychrophiles	Low temperatures	Antarctic sea water	*Bacillus* TA41	4°C
Acidophiles	Low pH	Acid mine drainage	*Metallosphaera sedula*	pH 2
Alkalophiles	High pH	Sewage sludge	*Clostridium paradoxum*	pH 10.1
Halophiles	High salt concentrations	Hypersaline waters	*Halobacterium halobium*	4 – 5 M NaCl
Piezophiles (Barophiles)	High pressure	Deep sea hydrothermal vents	*Methanococcus janaschii*	250 atm

Physiologically, metals can be grouped into three main categories: metals essential and basically non toxic (e.g. Ca and Mg), metals essential, but harmful at high concentrations (e.g. Fe, Mn, Zn, Cu, Co, Ni and Mo) and lastly toxic metals (e.g. Hg or Cd) (Valls & Lorenzo, 2002). Most of the heavy metals are of non-biological origin and are toxic at high concentrations but with nonspecific actions (Nies, 2000) and depending on the metal, can be ranked through the use of the *E. coli* based definition (Table 1.2; Nies, 1999). This recent anthropogenic mobilization of heavy metals from metal ores has created metal-loaded niches exerting strong selective pressure for metal endurance (Valls & Lorenzo, 2002). Bacteria able to grow in these environments could thus be designated metallophiles (Nies, 2000).

Table 1.2: Toxicity of heavy–metal ions in *Escherichia coli* (Nies, 1999).

MIC (mM)	Heavy–metal ions
0.01	Hg^{2+}
0.02	Ag^{+}, Au^{3+}
0.2	CrO_4^{2-}, Pd^{2+}
0.5	Pt^{4+}, Cd^{2+}
1	Co^{2+}, Ni^{2+}, Cu^{2+}, Zn^{2+}
2	Tl^{+}, UO_2^{2-}, (La^{3+}, Y^{3+}, Sc^{3+})[a], (Ru^{3+}, Al^{3+})[b]
5	Pb^{2+}, (Ir^{3+}, Os^{3+}, Sb^{3+}, Sn^{2+}, In^{3+}, Rh^{2+}, Ga^{3+}, Cr^{3+}, V^{3+}, Ti^{3+}, Ti^{3+}, Be^{2+})[b]
10	(Cr^{2+})[b]
20	Mn^{2+}

The minimal inhibitory concentration (MIC) was determined on TRIS–buffered mineral salts medium, starting pH 7.0, containing 2 $g.L^{-1}$ sodium gluconate as carbon source, and 1$g.L^{-1}$ yeast extract to complement *E. coli* auxotrophies. The plates were incubated for 2 days at 30°C

[a] Weak acidification of the medium had to be allowed to keep the metal ion in solution

[b] Acidification of the medium had to be allowed to keep the metal ion in solution

The contamination of environment with hexavalent chromium is becoming an increasing concern, as the widespread use of chromium and the frequent incorrect disposal of the by-products and wastes from industrial activities such as the metallurgical, electroplating, paint and pigment production, tanning and wood preservation (Losi *et al*., 1994; Zayed & Terry, 2003) has created serious environmental pollution.

1.2 CHROMIUM

Chromium, the seventh most abundant element on earth, is a transition metal from group VI-B, occurring in nature as the bound form constituting approximately 0.1 – 0.3 $mg.g^{-1}$ of the earth's crust. Cr is able to exist in several oxidation states (Table 1.3) of which the trivalent Cr(III) and hexavalent Cr(VI) species are the most stable and abundant forms (Zayed & Terry, 2003).

The trivalent oxidation state is the most stable form of chromium and is primarily found geologically as chromite ($FeCr_2O_4$) (Cervantes *et al*., 2001; Oze *et al*., 2007). In contrast, Cr(VI) is mainly of anthropogenic origin, although naturally occurring Cr(VI) has recently been found and shown to be a result of the dissolution of chromite and the subsequent oxidation of Cr(III) to aqueous Cr(VI) in the presence of the common manganese mineral, birnessite (Oze *et al.*, 2007). Cr(VI) usually associates with oxygen to form the oxyanions chromate (CrO_4^{2-}) and dichromate ($Cr_2O_7^{2-}$). Chromate and dichromate are in equilibrium which is sensitive to pH changes, where lower pH pushes the equilibrium towards the dichromate ion (Ebbing, 1996). Cr(VI) compounds are highly soluble and therefore mobile within aquatic systems, whereas derivatives of Cr(III) in the forms of hydroxides, oxides and sulphates, are water insoluble and exist mostly bound to organic matter in soils and aquatic systems (Rai *et al*., 1987; Cervantes *et al*., 2001; Zayed & Terry, 2003).

Although Cr(VI) is reduced in the presence of organic matter to Cr(III), high levels of Cr(VI) can overcome the reducing capacity of an environment and therefore persists as a pollutant (Cervantes *et al*., 2001).

Table 1.3: Chemical species of Cr in the environment (Zayed & Terry, 2003).

Chemical species	Oxidation state	Examples	Remarks
Elemental Cr	Cr(0)		Does not occur naturally
Divalent Cr	Cr(II)	$CrBr_2$, $CrCl_2$, CrF_2, CrSe, Cr_2Si	Relatively unstable and is readily oxidized to the trivalent state
Trivalent Cr	Cr(III)	CrB, CrB_2, $CrBr_3$, $CrCl_3.6H_2O$, $CrCl_3$, CrF_3, CrN	Forms unstable compounds and occurs in nature in ores, such as ferrochromite ($FeCr_2O_4$)
Tetravalent Cr	Cr(IV)	CrO_2, CrF_4	Does not occur naturally. The Cr(IV) ion and its compounds are not very stable and because of short half–lives, defy detection as reaction intermediates between Cr(VI) and Cr(III)
Pentavalent Cr	Cr(V)	CrO_4^{3-}, potassium perchromate	Does not occur naturally. Chromium (V) species are derived from the anion CrO_4^{3-} and are long-lived enough to be observed directly. However, there are relatively few stable compounds containing Cr(V)
Hexavalent Cr	Cr(VI)	$(NH_4)_2CrO_4$, $BaCrO_4$, $CaCrO_4$, K_2CrO_4, $K_2Cr_2O_7$	The second most stable state of Cr. However, Cr(VI) rarely occurs naturally, but is produced from anthropogenic sources. It occurs naturally in the rare mineral crocoite ($PbCrO_4$)

1.3 CHROMIUM TRANSPORT

To have any physiological or toxic effect, most heavy metal ions have to enter the cell (Nies, 1999). As Cr(VI) mainly exists in the oxyanion form, it cannot be trapped by the anionic components of bacterial envelopes (Cervantes *et al*. 2001; Neal *et al*., 2002) in contrast to the cationic Cr(III) derivates that have been shown to bind tightly to various components of bacterial envelopes of bacteria (Cervantes *et al*., 2001).

Chromate is actively transported across biological membranes in both prokaryotes and eukaryotes (Cervantes *et al*., 2001). By virtue of its structural similarity to SO_4^{2-}, bacteria readily transport Cr(VI) into the cell via the sulphate transport system. This analogous-transport pathway has been demonstrated in *Pseudomonas* (Ohtake *et al*., 1987) and *Cupriavidus* (Nies *et al*., 1989). In contrast, biological membranes are virtually impermeable to Cr(III) due to the insolubility of Cr(III)-compounds.

1.4 CHROMIUM TOXICITY

The biological effect of chromium is highly dependent on its oxidation state. Cr(VI) is highly toxic and has been shown to be a mutagen and carcinogen, whereas Cr(III) is considered to be relatively innocuous, probably due to the inability of Cr(III) to penetrate cells (Vennit & Levy, 1974; Cervantes *et al*., 2001; Codd *et al*., 2001).

Chromate alone does not react with DNA *in vitro*, however, in the presence of reductants a wide variety of DNA lesions, including Cr-DNA adducts, DNA-DNA crosslinks, DNA-protein crosslinks and oxidative damage occurs (Codd *et al*., 2001). Intracellular reduction of Cr(VI) through physiological reducing agents such as NAD(P)H, $FADH_2$, pentoses, glutathione as well as one-electron reducers such as glutathione reductase to transiently formed intermediates such as Cr(V) and the related free radical generation is considered a major cause of Cr(VI) carcinogenesis (Shi & Dalal, 1989; Shi & Dalal, 1990C; Codd *et al.*, 2001; Liu & Shi, 2001) as well as apoptosis (Ye *et al*., 1999).

Cr(V) in chemical solutions has been shown capable of generating free radicals such as hydroxyl radicals and superoxide, commonly referred to as reactive oxygen species (ROS) through Fenton-like reactions (Shi & Dalal, 1990A, 1990C; Liu & Shi, 2001). This redox cycle regenerates Cr(VI) which in turn can again be reduced through the continued action of cellular constituents and one-electron reducers, generating large quantities of ROS and oxidative stress (Ackerley *et al*., 2004A).

The genotoxic effect of Cr however cannot be fully explained by the sole action of ROS (Codd *et al*., 2001). Intracellular cationic Cr(III) complexes can interact electrostatically with negatively charged phosphate groups of DNA (Codd *et al*., 2001) which could affect replication, transcription and cause mutagenesis (Cervantes *et al*., 2001).

The physiological effects of chromate stress on bacteria is often observed through a decreased growth rate with increasing chromate concentration (Garbisu *et al*., 1998) or longer lag phases before growth is observed (Nepple *et al*., 2000). Chardin and co-workers (2002) showed an uncoupling of energy expenditure and growth in sulphate reducing bacteria during chromate-stress, comparable to that observed in bacteria due to oxidative stress. Chromate also frequently cause morphological changes (Michel *et al*., 2001; Ackerley *et al*., 2006; Chourey *et al*., 2006) observed as filamentous growth (Figure 1.1) as is often seen with bacterial-stress responses.

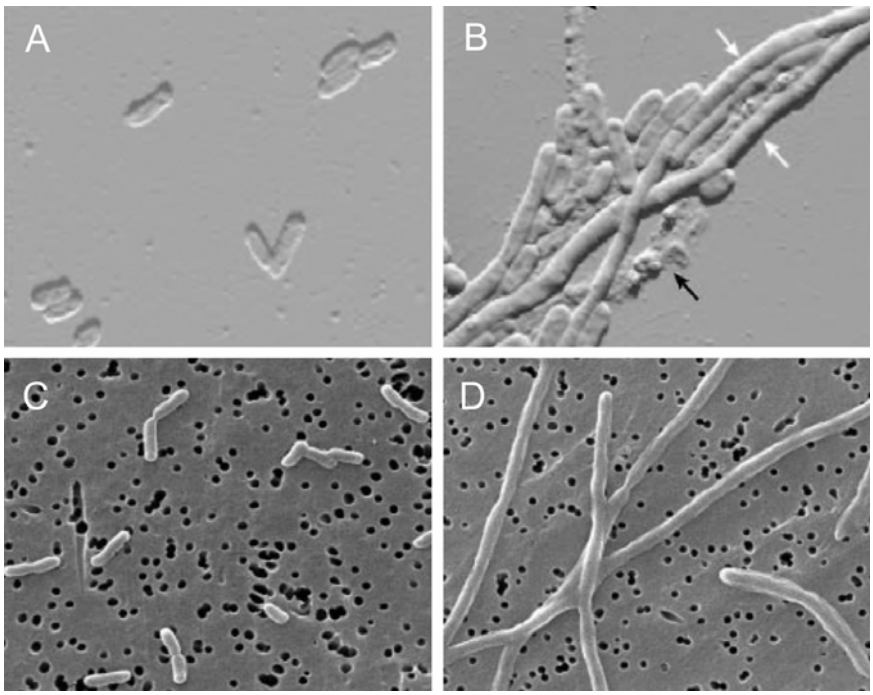

Figure 1.1: Micrographs of *Shewanella oneidensis* and *Escherichia coli* grown in the absence (A and C respectively) and presence of chromate (B and D respectively) indicating the morphological changes towards filamentous growth due to Cr(VI)-stress. (Adapted from Ackerley *et al*., 2006 and Chourey *et al*., 2006).

Recently, the molecular effects and global changes in protein expression due to chromate stress on *Shewanella oneidensis* (Chourey *et al*., 2006) and *E. coli* (Ackerley *et al*., 2006) were examined. *E. coli* Cr(VI)-stressed cells showed primarily the activation of the SOS response to counter oxidative stress (Ackerley *et al*., 2006), where as *Shewanella* showed induction of prophage-related genes. Genes involved in DNA metabolism, cell division, biosynthesis and degradation of murein, membrane response as well as environmental stress protections were upregulated, while genes encoding chemotaxis, motility and transport/binding proteins were repressed (Chourey *et al*., 2006).

1.5 BACTERIAL CHROMIUM RESISTANCE

Bacterial resistance mechanisms for essentially all toxic metal ions have been identified, including Ag^{+}, AsO_2^{-}, AsO_4^{3-}, Cd^{2+}, Co^{2+}, CrO_4^{2-}, Cu^{2+}, Hg^{2+}, Ni^{2+}, Sb^{3+}, Pb^{2+}, TeO_3^{2-}, Tl^{+} and Zn^{2+} (Silver & Phung, 1996; Ji & Silver, 1995). Ji & Silver (1995) hypothesizes that microbial resistance systems will be found in all bacterial types since these systems probably arose shortly after prokaryotic life started in an already metal-polluted world. Most resistance mechanisms are found on plasmids with related systems found as chromosomal genes, with efflux pumps currently the major known group responsible for heavy metal resistance in bacteria (Silver & Phung, 1996).

Chromate resistance, usually associated with plasmids, appears to be an independent mechanism from chromate reduction and was originally shown to confer chromate resistance through a decrease in intracellular accumulation of chromate (Bopp *et al.*, 1983; Ohtake *et al*., 1987; Cervantes & Ohtake, 1988; Nies *et al*., 1989).

Two homologous plasmid-conferred chromate resistance mechanisms (CHR) have been identified in *Pseudomonas* (Cervantes *et al*., 1990) and *Cupriavidus metallidurans* (formerly *Alcaligenes eutrophus* and *Ralstonia metallidurans*; Nies *et al*., 1990) through cloning and sequencing of the *chrA* genes. The *chrA* genes from *Pseudomonas* and *Cupriavidus* encode hydrophobic proteins (ChrA) of 416 and 401 amino acid residues respectively, sharing 29% amino acid identity (Nies *et al*., 1990; Cervantes *et al*., 1990).

Hydropathic profiles suggest that both ChrA from *Pseudomonas* and *Cupriavidus* are membrane proteins, originally thought to consist of 12 (Cervantes & Silver 1992) or 10 (Nies *et al*., 1998) transmembrane regions. Recently Jiménez-Mejía and co-workers (2006) determined the ChrA of *Pseudomonas* to posses a 13 transmembrane segment topology (Figure 1.2) arising from the duplication of a 6 transmembrane segment ancestral protein whereby the two halves of ChrA could carry out distinct functions in the transport of chromate.

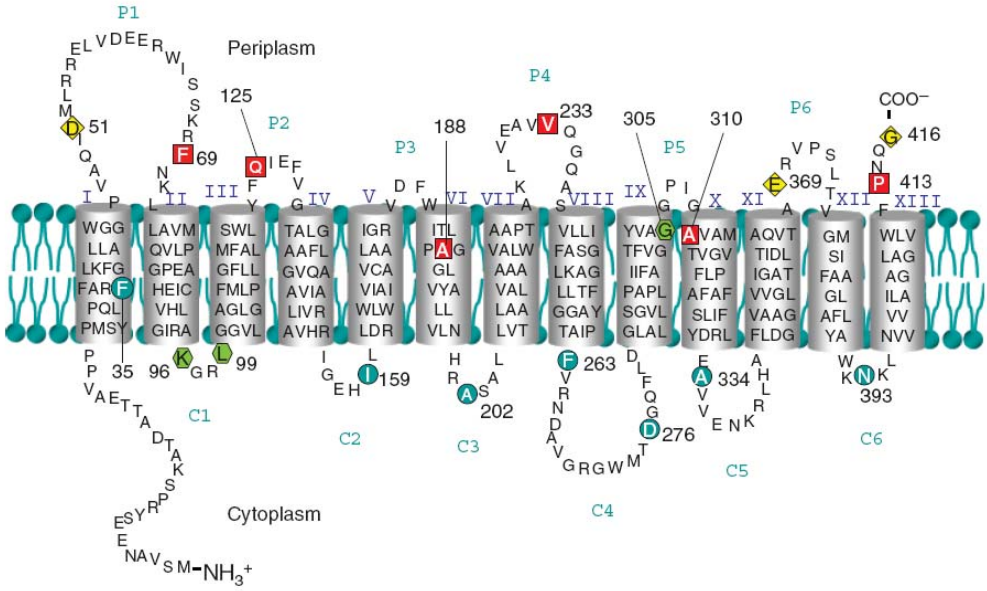

Figure 1.2: Schematic representation of the transmembrane topology of the ChrA of *Pseudomonas aeruginosa*. Amino acid sequence is given by single-letter abbreviations and transmembrane segments are indicated as grey cylinders (Adapted from Jiménez-Mejía *et al*., 2006).

The diminished uptake of chromate conferred by ChrA of *Pseudomonas* is based on an energy dependent chemiosmotic efflux system of chromate from the cytoplasm (Alvarez *et al*., 1999, Pimentel *et al*., 2002). The efflux of chromate is inhibited by sulphate, although sulphate has not been demonstrated to be transported by the ChrA proteins. Nies and co-workers (1998) proposed that ChrA might function as chromate/sulphate antiporters.

The chromate resistance mechanisms is however not limited to plasmids. In addition to the plasmid-encoded *chrA*$_1$ gene, a ChrA homolog (*chrA*$_2$) has been found on the chromosome of *Cupriavidus* also conferring chromate resistance (Juhnke *et al*., 2002).

1.6 CHROMATE REDUCTION

Dissimilatory Cr(VI)–reducing bacteria appear to be ubiquitous in soils and sediments as they have been isolated from numerous and diverse environments, both contaminated and uncontaminated with Cr(VI) (Cooke *et al*., 1995; Turick *et al*., 1996; Bader *et al*., 1999; Pattanapipitpaisal *et al*., 2001; Camargo *et al*., 2003A).

A variety of genera of bacteria have been reported to be able to reduce Cr(VI) to Cr(III), including *Pseudomonas* (Bopp & Ehrlich,1988; DeLeo & Ehrlich, 1994; Ganguli & Tripathi, 1999; Ishibashi *et al*., 1990), *Bacillus* (Campos *et al*., 1995; Garbisu *et al*., 1998; Camargo *et al*., 2003B), *Deinococcus* (Fredrickson *et al*., 2000), *Enterobacter* (Wang *et al*., 1989, 1990; Komori *et al*., 1989, 1990A, 1990B; Clark, 1994), *Agrobacterium* (Llovera *et al*., 1993A, 1993B), *Escherichia* (Shen & Wang, 1993), *Shewanella* (Myers *et al*., 2000; Middleton *et al*., 2003; Viamajala *et al*., 2002A, 2002B, 2004), *Thermus* (Kieft *et al*., 1999) and other species.

Chromate reduction by microorganisms is not only restricted to bacteria, but have been shown in species of *Streptomyces* (Das & Chandra, 1990; Laxman & Moore, 2002), *Candida* (Muter *et al*., 2001; Ramírez-Ramírez *et al*., 2004) as well as the hyperthermophilic archaeal *Pyrobaculum islandicum* (Kashefi & Lovley, 2000).

Three mechanisms involved in Cr(VI) reduction have been described (Wang & Shen, 1995; Ramírez-Díaz, 2007):

a) Reduction of Cr(VI) due to chemical reduction through cellular compounds such as amino acids, nucleotides, sugars, vitamins, organic acids or glutathione.
b) Aerobic Cr(VI) reduction that is generally associated with soluble proteins requiring NAD(P)H as an electron donor.
c) Anaerobic Cr(VI) reduction often through membrane-associated reductases of which some can utilize H_2 as electron donor. Anaerobic Cr(VI) reduction whereby Cr(VI) is an electron acceptor in the electron transport chain (Lovley & Phillips, 1994; Tebo & Obraztsova, 1998; QuiIntana *et al*., 2001) has also been demonstrated.

Several researchers have proposed that these chromate reductases might be the serendipitous activity of enzymes with other primary physiological functions, since Cr(VI) is mostly of anthropogenic origins and these fortuitous reactions are often carried out by constitutive enzymes (Bopp & Ehrlich, 1988; Ishibashi *et al*., 1990; Cervantes, 1991). However, very few of the responsible chromate reductases have been purified and characterized with respect to their gene sequence to elucidate their true function.

Most research has focused on a group of cytoplasmic flavoproteins identified as chromate reductases in *Pseudomonas putida* (ChrR) and *E. coli* (YieF) which fully reduces Cr(VI) to Cr(III) (Park *et al*., 2000; Gonzalez *et al*., 2003; Ackerley *et al*., 2004B; Gonzalez *et al*., 2005). These enzymes are NAD(P)H dependent homodimeric proteins with monomer molecular masses of approximately 20 kDa, containing non-covalently bound FMN and belongs to the NADH_dh2 family of proteins which consists of obligatory two-electron reducers of electrophiles. During the reduction of Cr(VI) to Cr(III), ChrR of *P. putida* generates Cr(V) transiently, whereas YieF from *E. coli* seems to transfer three electrons directly to Cr(VI) (Ackerley *et al*., 2004B). Both these enzymes also reduced quinones, potassium ferricyanide and 2,6-dichloroindophenol, with YieF also able to reduce other high-valence metals such as V(V) and Mo(VI) and even cytochrome c. Sequence similarities however indicate these enzymes likely to be quinone reductases, and the authors suggest that ChrR and YieF might be bacterial counterparts of the mammalian DT-diaphorase of which the main biological function is the detoxification of quinonoid compounds. Nevertheless, both these enzymes have been shown to protect against chromate toxicity, possibly through minimizing the amount of reactive oxygen species (ROS) formed by pre-empting chromate reduction by cellular one-electron reducers.

The chromate reductase purified from *Pseudomonas ambigua* (Suzuki *et al*., 1992) is also a homodimeric flavoprotein with an approximate monomer molecular mass of 25 kDa and non-covalently bound FMN, which utilized NAD(P)H as electron donor, forming a Cr(V) intermediate during Cr(VI) reduction. The chromate reductase however showed high homology to nitroreductases (NfsA) from both *E. coli* and *Vibrio harveyi* which also have chromate reductase activity (Kwak *et al*., 2003). NfsA is also an obligatory two-electron reducer of nitrocompounds and quinones (Ackerley *et al*., 2004A).

A soluble homodimeric iron(III) reductase (FerB) with a noncovalently bound FAD coenzyme from *Paracoccus denitrificans* also shows high sequence homology with the chromate reductase from *P. putida* and flavin reductases (Fre) from *P. syringae* and has been shown to be able to reduce Cr(VI) and quinones but not free flavins (Mazoch *et al*., 2004). A flavin reductase (Fre) system from *E. coli* also reduces Cr(VI) to a soluble Cr(III)-NAD^+ complex via unbound, highly active reduced flavins (Puzon *et al.*, 2005). The close relatedness of the nitroreductases (NfsA) and flavin reductases has previously been shown by Zenno and co-workers when the NfsA from *E. coli* was transformed from a nitroreductase into a flavin reductase with activity comparable to that of the native Frp of *Vibrio harveyi* (Zenno *et al*., 1998) through a single amino acid substitution within the active site.

In addition, some NADPH-dependent flavoenzymes, such as glutathione reductase, lipoyl dehydrogenase and ferrodoxin-$NADP^+$ oxidoreductase can also catalyze the reduction of Cr(VI) through a series of one-electron transfers (Shi & Dalal, 1990A, 1990B).

Recently, an additional Cr(VI) reductase from *E. coli* was purified by Bae and co-workers (2005). This cytoplasmic chromate reductase also showed a homodimeric quaternary structure with a monomer molecular mass of approximately 42 kDa and utilizes NAD(P)H as electron donor for Cr(VI) reduction. In contrast to the above mentioned purified chromate reductases, this enzyme did not contain any bound flavin-cofactor nor nitroreductase activity.

As these enzymes capable of chromate reduction utilizes different modes of electron transfer to chromate, Ackerley and co-workers (2004A) have suggested the terminology “tight”, “semi-tight” and “single-electron” to classify enzyme-mediated electron transfer. “Tight” chromate reduction occurs through the action of four-electron reducers that brings about Cr(VI) reduction to Cr(III) in a single step without redox cycling. Three electrons are simultaneously transferred to chromate, without the formation of a flavin semiquinone, and the remaining electron is transferred to molecular oxygen, whereby only 25% of the electrons are thus utilized in ROS generation. During “semi-tight” chromate reduction, chromate is reduced by a combination of two- and one-electron reductions steps with the

concomitant formation of a flavin semiquinone, allowing redox cycling of Cr and subsequent generation of more ROS. "Single-electron" reducers produces the most ROS, as Cr(VI) reduction to Cr(III) is mediated via a series of one-electron reductions, allowing significant redox cycling of the Cr.

1.7 APPLICATION

Most microbial remediation strategies have focused on the degradation of organic contaminants as most organic contaminant can be destroyed through oxidation to carbon dioxide whereas microorganisms can only alter the speciation of metal contaminants (Lovley & Coates, 1997). In recent years there has been a dramatic increase in the interest in utilizing bioremediation to treat heavy-metal contaminated environments (Valls & Lorenzo, 2002; Mulligan *et al*., 2001; Dua *et al*., 2002) and especially Cr(VI) contamination (Vainshtein *et al*., 2003; Zayed & Terry, 2003). Microorganisms can remove toxic heavy metals and metalloids through precipitation or volatilization as well as the alteration of the redox state of the metals and metalloids to more soluble forms that could aid in the leaching of these contaminants from soils (Lovley & Coates, 1997).

As mentioned previously, contamination of soils and groundwater by Cr(VI) is a significant problem and most microbial Cr(VI) reduction studies have mentioned their potential use for removing chromate from contaminated environments.

In situ microbial reduction can circumvent many of the limitations posed by physical or chemical treatment methods. Some of the main advantages of using bacterial Cr(VI) reduction are that it does not require the use of toxic chemicals or high energy input as well as the potential of using native non-hazardous microbial strains (Cervantes *et al*., 2001). Difficulties are however often encountered in real chromate-contaminated waste streams. Although *Enterobacter cloacae* can rapidly reduce Cr(VI) concentrations as high as 10 mM, other heavy metal contaminants and sulphates in industrial materials inhibit its Cr(VI) reduction (Ohtake *et al*., 1990). However, enzymatic Cr(VI) treatment could have advantages in mixed-waste where organic contaminants and Cr(VI) could be treated

simultaneously (Shen *et al*., 1996) potentially through coupling the oxidation of organic contaminants to the reduction of Cr(VI) (Lovley, 1995).

1.8 INTRODUCTION TO PRESENT STUDY

Gold mines in South Africa provide unique opportunities to study subsurface microbiology and biogeochemistry as they are among the deepest excavations in the world and provide novel extreme conditions that include, amongst others, high temperatures, high pressure, high salinity and low availability of energy sources. Numerous studies over the past few years have indicated that this deep-subsurface harbors a variety of microorganisms from both bacteria and archaea (Fredrickson & Onstott, 1996; Takai *et al*., 2001A; Onstott *et al.*, 2003) and have yielded novel extremophiles (Takai *et al*., 2001B).

In 1999, Kieft and co-workers described a thermophilic bacterium, later identified as *Thermus scotoductus* (Balkwill *et al*., 2004), isolated from groundwater samples collected from a South African Gold mine (Mponeng) at a depth of 3.2 km, with ambient rock-temperatures of 60°C, in the Witwatersrand Supergroup operated by Anglogold Ashanti (previously known as Western Deep Levels). The Witwatersrand Supergroup is a 2.9-billion-year-old formation of low-permeability sandstone and shale with minor volcanic units and conglomerates, overlain by the 2.7 Ga. Ventersdorp Supergroup volcanics and the 2.3 Ga Transvaal Supergroup dolomites.

Thermus scotoductus SA-01 was shown to be able to use O_2, NO_3^-, Fe(III) and S^0 as terminal electron acceptors for growth at 65°C. In addition, *T. scotoductus* SA-01 was also shown to be able to couple to oxidation of lactate or H_2 to the reduction of a variety of metals including Fe(III), Mn(IV), Co(III)-EDTA, Cr(VI) and U(VI) (Kieft *et al*., 1999; Möller & van Heerden, 2006).

This study into the mechanisms of *T. scotoductus* SA-01's ability to reduce Cr(VI) is part of an ongoing investigation into *T. scotoductus*'s metal-interaction and reduction abilities.

CHAPTER 2

Cr(VI) REDUCTION BY *THERMUS SCOTODUCTUS* STRAIN SA–01

2.1 INTRODUCTION

The use of microorganisms has become an important alternative to currently available conventional physical and chemical treatment technologies for the removal of toxic heavy metals from polluted areas. Many bacteria can reduce chromium, and dissimilatory Cr(VI)–reducing bacteria appear to be ubiquitous in soils and sediments since they have been isolated from numerous and diverse environments, both contaminated and uncontaminated with Cr(VI) (Turick *et al*., 1996; Pattanapipitpaisal *et al*., 2001; Luli *et al*., 1983; Cooke *et al*., 1995). A variety of genera of bacteria have been reported to be able to reduce Cr(VI) to Cr(III), including strains of *Pseudomonas* (Bopp & Ehrlich, 1988; Park *et al*., 2000), *Enterobacter* (Wang *et al*., 1989; Ohtake *et al*., 1990), *Bacillus* (Campos *et al*., 1995; Garbisu *et al*., 1998), *Thiobacillus* (Sisti *et al*., 1996), *Shewanella* (Myers *et al*., 2000) *Agrobacterium* (Llovera *et al*., 1993A) and *Thermus* (Kieft *et al*., 1999).

Since hexavalent chromium in the environment is primarily anthropogenic, the reason why some microorganisms have developed a capacity for Cr(VI) reduction has not yet been adequately explained.

This chapter describes Cr(VI)–reduction in batch cultures as well as under non–growth conditions, which were used to assess the aerobic Cr(VI)–reduction ability of *Thermus scotoductus* SA–01.

2.2 MATERIALS AND METHODS

2.2.1 Bacterial strains and culture conditions

The thermophilic bacterium used throughout this study was isolated in 1999 by Kieft and co-workers from groundwater sampled at a depth of 3.2 km in the South African gold mine, Mponeng, from the Witwatersrand Supergroup, operated by AngloGold Ashanti. This strain was identified as belonging to the genus *Thermus*, as determined by 16S rRNA gene sequence analysis (Kieft *et al*., 1999), and later classified as *Thermus scotoductus* strain SA–01 (Balkwill *et al*., 2004) [ATCC 700910; Subsurface Microbial Culture Collection (SMCC; Balkwill, 1993) LX–001]. The strain was provided by Prof. T.L. Kieft (Department of Biology, New Mexico Institute of Mining and Technology, Socorro, New Mexico).

SA–01 was routinely cultured aerobically in a complex organic medium, TYG [5 g tryptone (Biolab), 3 g yeast extract (Saarchem) and 1 g glucose in 1 L ddH_2O] at 65°C, pH 7.0, with shaking (200 rpm). The strain was examined for purity by streaking onto TYG medium solidified with 2% agar and by obtaining isolated colonies twice in succession. Gram staining and microscopic analysis showed only gram–negative rods. Frozen stocks were maintained in 15% glycerol at –80°C.

Escherichia coli TOP10 (Invitrogen) competent cells were used for cloning host purposes and was grown in Luria-Bertani (LB) medium [10 $g.L^{-1}$ tryptone (Biolab), 5 $g.L^{-1}$ yeast extract (Biolab) and 5 $g.L^{-1}$ NaCl (pH 7)] at 37°C with aeration (200 rpm). Ampicillin (100 $\mu g.ml^{-1}$) was added when required.

2.2.2 Strain verification

Strain identity was verified using 16S rDNA PCR amplification and sequencing of whole-cells or genomic DNA (section 5.2.2.1)

2.2.2.1 Polymerase chain reaction (PCR)

PCR reactions were performed in a total reaction volume of 50 µl using a Thermal Cycler (PxE 0.2, Thermo electron corporation). Reaction mixture consisted of 10X Super-Therm reaction buffer (5 µl), $MgCl_2$ (2 mM), dNTP's (0.8 mM), Super-Therm polymerase (2.5 U), 0.2 µM of both the universal 16S forward (27F) and reverse (1492R) primers and 50 ng of template. Reaction conditions consisted of an initial denaturing step at 95°C for 5 min, followed by 30 cycles of denaturing at 95°C (30 sec), annealing at 54°C (30 sec) and elongation at 72°C (1.5 min). A final elongation step of 10 min at 72°C was added to ensure complete elongation of amplified product.

Purification of the PCR product from the agarose gel was achieved by excising the desired band from the agarose gel and extracted using the GFX PCR DNA and Gel Band Purification Kit from Amersham Biosciences according to the manufacturer's instructions.

2.2.2.2 Ligations

The approximate 1.5 kbp PCR product purified from the agarose gel was ligated into pGEM®-T Easy Vector system (Promega). Protocols for ligations were performed as per manufacturer's instructions. The ligation reaction were performed in a total reaction volume of 10 µl and consisted of 2X Rapid Ligation Buffer (5 µl), pGEM®-T Easy vector (2.5 ng), PCR product (3.5 µl) and T4 DNA Ligase (0.3 Weiss units). The ligation reactions were incubated overnight at 4°C.

2.2.2.3 Transformations

Competent *Escherichia coli* One Shot TOP10 (Invitrogen) cells were prepared according to the method described by Hanahan (1983) with modifications. Flasks containing Psi broth (5 $g.L^{-1}$ yeast extract, 20 $g.L^{-1}$ tryptone, 5 $g.L^{-1}$ magnesium sulphate, pH 7.6 with KOH) were inoculated with 1 ml of an overnight culture and grown at 37°C until an absorbance of 0.6 at 600 nm was reached. Cells were placed on ice for 30 min and centrifuged (3 000 x g) for 10 min at 4°C to collect cells. Cells were resuspended in 40 ml TfbI buffer (30 mM potassium acetate, 100 mM rubidium chloride, 10 mM calcium chloride, 15% glycerol, pH 5.8) and incubated on ice for 15 min. Cells were collected through centrifugation at 3 000 x g for 10 min at 4°C and resuspended in 4 ml TfbII buffer (10 mM MOPS-NaOH, 75 mM calcium chloride, 10 mM rubidium chloride, 15% glycerol, pH 6.5). The cell suspensions

were incubated on ice for 10 min, aliquated and snap frozen in liquid nitrogen followed by -70°C storage.

50 µl of *E. coli* One Shot TOP10 competent cells were allowed to thaw on ice. 5 µl of the ligated plasmid reactions were added to the cells and incubated on ice for 30 min. The cell-suspension was heat shocked at 42°C for 40 s and immediately returned to ice-water for 2 min. 250 µl of SOC medium (pGEM®-T Easy Technical Manual) was added to the transformation reactions and incubated at 37°C for 1 h with gentle shaking. Various aliquots were plated out on separate LB plates containing ampicillin (0.1 $mg.ml^{-1}$), isopropyl β-D-thiogalactoside (IPTG, 0.12 $mg.ml^{-1}$) and 5-bromo-4-chloro-3-indolyl β-D-galactoside (X-Gal, 0.08 $mg.ml^{-1}$) and incubated overnight at 37°C to verify DNA ligation using blue/white selection.

Single white colonies were inoculated into 5 ml LB media containing ampicillin (0.1 $mg.ml^{-1}$) and incubated overnight at 37°C. Plasmids were isolated using the FastPlasmid™ Mini kit (Eppendorf) as per manufacturer's recommendations.

2.2.2.4 Sequencing

Plasmid inserts were sequenced by Inqaba Biotechnical Industries (South Africa) using a Spectrumedix SCE2410 genetic analysis system (SpectruMedix LLC). Sequencing reactions were performed using the BigDye (v3.1) dye terminator cycle sequencing kit (Applied Biosystems) using the universal SP6 and T7 promoter primers.

2.2.2.5 DNA electrophoresis

DNA was analyzed on a horizontal agarose slab gel [0.8% (w/v)] containing 1.5 $µg.ml^{-1}$ ethidium bromide in TAE buffer [Tris (40 mM), acetic acid (20 mM) and EDTA (1 mM)]. Electrophoresis was done for approximately 1 h at 90 V and the DNA visualized using a ChemiDox XRS Gel Documentation system (Biorad).

DNA fragment size was estimated based on electrophoretic mobility relative to that of MassRuler™ DNA Ladder (Fermentas) standards during the same electrophoretic run.

2.2.3 Aerobic batch culture studies

The chromate tolerance and reduction capability of SA–01 was investigated under aerobic conditions in TYG medium supplemented with various Cr(VI) concentrations. Growth was initiated in 500 ml Erlenmeyer flasks containing 100 ml medium using standardized inocula (5% v/v) to approximately 0.06 $g.L^{-1}$ cells (dry weight) from cultures that were transferred twice into fresh medium over a period of approximately 20 h. Inoculations were timed to ensure that cultures were under excess nutrient conditions, and thus in an environment allowing balanced exponential growth. Incubation proceeded for 24 h at 65°C with shaking (200 rpm), under aerobic conditions. The growth was assayed by aseptically withdrawing samples from the shake flasks and measuring the turbidity/optical density on a UV–vis spectrophotometer (Milton Roy Company Spectronic GENESYS 5) at 660 nm (OD_{660}) in disposable cuvets. After recording the optical density, the sample was centrifuged at 7 000 x g for 3 min. Portions of the supernatant were then used to measure the remaining hexavalent chromium levels. pH and E_h were monitored over the experimental time course. E_h was a measure of the relative reduction potential of the bulk solution, which can be due to a combination of several redox couples. Cell–free controls were included to measure the rate of abiotic chromate reduction. Growth experiments were repeated three times with consistent results. Data from representative experiments are presented.

2.2.4 Reduction of Cr(VI) by resting cells

To determine whether SA–01 could reduce Cr(VI) under conditions that do not favor cell growth (non–growth) or resting conditions, cells were grown in TYG medium until mid exponential (logarithmic) phase, harvested by centrifugation at 10 000 x g for 15 min, washed three times with 20 mM MOPS (pH 7) buffer and resuspended in the same buffer.

Aerobic reduction tests of resting cells were carried out in crimp–sealed Balch tubes (Bellco Glass, Inc.) in a final volume of 4 ml in 20 mM MOPS–NaOH buffer, pH 7, with a headspace filled with air. The mixture contained 1 g cells L^{-1}, CrO_3 (0.1 mM) and electron donor (10 mM). Cell suspensions were incubated at 65°C in a water bath while shaking. Cell suspensions were given a 5 min pre–incubation with the electron donor before the

reaction was initiated by addition of the hexavalent chromium. Samples (0.5 ml) were withdrawn periodically and centrifuged immediately (7 000 x g, 3 min) and supernatants were analyzed for residual Cr(VI). All experiments were done in duplicate using independent biomass preparations and averages are shown. For each treatment, cell–free controls were prepared to monitor whether abiotic chromate reduction occurred.

2.2.5 Factors affecting chromate reduction

2.2.5.1 Effect of pH and temperature

The effect of pH on the activity of whole cells to reduce Cr(VI) under non–growth conditions was assessed by constructing a pH range (5.5 – 8.5) by adjusting the pH of a 20 mM MES–MOPS–Bicine buffer with HCl or NaOH. The reaction was allowed to proceed for 30 min at 65°C and the residual Cr(VI) measured afterwords.

A temperature range of 50°C to 90°C was used to evaluate the optimum temperature for Cr(VI) reduction using resting whole–cells. The cell suspensions in the assay buffer was equilibrated as the required temperature before the reaction was initiated as described in section 2.2.4. The reacting mixture was allowed to proceed for 30 min at pH 7 and the residual Cr(VI) was measured afterwords.

Assays were done in duplicate with blank rates taken at each assayed pH and temperature value.

2.2.5.2 Effect of electron donor

The ability of SA–01 whole–cells to utilize various electron donors under non–growth conditions for Cr(VI) reduction was assessed under the standard assay conditions as described in section 2.2.4 using 10 mM of each electron donor. As many of the electron donors naturally have buffering capabilities, the pH of the electron donor stock solutions was adjusted to 7 to ensure no discrepancies due to difference in reaction pH. Assays were done in duplicate with chemical Cr(VI) reduction by each electron donor considered.

2.2.5.3 Effect of metabolic inhibitors

Metabolic inhibitors of glycolysis, the Krebs–cycle as well as the electron transport system was used to evaluate Cr(VI) reduction using resting whole–cells of SA–01. Sodium fluoride and iodoacetate was added to the standard whole–cell reduction assays to a final concentration of 1 – 20 mM with glucose as the electron donor to assess the inhibition of glycolysis. Sodium cyanide and sodium fluoroacetate (1 – 20 mM) was used for the inhibition of the electron transport system and the Krebs–cycle respectively, using pyruvate as the electron donor under the standard assay conditions. A 1 min pre–incubation of the cells with the metabolic inhibitors was allowed before the addition of the electron donor and the start of the reaction.

2.2.5.4 Steady–state kinetics

The effect of substrate concentration on the Cr(VI)–reducing activity of whole–cells under non–growth conditions was evaluated with different concentrations of both Cr(VI) and pyruvate. For evaluation of the effect of Cr(VI), the pyruvate concentrations was kept constant at 10 mM, and similarly for the evaluation of electron donor concentration, the Cr(VI) concentration was 0.1 mM under the standard assay conditions (65°C; pH 7). Assays were performed in duplicate with averages used for non–linear regression analysis [SigmaPlot 8.0 (SPSS Inc.)].

2.2.5.5 Effect of complexing agents

The effect of ethylenediaminetetraacetate (EDTA) and nitrilotriacetic acid (NTA) on chromate reduction activity by resting whole–cells was tested by incubating the enzyme with disodium-EDTA or trisodium–NTA to final concentrations in the range of 0.1 – 50 mM. The remaining activity was determined, with the control (no Na_2-EDTA or Na_3–NTA) taken as 100%.

2.2.6 Preparation of subcellular fractions

Subcellular fractions were prepared using a modification of the method of Gaspard *et al*., (1998), as described by Kaufmann & Lovley in 2001. SA–01 was grown in TYG medium without chromate until mid exponential growth. Cells were harvested by centrifugation at

10 000 x g for 15 min at 4°C and washed three times with 20 mM MOPS–NaOH buffer (pH 7.0). For the preparation of spheroplasts, cells were resuspended in MOPS–NaOH buffer (20 mM) containing 25% (w/v) sucrose [approximately 1 g cells (wet weight) in 20 ml buffer]. To accomplish cell wall lysis, lysozyme was added to a final concentration of 0.1% (w/v) and shaken for 30 min at 37°C. Following the addition of Na_2–EDTA (pH 8.0) to a final concentration of 5 mM and shaking for 20 min, $MgCl_2$ was added to a final concentration of 13 mM and the suspension was shaken for another 20 min. Separation of spheroplasts from the periplasmic fraction was obtained by centrifugation at 20 000 x g for 30 min. Spheroplasts were resuspended in 20 mM MOPS–NaOH buffer (pH 7.0).

To obtain the membrane and cytoplasmic fractions, a few DNase crystals and Complete, EDTA-free protease inhibitor cocktail (Roche) were added to the EDTA-lysozyme-treated cell suspension, and cells broken by ultrasonic treatment (10 times, 100 W, 30 s) with a sonifier (Branson Sonic Power Sonifier Cell Disruptor B-30) in an ice-water bath. Cell debris was removed by centrifugation at 4 000 x g for 10 min at 4°C. The crude extract (supernatant) was subsequently centrifuged at 110 000 x g for 1.5 h at 4°C, yielding the cytoplasmic fraction (supernatant) and a membrane fraction (pellet). The latter was resuspended in MOPS–NaOH buffer (20 mM, pH 7.0).

2.2.7 Analytical methods

2.2.7.1 Cell concentrations

Cell concentrations were determined by extrapolating optical density readings at 660 nm (OD_{660}) to dry biomass values using a calibration curve relating OD_{660} to dry biomass (Figure 2.1).

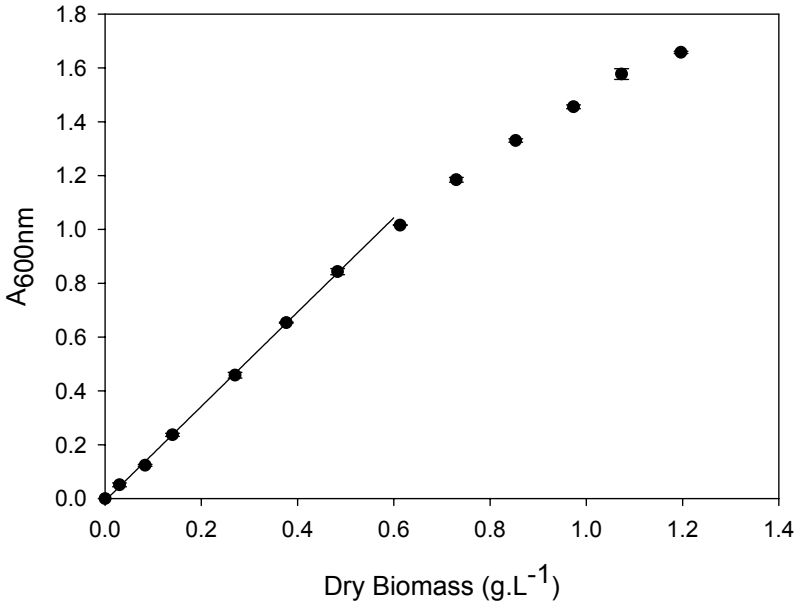

Figure 2.1: Standard curve relating dry biomass to absorbance at 600 nm. Error bars indicate standard deviation.

2.2.7.2 Cr(VI) concentration determination

Chromate reductase activity was determined by measuring the decrease of hexavalent chromium. Cr(VI) was analysed by the *s*-diphenylcarbazide method as described by Urone (1955). Samples (0.3 ml) were withdrawn and added to 2.5 ml of a 0.12 M H_2SO_4 stock solution. 0.2 ml of the *sym*-diphenylcarbazide reagent (dissolved in acetone) was added to the reaction mixture to a final concentration of 0.01% (w/v). Absorbance was measured using a Spectronic GENESYS 5 spectrophotometer (Milton Roy Company) at 540 nm and chromate was quantified using a calibration curve relating chromate concentration to A_{540nm} (Figure 2.2).

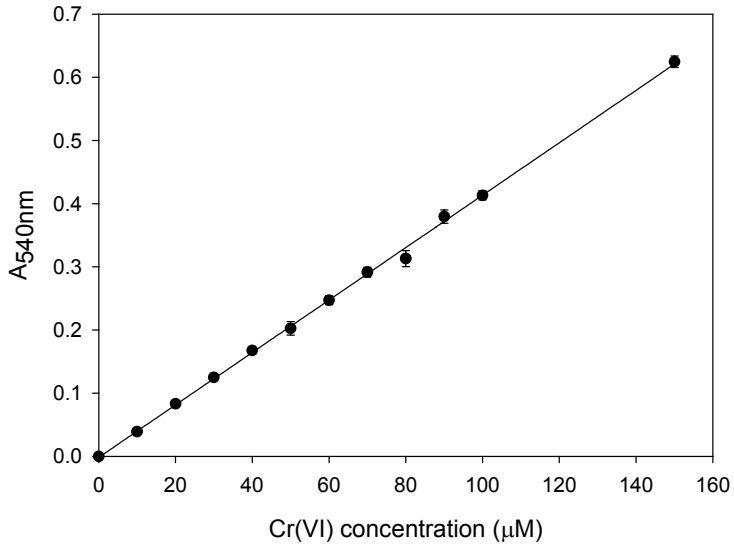

Figure 2.2: Standard curve for the determination of hexavalent chromium with the *s*–diphenylcarbazide method using chromium trioxide as standard. Error bars indicate standard deviation.

After cell fractionation, the fractions were assayed in 1 ml reaction mixtures containing 20 mM MOPS–NaOH buffer (pH 7.0), 0.1 mM CrO_3, 0.3 mM NADH and 0.05 ml of the enzyme preparation at 65°C.

2.2.7.3 Protein concentrations

Protein concentrations were determined using the bicinchoninic acid (BCA) method (Smith *et al*., 1985). BCA Protein Assay Kit from Pierce (Rockford, IL, USA) was used according to the manufacturer's instructions with bovine serum albumin (BSA) as standard (supplied with kit).

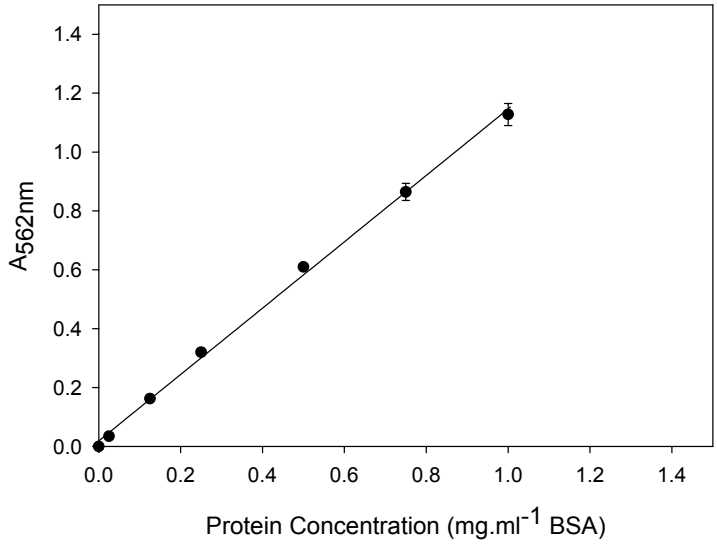

Figure 2.3: Standard curve for the BCA protein assay kit (Pierce) at 37°C using BSA as protein standard. Error bars indicate standard deviation.

2.3 RESULTS AND DISCUSSION

2.3.1 Strain verification

Strain verification and purity of *Thermus scotoductus* SA-01 was done using 16S rDNA PCR amplification (Figure 2.4) and sequencing of 5 representative clones. Figure 2.5 shows the alignment of the sequence obtained with the partial 16S ribosomal RNA gene of *Thermus* SA-01 (NCBI: AF020205; Kieft *et al.*, 1999).

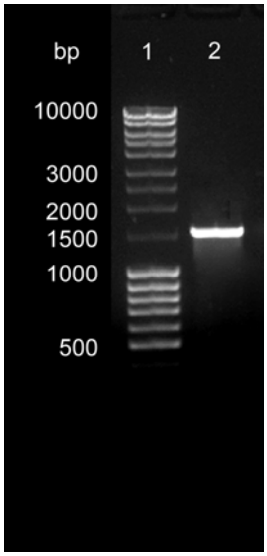

Figure 2.4: 16s rDNA gene PCR amplification of *Thermus scotoductus* SA-01. Lane 1, molecular weight marker; lane 2, 16S rDNA amplicon.

```
SA-01         1    -AGAGTTTGA TCATGGCTCA GGGTGAACGC TGGCGGCGTG CCTAAGACAT GCAAGTCGAG CGGGGCAGGT TTATACCTGT CCAGCGGCGG ACGGGTGAGT  99
Kieft et al   1    AAGAGTTTGA TCGTGGCTCA GGGTGAACGC TGGCGGCGTG CCTAAGACAT GCAAGTCGAG CGGGGCAGGT TTATACCTGT CCAGCGGCGG ACGGGTGAGT  100

SA-01         100  AACGCGTGGG TGACCTACCC GGAAGAGGCG GACAACCTGG GGAAACCCAG GCTAATCCGC CATGTGGTCC TGTCCTGTGG GGCAGGACTA AAGGGTGAAT  199
Kieft et al   101  AACGCGTGGG TGACCTACCC GGAAGAGGCG GACAACCTGG GGAAACCCAG GCTAATCCGC CATGTGGTCC TGTCCTGTGG GGCAGGACTA AAGGGTGAAT  200

SA-01         200  AGCCCGCTTC CGGATGGGCC CGCGTCCCAT CAGCTAGTTG GTGGGGTAAA GGCCCACCAA GGCGACGACG GGTAGCCGGT CTGAGAGGAT GGCCGGCCAC  299
Kieft et al   201  AGCCCGCTTC CGGATGGGCC CGCGTCCCAT CAGCTAGTTG GTGGGGTAAA GGCCCACCAA GGCGACGACG GGTAGCCGGT CTGAGAGGAT GGCCGGCCAC  300

SA-01         300  AGGGGCACTG AGACACGGGC CCCACTCCTA CGGGAGGCAG CAGTTAGGAA TCTTCCGCAA TGGACGGAAG TCTGACGGAG CGACGCCGCT TGGAGGAGGA  399
Kieft et al   301  AGGGGCACTG AGACACGGGC CCCACTCCTA CGGGAGGCAG CAGTTAGGAA TCTTCCGCAA TGGACGGAAG TCTGACGGAG CGACGCCGCT TGGAGGAGGA  400

SA-01         400  AGCCCTTCGG GGTGTAAACT CCTGAACTGG GGACGAAAGC CCCGTGTAGG GGGATGACGG TACCCAGGTA ATAGCGCCGG CCAACTCCGT GCCAGCAGCC  499
Kieft et al   401  AGCCCTTCGG GGTGTAAACT CCTGAACTGG GGACGAAAGC CCCGTGTAGG GGGATGACGG TAACCAGGTA ATAGCGCCGG CCAACTCCGT GCCAGCAGCC  500

SA-01         500  GCGGTAATAC GGAGGGCGCG AGCGTTACCC GGATTTACTG GGCGTAAAGG GCGTGTAGGC GGCCTGGGGC GTCCCATGTG AAAGGCCACG GCTCAACCGT  599
Kieft et al   501  GCGGTAATAC GGAGGGCGCG AGCGTTACCC GGATTTACTG GGCGTAAAGG GCGTGTAGGC GGCCTGAGGC GTCCCATGTG AAAGGCCACG GCTCAACCGT  600

SA-01         600  GGAGGAGCGT GGGATACGCT CAGGCTAGAG GGTGGGAGAG GGTGGTGGAA TTCCCGGAGT AGCGGTGAAA TGCGCAGATA CCGGGAGGAA CGCCGATGGC  699
Kieft et al   601  GGAGGAGCGT GGGATACGCT CAGGCTAGAG GGTGGGAGAG GGTGGTGGAA TTCCCGGAGT AGCGGTGAAA TGCGCAGATA CCGGGAGGAA CGCCGATGGC  700

SA-01         700  GAAGGCAGCC ACCTGGTCCA CTTCTGACGC TGAGGCGCGA AAGCGTGGGG AGC**ACCGG ATTAGATACC CGGGTAGTCC ACGCCCTAAA CGATGCGCGC  799
Kieft et al   701  GAAGGCAGCC ACCTGGTCCA CTTCTGACGC TGAGGCGCGA AAGCGTGGGG AGCAAACCGG ATTAGATACC CGGGTAGTCC ACGCCCTAAA CGATGCGCGC  800

SA-01         800  TAGGTCTTTG GGGTTTACCT GGGGGCCGAA GCCAACGCGT TAAGCGCGCC GCCTGGGGAG TACGGCCGCA AGGCTGAAAC TCAAAGGAAT TGACGGGGGC  899
Kieft et al   801  TAGGTCTTTG GGGTTTACCT GGGGGCCGAA GCCAACGCGT TAAGCGCGCC GCCTGGGGAG TACGGCCGCA AGGCTGAAAC TCAAAGGAAT TGACGGGGGC  900

SA-01         900  CCGCACAAGC GGTGGAGCAT GTGGTTTAAT TCGAAGCAAC GCGAAGAACC TTACCAGGCC TTGACATGCT AGGGGACCTA GGTGAAAGCC TGGGGTACCC  999
Kieft et al   901  CCGCACAAGC GGTGGAGCAT GTGGTTTAAT TCGAAGCAAC GCGAAGAACC TTACCAGGCC TTGACATGCT AGGGGACCTA GGTGAAAGCC TGGGGTACCC  1000

SA-01         1000 GCGAGGGAGC CCTAGCACAG GTGCTGCATG GCCGTCGTCA GCTCGTGTCG TGAGATGTTG GGTTAAGTCC CGCAACGAGC GCAACCCCTG CCCTTAGTTG  1099
Kieft et al   1001 GCGAGGGAGC CCTAGCACAG GTGCTGCATG GCCGTCGTCA GCTCGTGTCG TGAGATGTTG GGTTAAGTCC CGCAACGAGC GCAACCCCTG CCCTTAGTTG  1100

SA-01         1100 CCAGCGGGAT AGGCCGGGCA CTCTAAGGGG ACTGCCTGCG AAAGCAGGAG GAAGGCGGGG ACGACGTCTG GTCATCATGG CCCTTACGGC CTGGGCGACA  1199
Kieft et al   1101 CCAGCGGGAT AGGCCGGGCA CTCTAAGGGG ACTGCCTGCG AAAGCAGGAG GAAGGCGGGG ACGACGTCTG GTCATCATGG CCCTTACGGC CTGGGCGACA  1200

SA-01         1200 CACGTGCTAC AATGCCCACT ACAGAGCGAG GCGACCCAGT GATGGGGAGC GAATCGCAAA AAGGTGGGCG TAGTTCGGAT TGGGGTCTGC AACCCGACCC  1299
Kieft et al   1201 CACGTGCTAC AATGCCCACT ACAGAGCGAG GCGACCCAGT GATGGGGAGC GAATCGCAAA AAGGTGGGCG TAGTTCGGAT TGGGGTCTGC AACCCGACCC  1300

SA-01         1300 CATGAAGCCG GAATCGCTAG TAATCGCGGA TCAGCCATGC CGCGGTGAAT ACGTTCCCGG GCCTTGTACA CACCGCCCGT CACGCCATGG GAGCGGGTTC  1399
Kieft et al   1301 CATGAAGCCG GAATCGCTAG TAATCGCGGA TCAGCCATGC CGCGGTGAAT ACGTTCCCGG GCCTTGCACA CACCGCCCGT ---------- ----------  1380

SA-01         1400 TACCCGAAGT CGCCGGGAGC CTTAGGGCAG GCGCC 1434
Kieft et al   1380 ---------- ---------- ---------- ----- 1380
```

Figure 2.5: Alignment of the 16S rDNA sequence obtained with *Thermus scotoductus* SA-01 NCBI: AF020205 (Kieft *et al.*, 1999).

2.3.2 Cr(VI) reduction during aerobic growth

The Cr(VI) tolerance and reduction capacity of *Thermus scotoductus* SA–01 during aerobic growth in a complex organic medium was determined by adding varying concentrations of Cr(VI) to the culture medium during inoculation (lag–phase) and the logarithmic phase of growth respectively. When Cr(VI) was added during inoculation, SA–01 actively grew in the presence of up to 0.3 mM Cr(VI) and Cr(VI) reduction began immediately (Figures 2.6 & 2.7), as evidenced by a decrease in yellow colour in the medium. No insoluble Cr(VI) precipitation or white colloidal suspensions were evident, as insoluble Cr(III) complexes such as $Cr(OH)_3$ and Cr_2O_3 are only formed in the absence of substances with which Cr(III) can form soluble complexes or insoluble salts (Pourbaix, 1966). At these concentrations, the specific growth rate decreased with increasing chromate concentrations (Figure 2.6), however a higher rate of Cr(VI) reduction coincided with higher initial Cr(VI) concentrations (Figure 2.7).

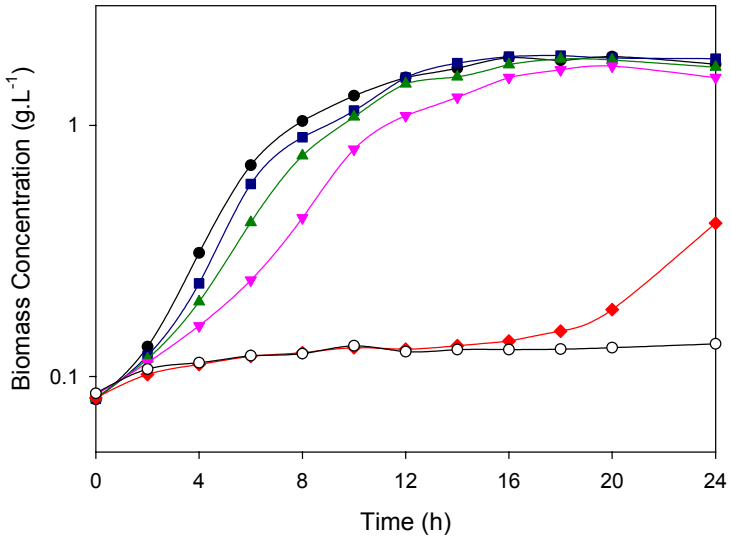

Figure 2.6: Growth of *Thermus scotoductus* SA–01 in TYG medium (●) amended with 0.1 mM (■), 0.2 mM (▲), 0.3 mM (▼), 0.5 mM (♦) and 1 mM (○) of Cr(VI) during inoculation (t = 0).

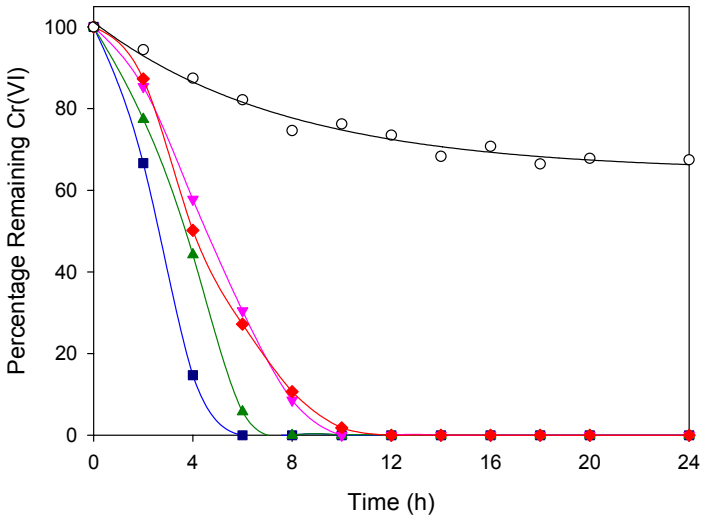

Figure 2.7: Cr(VI) reduction during growth of *Thermus scotoductus* SA–01 when amended with 0.1 mM (■), 0.2 mM (▲), 0.3 mM (▼), 0.5 mM (♦) and 1 mM (○) Cr(VI) at time of inoculation (t = 0).

When grown in the presence of 0.5 mM Cr(VI), a 16 h lag phase was observed during which the cells actively reduced all the Cr(VI) in the growth medium (Figure 2.6), after which growth was initiated. In 2000, Nepple *et al*. showed that *Rhodobacter sphaeroides* starts growing only after a certain amount of the chromate added has been reduced, as the cells have to partially detoxify their environment before growth is initiated. Concentrations of 1 mM Cr(VI) proved to be toxic as growth and enzymatic reduction of the Cr(VI) was completely inhibited.

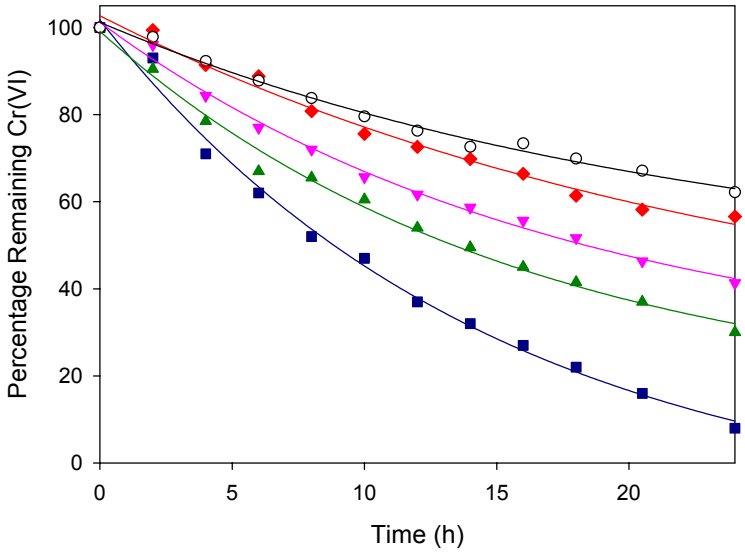

Figure 2.8: Chemical Cr(VI) reduction by the complex organic media (TYG) amended with 0.1 mM (■), 0.2 mM (▲), 0.3 mM (▼), 0.5 mM (♦) and 1 mM (○) Cr(VI).

Abiotic Cr(VI) reduction resulted from the medium constituents (tryptone and yeast extract) but was significantly less than that observed during growth in 0.5 mM Cr(VI) and less (Figure 2.8).

Changes in pH and oxidation–reduction potential (ORP) during growth on 0.2 mM Cr(VI) were compared to control cultures containing no Cr(VI). In cultures containing 0.2 mM Cr(VI) the pH increased from approximately 6.5 to 8.8 during 24 h of growth (Figure 2.10) similar to the control containing no Cr(VI) (Figure 2.9). During exponential growth, both the cultures exhibited a rapid drop of oxidation–reduction potential (ORP) from about +150 to –250 mV (Figures 2.9 & 2.10). Cr(VI) reduction was observed throughout this ORP range, which is in accordance with Wang & Xiao (1995) who also found no correlation between Cr(VI) reduction and the ORP values of the culture medium. No definite redox potential requirement has been made for bacterial Cr(VI) reduction as varying ORP requirements with different bacteria have been found (Gvozdyak *et al*., 1986; Llovera *et al*., 1993B; Shen & Wang, 1994).

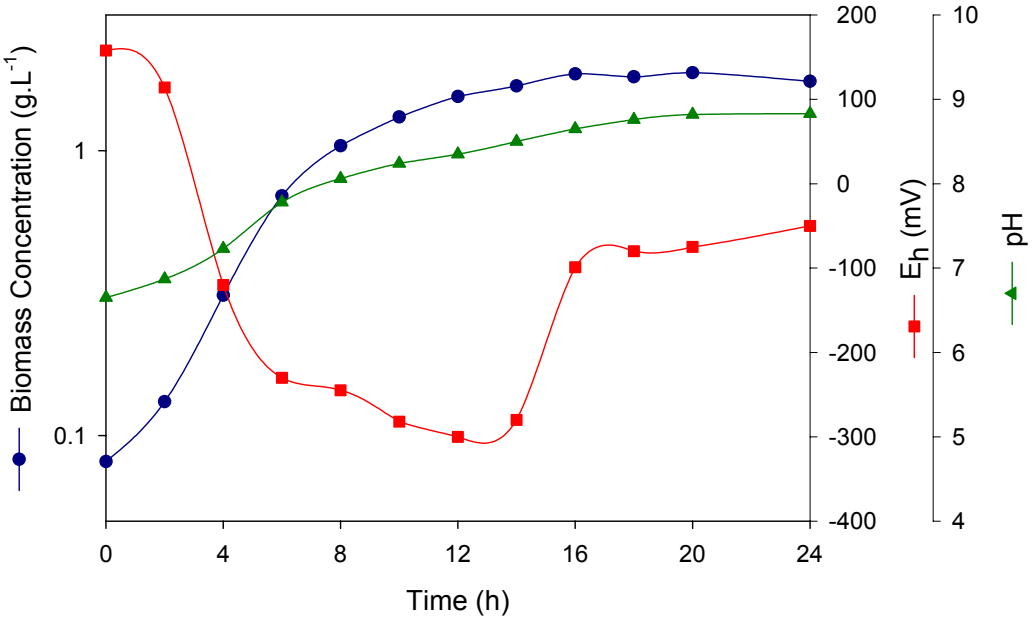

Figure 2.9: Growth of *Thermus scotoductus* SA–01 (●) and associated changes in pH (▲) and E_h (■) in TYG medium.

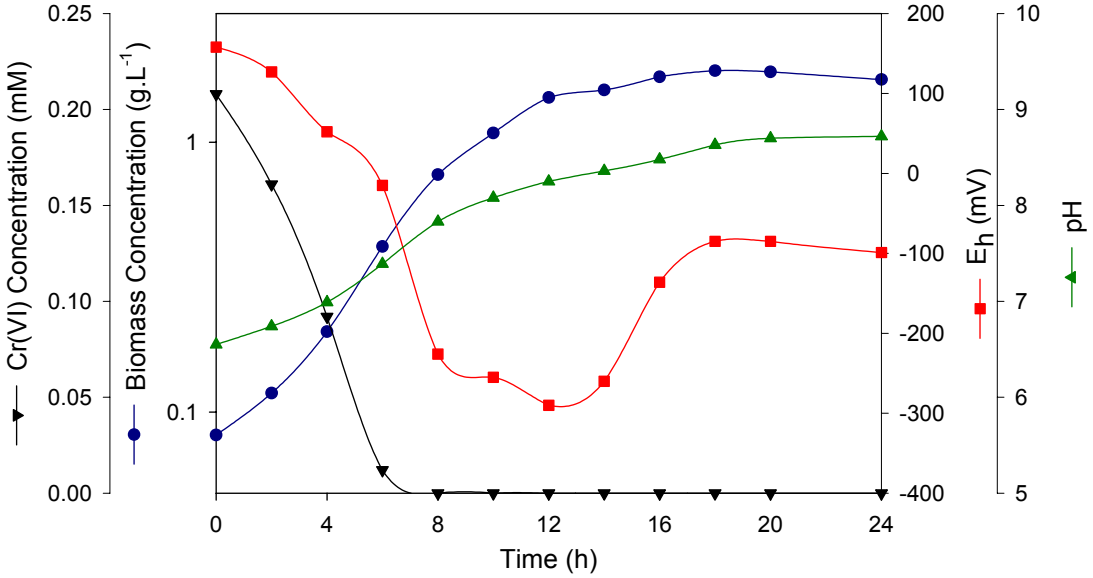

Figure 2.10: Growth of *Thermus scotoductus* SA–01 (●) in TYG medium containing 0.2 mM Cr(VI) and changes in chromate concentration (▼), pH (▲) and E_h (■).

The effect of chromate on logarithmic phase cells was assessed by the addition of chromate after 6 h of growth (Figure 2.11). Up to 0.5 mM chromate did not adversely affect the growth of SA–01, whereas at 1 mM Cr(VI), growth was inhibited, but active reduction of Cr(VI) was still observed (Figure 2.12). Chromate reduction slowed significantly after approximately 12 h of growth which is probably as a result of the bacterial cells entering the stationary phase. Wang & Shen (1997) analyzed Cr(VI) reduction of different genera of bacteria and demonstrated that the batch cultures had a finite capacity for Cr(VI) reduction (maximum amount of Cr(VI) that a batch culture can reduce). The batch cultures reduced Cr(VI) at rates which decreased progressively with the amount of Cr(VI) reduced and ceased whenever the maximum capacity was reached regardless of subsequent cell growth.

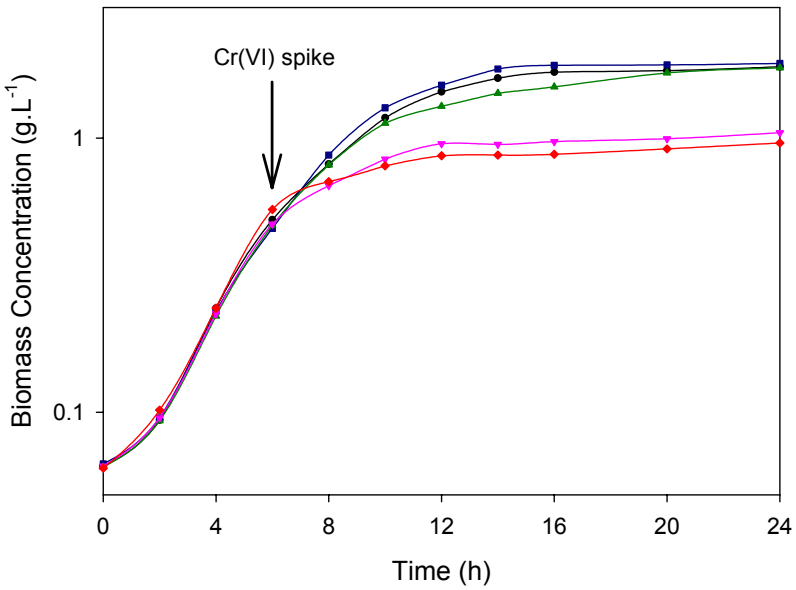

Figure 2.11: Growth of *Thermus scotoductus* SA–01 in TYG medium (●) when spiked with 0.2 mM (■), 0.5 mM (▲), 1 mM (▼) and 10 mM (♦) Cr(VI) during mid–exponential growth.

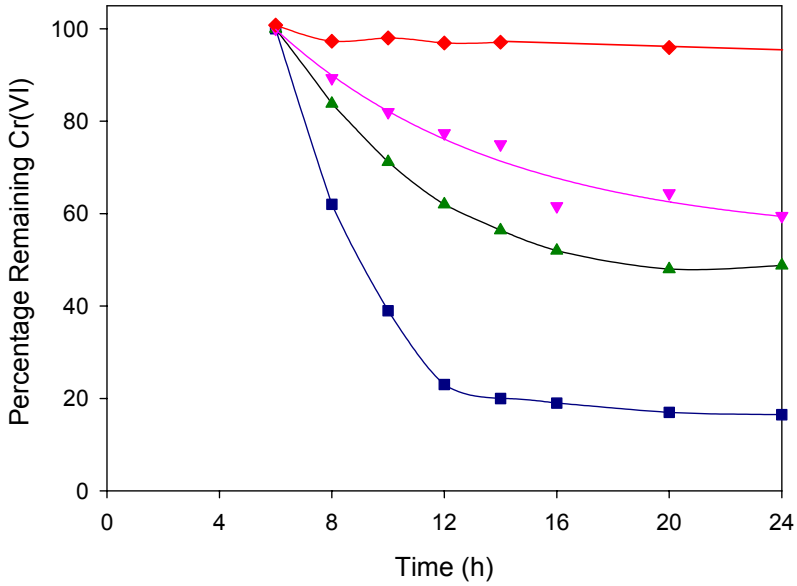

Figure 2.12: Cr(VI) reduction during growth of *Thermus scotoductus* SA–01 when spiked with 0.2 mM (■), 0.5 mM (▲), 1 mM (▼) and 10 mM (♦) Cr(VI) during mid–exponential growth (t = 6).

2.3.3 Cr(VI) reduction under non–growth conditions

To determined whether SA–01 could reduce Cr(VI) under conditions that do not favor cell growth, washed logarithmic phase cells were incubated with only 10 mM pyruvate and 0.1 mM chromate in a MOPS buffer (pH 7, 65°C). Although Cr(VI) reduction was observed during the growth phase, cell growth is not necessarily required for Cr(VI) reduction. Resting cell suspensions, both with and without pyruvate as an electron donor, reduced the chromate (Figure 2.13) starting immediately after the addition of Cr(VI). However, the rate of Cr(VI) reduction was significantly higher for cell suspensions containing electron donor.

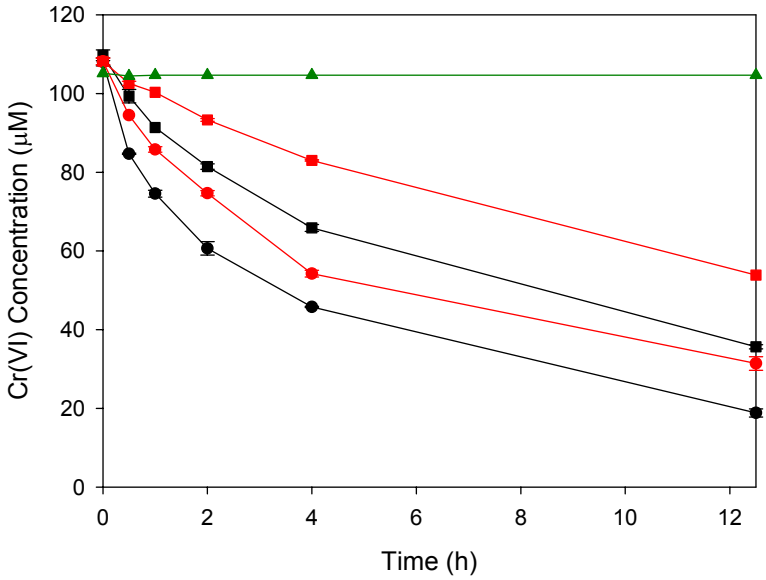

Figure 2.13: Cr(VI) reduction by resting cells of *Thermus scotoductus* SA–01 monitored over time when grown in TYG medium without electron donor (■) and pyruvate as electron donor (●) or grown in TYG medium containing 0.2 mM Cr(VI) without electron donor (■) and pyruvate as electron donor (●). Cell–free control with pyruvate showed no Cr(VI) reduction (▲). Error bars indicate standard deviations.

The ability of bacteria to reduce metal ions in the absence of exogenous electron donor has been observed for other metal–reducing microorganisms such as *Cellulomonas* (Sani *et al*., 2002), *Deinococcus radiodurans* R1 (Fredrickson *et al*., 2000) and *Pseudomonas* sp CRB5 (McLean & Beveridge, 2001). The cell–free pyruvate controls showed no Cr(VI) reduction (Figure 2.13). SA–01 appears to use endogenous electron donors, stored as energy storage compounds during growth, for metal reduction. Sani and co–workers (2002) observed metal reduction by a *Cellulomonas* isolate in the absence of exogenous electron donor and suggested that endogenous electron donors (either through internal reserves or by endogenous decay) might be used for metal reduction. Microorganisms are known to accumulate energy storage polymers under growth conditions (Boe & Lovrien, 1990) and cells often undergo endogenous metabolism under starvation conditions (Van Loosdrecht & Henze, 1999) which may supply electrons for metal reduction.

Whole–cell reductions with cells grown in TYG medium without Cr(VI), using pyruvate as an electron donor, reduced almost 20% of the chromate within 30 min. The rate of Cr(VI) reduction however slowed over time. This phenomenon has been frequently observed with whole cells (Tucker *et al*., 1998). This might result from a decrease in Cr(VI) concentrations (Schmieman *et al*., 1998) or a combination of substrate decrease and inhibition by Cr(VI) (Yamamoto *et al*., 1993) due to the mutagenic and toxic effects of Cr(VI). Re–spiking with electron donor did not increase the chromate reduction rates of these cultures.

Whole cell reduction with cells grown in TYG medium containing 0.2 mM Cr(VI) showed lower reduction rates. Chromate–reducing activity was thus independent of whether chromate was present during growth and thus not induced by chromate. The chromate reductase may thus either be constitutively expressed or a fortuitous reaction by an enzyme with another primary physiological function. Since Cr(VI) is primarily of anthropogenic origin, several researchers have proposed that chromate reduction might be the serendipitous activity of enzymes with other primary substrates (Clark, 1994; Ishibashi *et al*., 1990; Park *et al*., 2000) and that these enzymes are often constitutively expressed (Bopp & Ehrlich, 1988; Ishibashi *et al*., 1990; Cervantes, 1991).

It has also been suggested that some metal–bacterium interactions in resting cells are mediated via cell activities induced during heavy–metal–free pregrowth (Macaskie *et al*., 1992). Inducible resistance mechanisms may also come into play as a decreased uptake of chromate most likely protects the cells. This phenomenon is however not consistently observed for chromate reducing bacteria as Bopp & Ehrlich (1988) showed that *Pseudomonas fluorescens* cells are equally active in reducing chromate whether or not they had been grown in the presence of chromate.

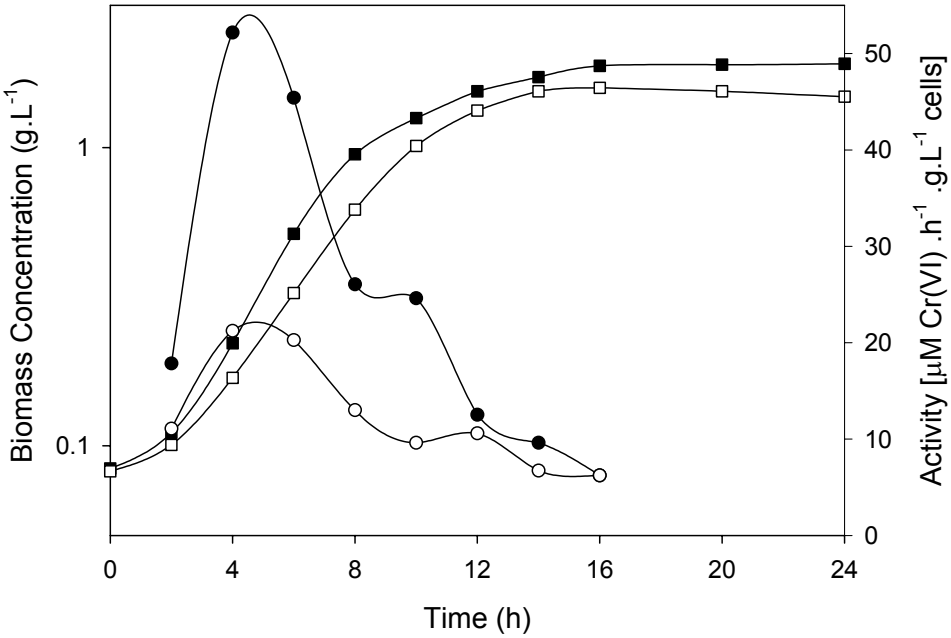

Figure 2.14: Growth of *Thermus scotoductus* SA–01 in TYG medium without (■) and with 0.2 mM Cr(VI) (□) and their respective activity [(●) and (○)] of whole–cells under resting conditions during different growth phases.

The chromate reducing capability of cells in different phases of growth was determined by harvesting cells at different stages of growth, and assessing their ability to reduce Cr(VI) under non–growth conditions. For both cultures [grown in TYG and TYG containing 0.2 mM Cr(VI)] maximum chromate reducing ability was reached after 5 h of growth, which corresponds to mid–exponential growth phase (Figure 2.14). Thereafter, the cells rapidly lose their Cr(VI) reducing ability; up to 50% less activity after only 3 h of further growth (late–exponential growth phase).

2.3.4 Factors affecting chromate reduction

2.3.4.1 Optimum temperature and pH

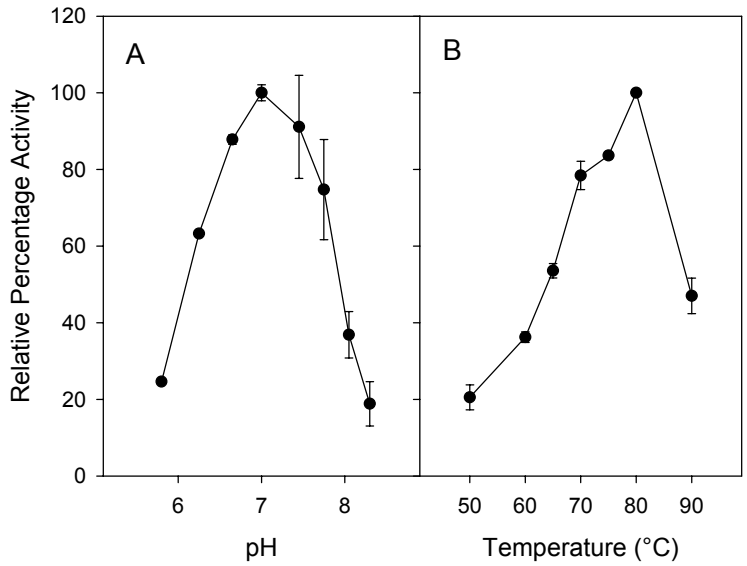

Figure 2.15: Effect of pH (A) and temperature (B) on Cr(VI) reduction by whole–cells under non–growth conditions. Error bars represent standard deviations.

When the reduction of Cr(VI) was studied using washed whole cells with pyruvate as an electron donor as described in section 2.2.5.1, the reduction occurred at pH 5.5 to 8.5. In the MES–MOPS–Bicine buffer, the optimum activity for chromate reduction occurred at a pH of 7 (Figure 2.15A). Reduction also occurred over a wide temperature range (Figure 2.15B), with an optimum temperature of 80°C. Optimal pH and temperature for Cr(VI) reduction generally coincides with the optimal growth conditions however, in 1999, Kieft *et al.* found that the optimum pH and temperature for SA–01 growth and iron reduction during growth was 7 and 65°C respectively.

2.3.4.2 Effect of electron donor

A variety of organic compounds can serve as electron donors for chromium reduction by chromate–reducing bacteria (Wang & Shen, 1995), with the majority of known electron donors being natural aliphatic compounds, mainly low–molecular–weight carbohydrates, amino acids and fatty acids. The reduction of Cr(VI) using washed whole cells of SA–01

was supported by a variety of organic electron donors (Figure 2.16), with pyruvate being the most effective electron donor for Cr(VI) reduction.

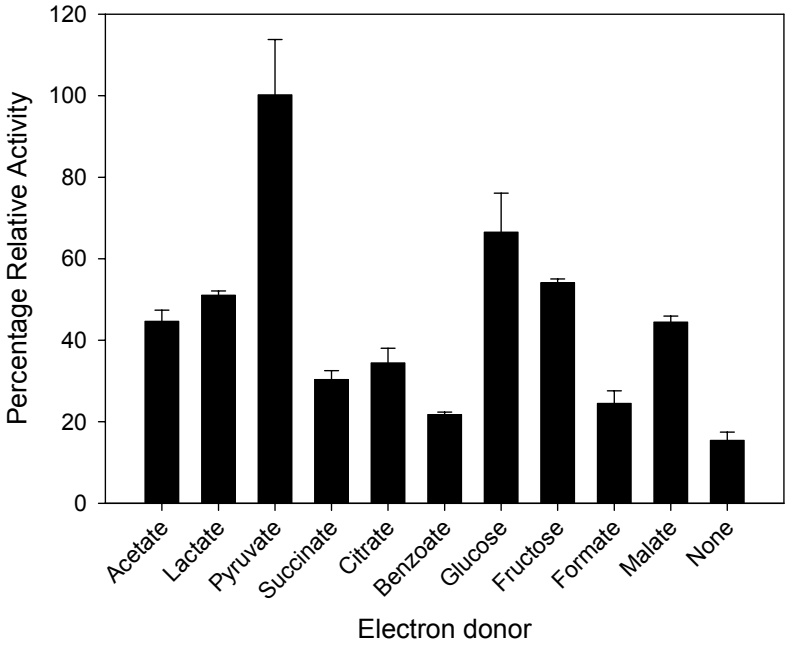

Figure 2.16: Assessment of various organic compounds as electron donor for Cr(VI) reduction by whole–cells under non–growth conditions. Error bars represent standard deviations.

2.3.4.3 Effect of metabolic inhibitors

Reduction was strongly inhibited by both sodium fluoride and iodoacetic acid (Figure 2.17A) when glucose was used as an electron donor during Cr(VI) reduction with washed whole–cells. Sodium fluoride and iodoacetate are both inhibitors of glycolysis through the inhibition of enolase and glyceraldehydes–3–phosphate dehydrogenase respectively (Mathews *et al.*, 2000). Using pyruvate as an electron donor, Cr(VI) was also strongly inhibited by both fluoroacetate and sodium cyanide (Figure 2.17B). Fluoroacetate is an inhibitor of the Krebs–cycle as it strongly inhibits aconitase (Mathews *et al.*, 2000). The inhibition of Cr(VI) reduction by sodium cyanide suggests the involvement of the electron transport system by wholecells during Cr(VI) reduction.

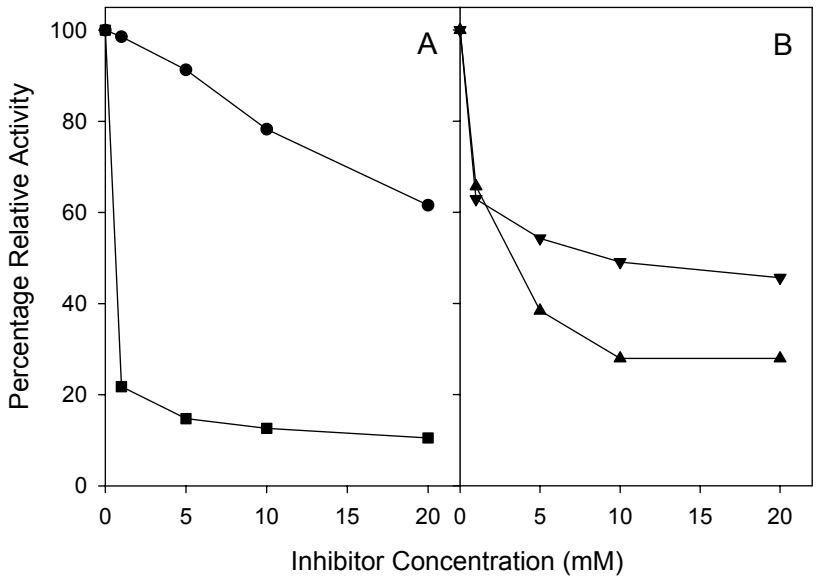

Figure 2.17: Effect of iodoacetic acid (■) and sodium fluoride (●) (A), and sodium cyanide (▲) and sodium fluoroacetate (▼) (B) on Cr(VI)–reducing activity of whole–cells under resting conditions, using either glucose (A) or pyruvate (B) as an electron donor.

2.3.4.4 Steady–state kinetics

Cr(VI) reduction followed saturation kinetic patterns, where the activity increased in proportion to the concentration of pyruvate and Cr(VI) (Figure 2.18) with the chromate reduction rates approaching a maximum at higher concentrations. As initial rates were used, the chromate reducing capability or transformation capacity was not taken into account.

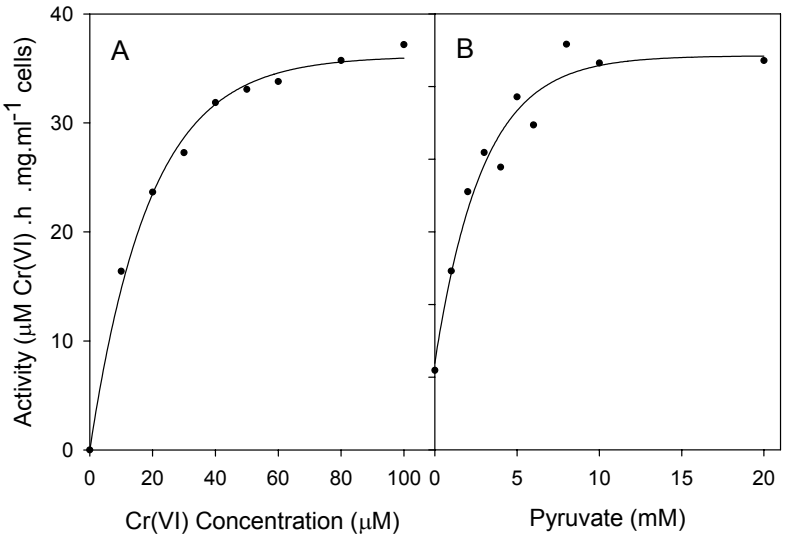

Figure 2.18: Effect of Cr(VI) (A) and pyruvate (B) concentrations on the Cr(VI)–reducing activity of whole–cells under non–growth conditions.

2.3.4.5 Effect of complexing agents

The presence of complexing agents is not required for Cr(VI) reducing activity and is virtually unaffected by EDTA and NTA up concentrations of 20 mM (Figure 2.19). At very high concentration (50 mM), the cells aggregate and a concomitant decrease in activity is seen. The only occurrence of an obligatory requirement for a complexing agent to enable Cr(VI) reduction was reported for *Desulfovibrio vulgaris* (Mabbett *et al*., 2002), and suggested that as Cr(III)–chelate complexes are extremely inert kinetically, an equilibrium consideration may be important.

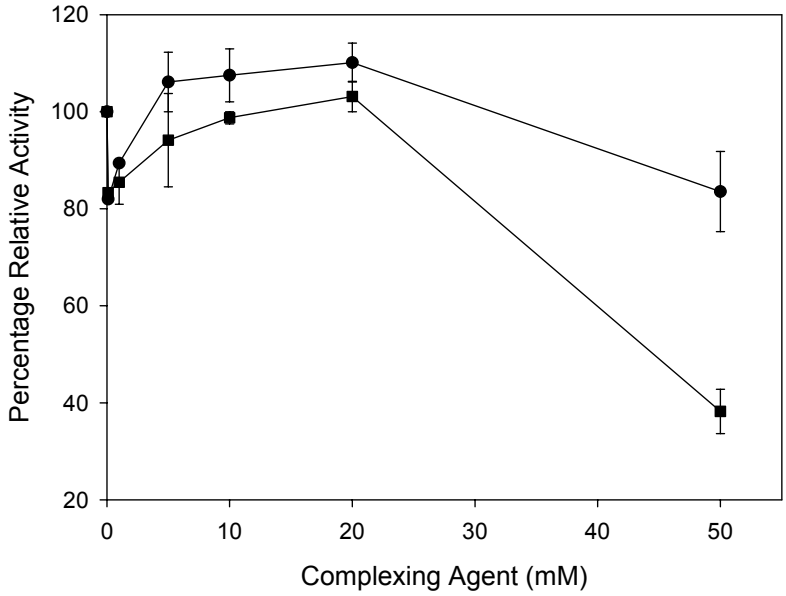

Figure 2.19: Effect of the complexing agents EDTA (●) and NTA (■) on the Cr(VI)–reducing activity of whole–cells under non–growth conditions. Error bars represent standard deviations.

2.3.5 Localization of the chromate reductase

The cell walls of many bacteria are made of peptidoglycan, which are heteroglycan chains linked to peptides. The heteroglycan component is composed of alternating residues of N–acetylglucosamine (GlcNAc) and N–acetylmuramic acid (MurNAc) joined by β–(1→4) linkages (Horton *et al*., 1996). The first cell fractionation step involved the action of hen egg white lysozyme (Sigma–Aldrich) for the preparation of spheroplasts and a periplasmic fraction. Lysozyme specifically catalyses hydrolysis of the glycosidic bond between C–1 of a MurNAc residue and the oxygen atom of C–4 of a GlcNAc residue (Horton *et al*., 1996). Sonification of the spheroplasts resulted in breaking of the spheroplasts, yielding a cytoplasmic (soluble) fraction and a membrane (pellet) fraction after ultracentrifugation (Kaufmann & Lovley, 2001). Thus, fractionation resulted in a periplasmic, membrane and cytosolic (soluble) fraction, of which the cytosolic contained 90% of the total aerobic chromate reducing activity (Table 2.1), suggesting a soluble NADH–dependent Cr(VI) reductase. The crude cytoplasmic fraction catalyzed the reduction of Cr(VI) with NADH as the electron donor at a rate of 1.08 mmol L^{-1} Cr(VI) h^{-1} ml^{-1} extract. The fraction also reduced Cr(VI) under anaerobic conditions, but an additional strictly anaerobic chromate

reduction mechanism was present in the membrane fraction. Both of these Cr(VI) reductases required NADH for activity. The aerobic Cr(VI) reduction activity of bacteria is typically associated with soluble proteins which require NADH as an electron donor (Wang and Shen, 1995).

Table 2.1: Localization of the aerobic Cr(VI) reductase activity.

Fraction	Chromate reductase Activity* (% of total)	Heat-killed Control Activity*
Membrane	0.031 (2.6)	0.082
Periplasm	0.089 (7.4)	0.151
Cytoplasm	1.082 (90)	0.104

* Activity given as mmol L^{-1} Cr(VI) reduced per hour per ml crude fraction

2.4 CONCLUSIONS

The results from this study demonstrate that *Thermus scotoductus* SA–01 has the ability to readily reduce Cr(VI) under aerobic conditions under both growth and non–growth conditions, in addition to the anaerobic Cr(VI) reduction under non–growth anaerobic conditions (Kieft *et al*., 1999). It is also shown that this bacterium can tolerate up to 0.5 mM Cr(VI) when grown in a complex organic medium. Data indicates that the chromate reduction activity might be constitutively expressed, as Cr(VI) in the growth medium is not required for subsequent Cr(VI)–reduction by whole–cells under resting conditions. No correlation could be drawn between the redox–potential or presence of chelating agents and the Cr(VI)–reducing ability. The aerobic reduction of Cr(VI) by SA–01 appears to be enzymatic as it is inhibited by a variety of metabolic inhibitors when whole–cell suspensions were used and as Cr(VI)–reduction is catalyzed by cell extracts using NADH as an electron donor. Whether this enzymatic reduction is a fortuitous reaction by an enzyme with another primary physiological function however still needs to be investigated.

The rate of Cr(VI) reduction was dependent on pH, temperature an initial Cr(VI) concentrations. SA–01 chromate reduction was shown to be optimal at a temperature of 80°C; however, this is not the first description of a thermophilic Cr(VI) reductase. Reduction of Cr(VI) by a thermophilic bacterium at 65°C (Zhang *et al*., 1996) and a hyperthermophilic archaea at 100°C (Kashefi & Lovley, 2000) has been reported.

The effect of other metals on the ability of SA–01 also warrants further investigation to assess its ability for bioremediation purposes. Its ability to tolerate and reduce various other toxic metals including Fe(III), Mn(IV), Co(III)–EDTA, Tc(VII) and U(VI) (Kieft *et al*., 1999) however lends great promise.

CHAPTER 3

PURIFICATION AND CHARACTERIZATION OF THE SOLUBLE Cr(VI) REDUCTASE

3.1 INTRODUCTION

Although researches have proposed that chromate reduction protects against chromate toxicity and serves as an additional "resistance" mechanism (Ackerley *et al*., 2004A; Gonzalez *et al*., 2003), the ability to reduce Cr(VI) is an independent mechanism from chromate resistance.

Enzymes capable of Cr(VI) reduction are often referred to in the literature as "chromate reductases". Bacterial Cr(VI) reduction can occur under anaerobic and/or aerobic conditions, where the aerobic Cr(VI) reduction activity is generally attributed to soluble proteins with NADH as an electron donor as either a requirement or for enhanced activity (Wang & Shen, 1995). By virtue of its structural similarity with sulphate, the oxyanion chromate is actively transported across biological membranes in bacteria via the sulphate transport system (Ohtake *et al*., 1987; Nies *et al*., 1989). Intracellular reduction can occur through various physiological reducing agents to transiently formed Cr(V) intermediates that redox-cycles, causing oxidative damage through free radicals and reactive oxygen species (ROS) formation (Shi & Dalal, 1990C; Liu & Shi, 2001). Appropriate cytoplasmic Cr(VI) reductases could pre-empt the formation of ROS, thereby protecting cells against Cr(VI) (Ackerley *et al*., 2004A; Gonzalez *et al.*, 2005)

Thus far, Cr(VI) reductases purified and characterized have been from mesophilic origins without extensive thermostability. This chapter describes the purification and characterization of the cytoplasmic chromate reductase from *Thermus scotoductus* SA–01.

3.2 MATERIALS AND METHODS

3.2.1 Bacterial strain and culture conditions

For protein purification *Thermus scotoductus* strain SA–01 was cultured aerobically in a complex organic medium, TYG (5 g tryptone [Biolab], 3 g yeast extract [Saarchem] and 1 g glucose in 1 L ddH_2O) at 65°C, pH 7.0, with aeration (200 rpm). SA–01 was cultured without added Cr(VI) until mid–exponential growth phase.

3.2.2 Preparation of subcellular fractions

Subcellular fractions were prepared using a modification of the method of Gaspard *et al*. (1998), as described by Kaufmann & Lovley in 2001 (section 2.2.6).

3.2.3 Purification of soluble Cr(VI) reductase

All purification steps were carried out at room temperature and enzyme preparations were stored at 4°C without any loss of activity. Purification to homogeneity entailed five chromatographic steps: anion–exchange, hydrophobic interaction, dye–affinity and size exclusion chromatography, using the ACTA Prime Purification System (Amersham Biosciences).

3.2.3.1 Anion–exchange chromatography

The cytoplasmic fraction (crude) was applied to a DEAE–Toyopearl 650M column (6 x 2.5 cm; TOSOH Corporation) equilibrated with 20 mM MOPS–NaOH buffer (pH 7) containing 5 mM NaCl. The Cr(VI) reductase was first eluted at a flow rate of 5 $ml.min^{-1}$ with 50 mM NaCl in the same buffer. Strongly bound proteins were then eluted with 1 M NaCl. The chromate reductase activity eluted as a single activity peak which were pooled and concentrated to a fifth the volume by ultrafiltration on a 10 kDa NMWL membrane (Millipore) in an Amicon stirrer cell system. 20 mM MOPS–NaOH buffer were added to the concentrate to re–adjust the final volume to the original amount, thereby decreasing the NaCl concentration in the sample to approximately 5 mM. This sample was re–applied to

the regenerated DEAE–Toyopearl column, again equilibrated with 20 mM MOPS–NaOH buffer (pH 7) containing 5 mM NaCl. The enzyme was eluted with a linear gradient of 5 – 100 mM NaCl (400 ml) in the same buffer (5 ml.min^{-1} flow rate). Fractions containing the Cr(VI) reductase activity eluted at about 30 mM NaCl. Fractions with high Cr(VI) reduction activity were pooled and used in the hydrophobic interaction step.

3.2.3.2 Hydrophobic–interaction chromatography

Solid ammonium sulphate was added to the sample to a final concentration of 0.4 M $(NH_4)_2SO_4$ and applied to a phenyl-toyopearl 650M column (6 x 2.5 cm, TOSOH Corporation) equilibrated with 20 mM MOPS-NaOH (pH 7) containing 0.4 M $(NH_4)_2SO_4$. Bound protein was eluted with a linear gradient of 0.4 to 0 M $(NH_4)_2SO_4$ (300 ml at 5 ml.min^{-1} flow rate). Fractions containing Cr(VI) reductase activity eluted at approximately 0.25 M $(NH_4)_2SO_4$. The active fractions were combined and dialyzed overnight against 20 mM MOPS-NaOH buffer using 7 kDa MWCO SnakeSkin pleated dialysis tubing (Pierce).

3.2.3.3 Dye-affinity chromatography

The dye-affinity chromatography step employed a Blue Sepharose CL–6B (Sigma–Aldrich) column (17 x 1.3 cm) equilibrated with 20 mM MOPS-NaOH (pH 7). Blue Sepharose CL–6B is Cibacron Blue attached to Sepharose CL–6B. After binding of the dialyzed sample, the column was washed sequentially with 100 ml 20 mM MOPS-NaOH containing 0.1 M NaCl, 100 ml 20 mM MOPS-NaOH and 100 ml 20 mM MOPS-NaOH containing 10 mM NAD^+. The enzyme was then eluted with 20 mM MOPS-NaOH containing both 10 mM NAD^+ and 0.1 M NaCl. Active fractions were pooled and concentrated to 3 ml using ultrafiltration on a 10 kDa NMCO cellulose membrane Vivaspin column (VivaScience).

3.2.3.4 Size-exclusion chromatography

The final purification step was size–exclusion chromatography, whereby the native molecular weight (M_r) of the chromate reductase was also determined. The concentrate was loaded onto a Sephacryl S-100HR column (2.6 x 65 cm; Sigma-Aldrich), equilibrated with 20 mM MOPS–NaOH (pH 7) containing 50 mM NaCl. Proteins were eluted with the same buffer at a flow rate of 0.5 ml.min^{-1}. Cytochrome c (12.4 kDa), chymotrypsin (25

kDa), bovine serum albumin (66 kDa) and Blue Dextran (2 000 kDa) were used as molecular weight standards (Figures 3.1 & 3.2).

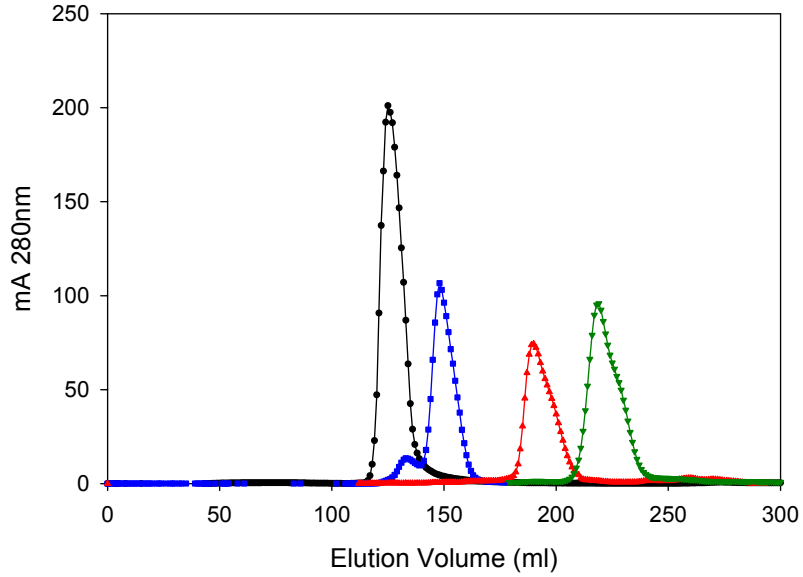

Figure 3.1: Elution profile from Sephacryl S-100HR column calibration using gel filtration molecular weight markers consisting of Blue Dextran [2 000 kDa (●)], bovine serum albumin [66 kDa (■)], chymotrypsin [25 kDa (▲)] and cytochrome c [12.4 kDa (▼)].

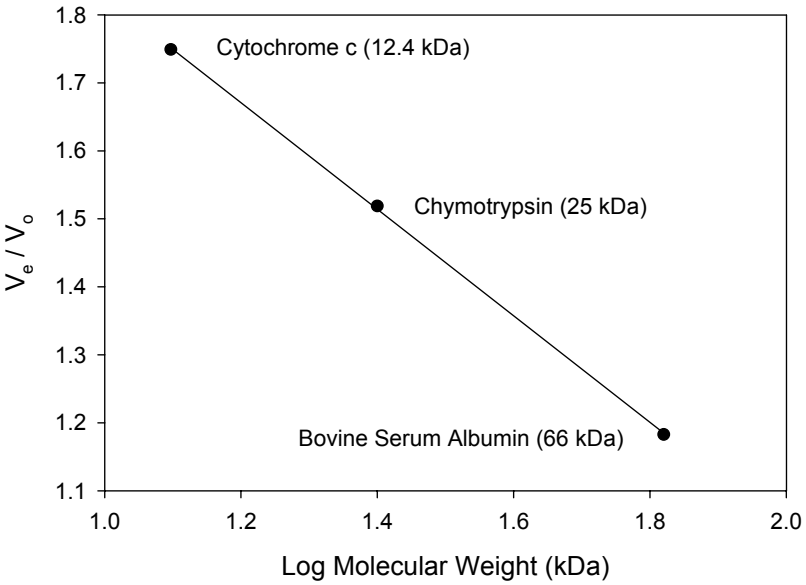

Figure 3.2: Calibration curve of Sephacryl S-100HR relating molecular weight to elution volume. The void volume (V_o) was calculated using the elution volume of Blue Dextran (2 000 kDa).

3.2.4 Characterization of purified enzyme

3.2.4.1 Effect of pH on enzyme activity

The effect of pH on the activity of the purified chromate reductase was measured under the standard conditions by incubation of the reaction mixture at various pHs at 65°C. The pH range was constructed by adjusting the pH of an equimolar 20 mM MES–MOPS–Bicine buffer with HCl or NaOH. Assays were done in triplicate with blank rates taken at each assayed pH value.

3.2.4.2 Effect of temperature on enzyme activity

The optimum temperature for the purified chromate reductase was determined by incubating the reaction mixture at different temperature ranging from 40°C to 80°C under the standard assay conditions at pH 7.0. Assays were done in triplicate with blank rates taken at each assayed temperature value.

3.2.4.3 Effect of metals and EDTA

The effect of various divalent metals as well as the metal-chelator, EDTA, on the activity of the cytoplasmic chromate reductase were determined by including 10 mM of each metal or chelator into the standard reaction mixture.

3.2.4.4 Steady–state kinetics

Kinetic constants were determined at a pH of 6.5 and 65°C by measurement of initial velocities at various concentrations of hexavalent chromium and NAD(P)H. Apparent maximum initial velocities (V_{max}) and apparent Michaelis constant (K_m) were determined from non–linear regressions of Michaelis–Menten plots using SigmaPlot 8.0 (SPSS Inc.).

3.2.4.5 Stoichiometric analysis

NADH consumption was related to Cr(VI) reduction, by measuring the oxidation of NADH through the decrease in absorbance at 340nm using a Beckman Coulter DU–800 spectrophotometer. NADH concentration was determined from A_{340nm} using the extinction coefficient 6.221 $mM.cm^{-1}$. Cr(VI) concentration was measured using the *s*–diphenylcarbazide method.

3.2.4.6 Alternative substrates

Alternative oxidants for the chromate reductase were assessed by monitoring NADH consumption as described above. NADH oxidase activity was determined under aerobic conditions allowing the oxidation of molecular oxygen. Flavin reduction activity was determined by including 0.5 mM FMN or FAD in a standard reaction mixture.

3.2.5 Analytical techniques

3.2.5.1 Standard enzyme assay

Chromate reductase activity was determined by measuring the decrease of hexavalent chromium. Cr(VI) was analysed by the *s*-diphenylcarbazide method as described by Urone (1955). Samples (0.3 ml) were withdrawn and added to 2.5 ml of a 0.12 M H_2SO_4 stock solution. 0.2 ml of the *sym*-diphenylcarbazide reagent (dissolved in acetone) was added to the reaction mixture to a final concentration of 0.01% (w/v). Absorbance was measured using a Spectronic GENESYS 5 spectrophotometer (Milton Roy Company) at 540 nm and chromate was quantified using a calibration curve relating chromate concentration to A_{540nm} (Figure 2.2). During purification the enzyme fractions were assayed in 1 ml reaction mixtures containing 20 mM MOPS–NaOH buffer containing 10 mM $CaCl_2$ (pH 7.0), 0.1 mM CrO_3, 0.3 mM NADH and 0.05 ml of the enzyme preparation at 65°C. One Unit is defined as the amount of enzyme required to reduce 1 nmol of Cr(VI) per minute.

3.2.5.2 Protein assay

Protein concentrations were determined using the bicinchoninic acid (BCA) method (Smith *et al*., 1985). BCA Protein Assay Kit (standard and enhanced method; Figures 2.3 & 3.3) and Micro BCA Protein Assay Kit (Figure 3.4) from Pierce (Rockford, IL, USA) was used according to the manufacturers instructions with bovine serum albumin (BSA) as standard (supplied with kit). During column chromatography, protein concentrations were estimated by measurement of A_{280nm}.

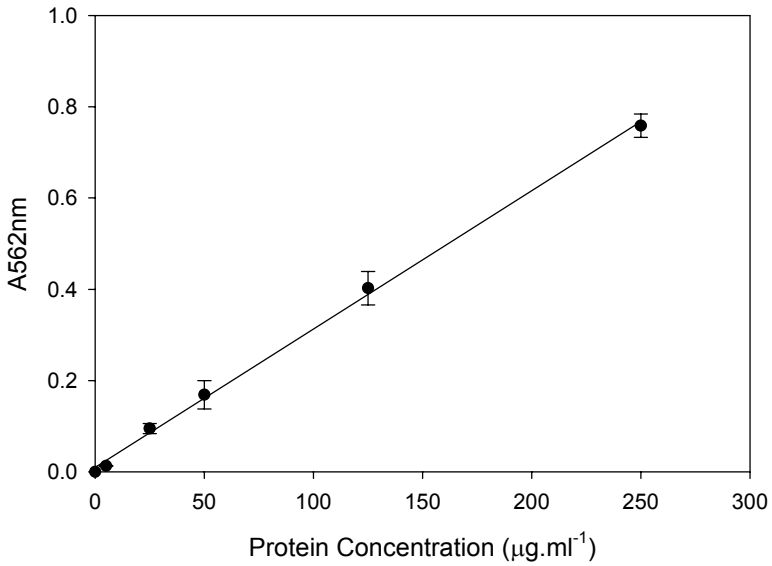

Figure 3.3: Standard curve for the BCA protein assay kit (Pierce) at 60°C (enhanced method) using BSA as protein standard. Error bars indicate standard deviation.

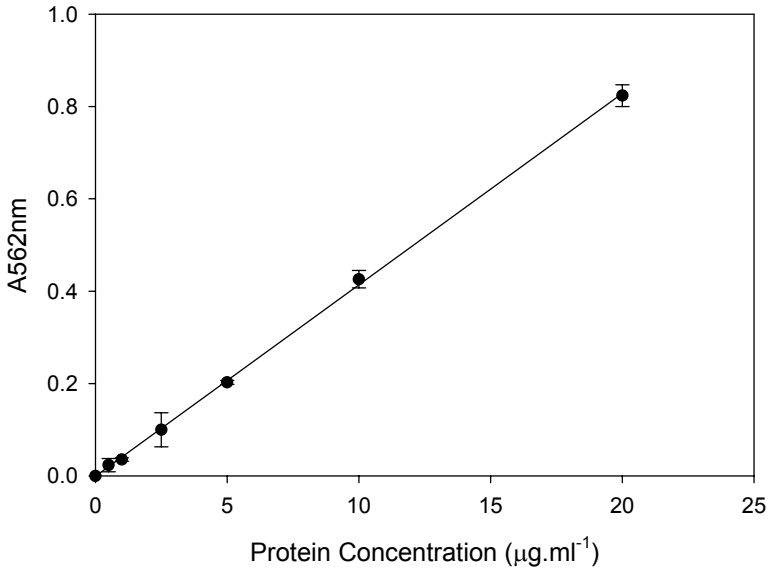

Figure 3.4: Standard curve for the Micro BCA protein assay kit (Pierce) at 60°C using BSA as protein standard. Error bars indicate standard deviation.

3.2.5.3 Gel electrophoresis

Electrophoresis under denaturing conditions or sodium dodecyl sulphate polyacrylamide gel electrophoresis (SDS-PAGE) was performed using the "Mighty Small" miniature slab gel electrophoresis unit, SE 200, from Hoefer Scientific Instruments. The protocol used was that described by Laemmli (1970) using a 10% resolving gel and 4% stacking gel. Precision Plus Protein Standards – Dual Color (BIO-RAD) was used as molecular weight markers in SDS–PAGE, and proteins were visualized by staining polyacrylamide gels with silver (Rabilloud *et al*., 1988).

Native polyacrylamide gel electrophoresis (Native–PAGE) was carried out according the methods described by Laemmli (1970), excluding the presence of SDS, again using a 10% resolving gel and 4% stacking gel.

3.2.5.4 Determination of flavin content

UV-visible spectra of the purified enzyme was recorded on a Beckman Coulter DU–800 spectrophotometer between 300 and 700 nm in a quartz cuvette. Flavin cofactor content was determined by thin layer chromatography (TLC). The enzyme-bound cofactor was released from the purified protein by autoclaving the sample, followed by centrifugation 14 000 x g for 10 min. The supernatant was applied to a Silicagel 60 TLC aluminium plates (Merck) using butanol-acetic acid-water (12:3:5) as solvent. Riboflavin, flavin mononucleotide (FMN) and flavin adenine dinucleotide (FAD) was used as standards and the fluorescence spots were visualized using UV light.

3.2.5.5 Determination of N-terminal amino acid sequence

N-terminal amino acid sequencing was performed using automated Edman-degradation on an Applied Biosystems 4774A gas-phase sequencer (Foster City, California) at the Protein Chemistry Facility of the Centro de Investigaciones Biologicas (CSIC, Madrid, Spain).

3.3 RESULTS AND DISCUSSION

3.3.1 Purification of the cytoplasmic chromate reductase

As discussed in chapter 2, the aerobic chromate reductase activity of *Thermus scotoductus* SA–01 is expressed constitutively and is present in the cytoplasmic fraction. Crude extracts, constituting the cytoplasm, were therefore prepared from approximately 12 g cells (wet weight) grown in TYG media containing no Cr(VI). The chromate reductase was purified to electrophoretic homogeneity with an overall yield of 9.1% and a purification fold of approximately 450. The purification parameters are summarized in Table 3.1.

The crude extract (cytoplasmic fraction) was applied through column adsorption to a DEAE Toyopearl anion–exchange resin and eluted as a single sharp activity peak through static ion exchange with 50 mM NaCl (Figure 3.5). Very low yields were recovered from the anion–exchange resin, but could be partly restored by the addition of 10 mM Ca^{2+} in the reaction mixture. Nearly one third of all known enzymes require the presence of metal ions for catalytic activity. Two classes of metal ion–requiring enzymes can be distinguished by the strength of their ion–protein interactions. The metalloenzymes contain tightly bound metal ions, in contrast with metal–activated enzymes which loosely binds metal ions from solution (Voet & Voet, 1990). Weakly bound Ca^{2+} ions required for activity possibly eluted in the non–binding fraction.

Total activity decreased by approximately 50%, which may partly be attributed to the removal of low–molecular weight compounds in the crude extract having chromate reducing properties. As the enzyme bound to an anion–exchange resin at pH 7, the isoelectric point (pI) is predicted to be 7 or lower.

Table 3.1: Purification parameters of the soluble chromate reductase.

Fraction	Volume	Activity	Total Activity	[Protein]	Total Protein	Specific Activity	Purification Fold	% Yield
	ml	Units.ml^{-1}	Units[a]	mg.ml^{-1}	mg	Units.mg^{-1}		
Crude Extract[b]	150	62.8	9420	3.200	480.0	19.6	1.0	100.0
DEAE Toyopearl (I)	49	98.1	4807	1.620	79.4	60.6	3.1	51.0
DEAE Toyopearl (II)	84	33.3	2798	0.183	15.4	182.1	9.3	29.7
Phenyl Toyopearl	88	29.0	2549	0.023	2.0	1250.0	63.7	27.1
Blue Sepharose	39.5	15.9	628	-[c]	-	-	-	6. 7
Sephacryl S-100HR	17.5	48.8	854	0.0055	0.10	8839.1	450.4	9.1

[a] Units are defined as amount of nmol Cr(VI) reduced . min^{-1}

[b] Cytoplasmic fraction

[c] NAD^+ interfere with BCA protein assay

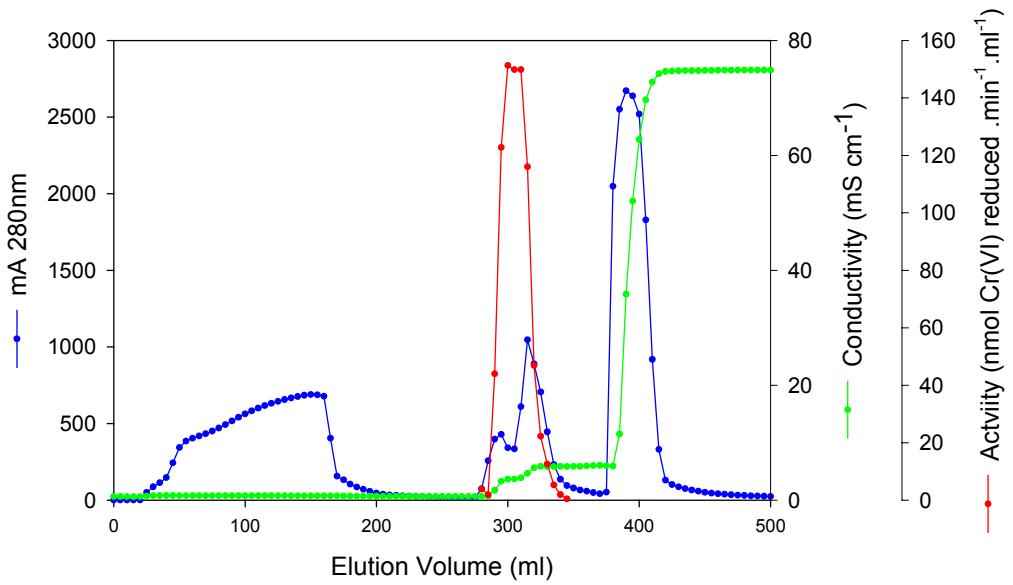

Figure 3.5: Typical elution profile of DEAE Toyopearl chromatographic column of crude extract eluted using static ion exchange. Both the non–binding and binding fractions are shown, with A_{280nm} for protein estimation (●), chromate reducing activity (●) and NaCl concentration (●).

The pooled active fractions was again applied to a DEAE Toyopearl resin but eluted with a linear NaCl gradient. The chromate reductase eluted as a symmetrical activity peak at approximately 30 mM NaCl, suggesting very weak binding to the anion–exchanger (Figure 3.6).

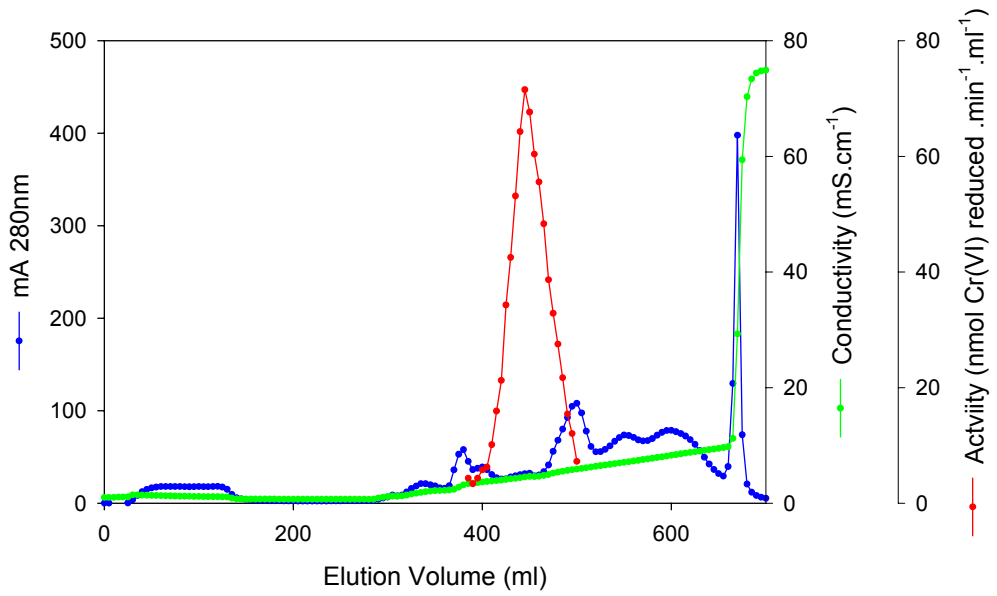

Figure 3.6: Typical elution profile of DEAE Toyopearl chromatographic column, using a NaCl concentration gradient to elute bound chromate reductase from pooled active fractions from first anion–exchange chromatography step. Both the non–binding and binding fractions are shown, with A_{280nm} for protein estimation (●), chromate reducing activity (●) and NaCl concentration (●).

The enzyme proved to be moderately hydrophobic as it adsorbed to a phenyl–toyopearl resin equilibrated with 0.4 M $(NH_4)_2SO_4$ and eluted with a negative linear gradient at approximately 0.25 M $(NH_4)_2SO_4$ (Figure 3.7). Although the enzyme is present in the cytoplasmic fraction, its hydrophobic properties suggest a possible weak interaction with the inner–membrane.

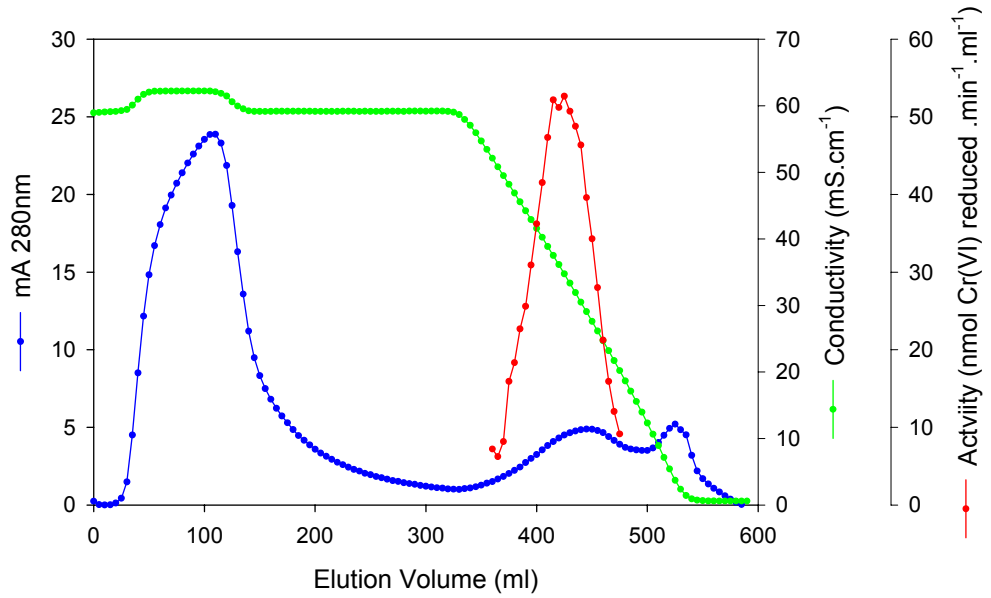

Figure 3.7: Typical phenyl Toyopearl chromatography column elution profile, using a negative $(NH_4)_2SO_4$ concentration gradient. Both the non–binding and binding fractions are shown, with A_{280nm} for protein estimation (●), chromate reducing activity (●) and $(NH_4)_2SO_4$ concentration (●).

Twenty µl's of each fraction containing chromate reductase activity was analyzed with SDS–PAGE. Assuming all variables are constant, the only basis for greater activity would be a higher concentration of the chromate reductase protein, which would be paralleled by a more prominent (darker) band (Park *et al*., 2000). The only protein where band intensity correlated directly to chromate reductase activity is the approximately 36 kDa band, suggesting that this might represent the chromate reductase protein.

For further purification through dye–affinity chromatography, Blue Sepharose CL–6B was employed. This product has been successfully used in the purification of NAD^+ and $NADP^+$ dependent enzymes, whereby specifically–bound proteins are eluted with low concentrations of the specific cofactor, a change in pH or ionic strength of the buffer. The bound chromate reductase activity did not elute with 20 mM NAD^+, nor completely with an increase in NaCl in the elution buffer. The column was therefore eluted with a combination of 10 mM NAD^+ and 0.25 M NaCl in 20 mM MOPS–NaOH (pH 7) (Figure 3.8). The NAD^+ in the elution buffer however interfered with the determination of protein concentrations (A_{280nm}) during the column elution as well as protein quantification using the BCA protein

assay. From SDS–PAGE analysis (data not shown) it is evident that very few proteins eluted with the chromate reductase, suggesting a high purification fold at this chromatographic step.

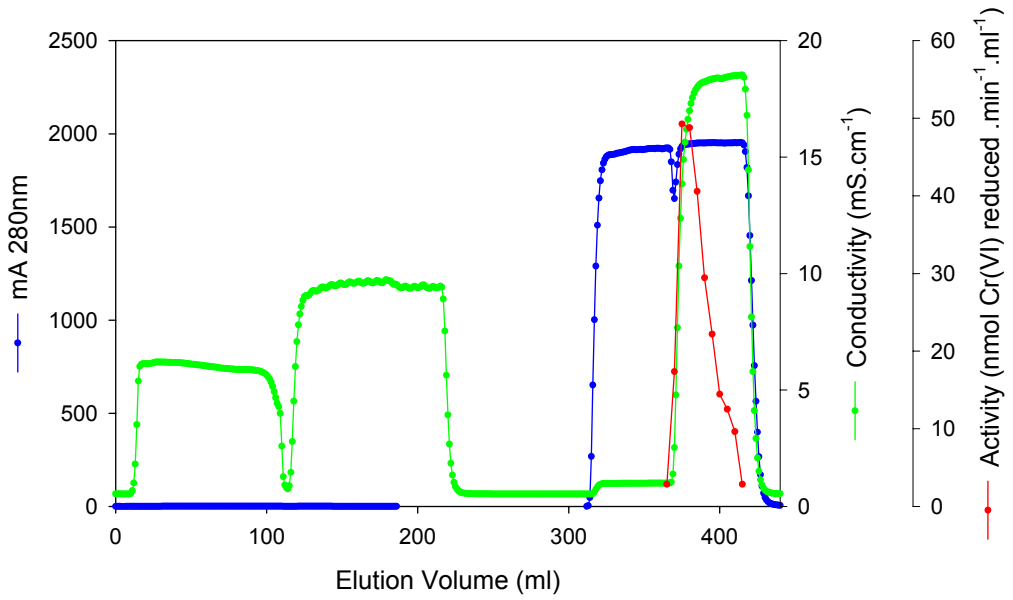

Figure 3.8: Typical elution profile of Blue Sepharose chromatography column. Bound chromate reductase was eluted with a combination of 0.25 M NaCl and 10 mM NAD^+ in the standard buffer. Both the non–binding and binding fractions are shown, with A_{280nm} for protein estimation (●) and chromate reducing activity (●). A_{280nm} values greater than 10 indicate NAD^+ interference.

The final purification step, size–exclusion chromatography on a Sephacryl S–100HR, yielded a single activity peak (Figure 3.9) under these non–denaturing conditions. Relative to the protein standards, a native molecular mass of approximately 72.4 kDa was determined for the chromate reductase. SDS–PAGE analysis shows an apparent monomer molecular weight for the denatured subunits of 35.8 kDa, suggesting that the native enzyme has a homodimeric quaternary structure.

Most purified Cr(VI) reductases give single bands with SDS–PAGE analysis, with higher native molecular weights determined by gel–filtration chromatography, suggesting either homodimeric or homotrimeric structures (Table 3.2). A monomeric Cr(VI) reductase haas however been purified from *Rhodobacter sphaeroides* (42 kDa; Nepple *et al*., 2000).

Table 3.2: Comparison of chromate reductases molecular weights (M_r) and quaternary structures.

Organism	**Monomer M_r** (kDa)[a]	**Native M_r** (kDa)[b]	**Structure**	**Reference**
Thermus scotoductus SA-01	36	72	Homodimeric	
Pseudomonas ambigua G-1	25	65	Homo– di/trimeric	Suzuki *et al*. 1992
Pseudomonas putida MK-1	20	50	Homodimeric	Park *et al*. 2000
Bacillus sp. QC1-2	24	44	Homodimeric	Campos-Garcia *et al*. 1997
Rhodobacter sphaeroides 158	42	42	Monomeric	Nepple *et al*. 2000
Pseudomonas putida (ChrR)	22	50	Homodimeric	Ackerley *et al*. 2004B
Escherichia coli (YieF)	22	50	Homodimeric	Ackerley *et al*. 2004B
Escherichia coli (NfsA)	26	65	Homo– di/trimeric	Ackerley *et al*. 2004A

[a] As determined by SDS–PAGE

[b] As determined by gel–filtration chromatography

The Sephacryl S–100HR was also effective in the removal of the NAD^+ from the previous purification step, which was important for the accurate kinetic characterization of the enzyme, as NAD^+ present in the reaction might have an effect on the chromate reduction reaction rates.

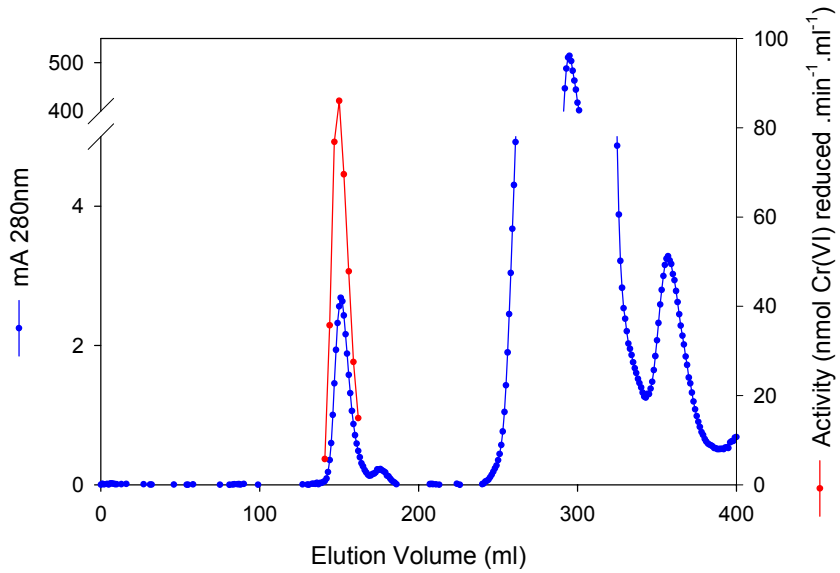

Figure 3.9: Typical Sephacryl S–100HR chromatography column elution profile with 20 mM MOPS–NaOH (pH 7) containing 50 mM NaCl. A_{280nm} indicates protein estimation (●) with chromate reducing activity (●). A_{280nm} values greater than 100 indicate NAD^+ interference.

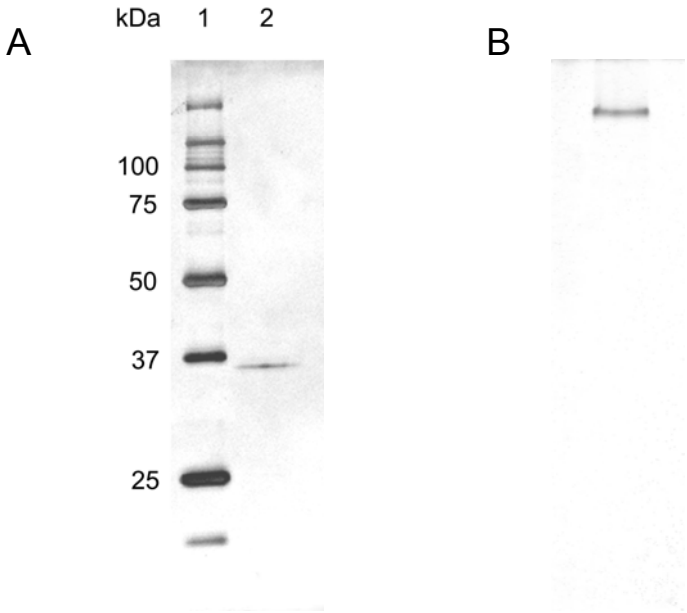

Figure 3.10: SDS–PAGE analysis of the purified chromate reductase from *Thermus scotoductus* SA-01 (A). Lane 1, standard molecular weight marker; lane 2, purified protein. Proteins were visualized by silver staining. Silver stained native (non-denaturing) PAGE gel of the cytoplasmic chromate reductase (B).

SDS-PAGE as well as non–denaturing PAGE analysis showed only a single band present. Throughout purification, the activity corresponded with a light yellow colour resistant to ultrafiltration. Near UV-visible absorption spectrum typical of flavoproteins were obtained for the air-oxidized protein with absorption maxima at 375 nm and 460 nm. The flavin group was non-covalently bound and was released at very high temperatures. The bound flavin was identified through thin layer chromatography as FMN (Figure 3.11).

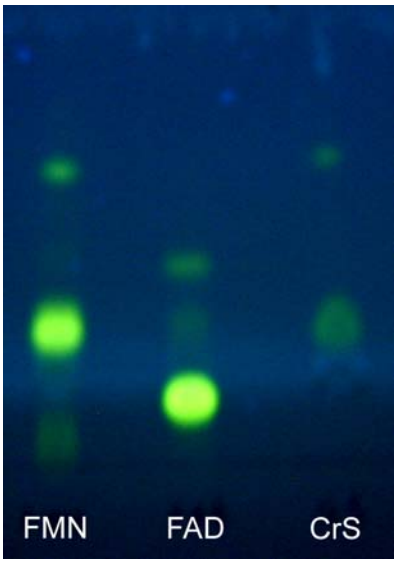

Figure 3.11: Thin layer chromatography (TLC) analysis of the non-covalently bound co-factor from the cytoplasmic chromate reductase through dissociation at high temperatures.

3.3.2 Characterization of the purified chromate reductase

3.3.2.1 Effect of pH

Maximal chromate reductase activity was achieved at a pH of 6.3 compared to the optimum pH for chromate reduction of whole cells under resting conditions at 7. Figure 3.12 depicts the effect of pH on enzyme activity in a MES–MOPS–Bicine buffer in the presence of 10 mM $CaCl_2$, with maximum activity taken as 100%. The chromate reductase was more than 50% active between pH 5.5 and 7.5. The optimum pH for chromate reductase correlates well with optimal growth pH for the organism, which is near neutrality (Kieft *et al*., 1999).

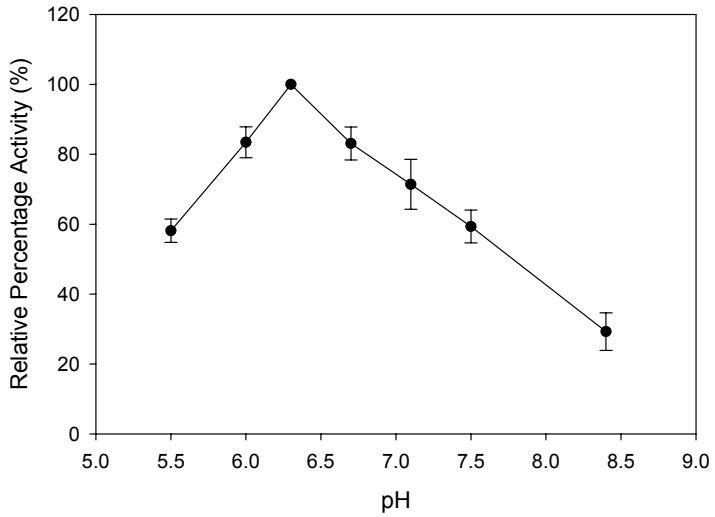

Figure 3.12: Effect of pH on the activity of purified *Thermus scotoductus* SA–01 soluble chromate reductase. Activity at pH 6.2 (optimum) was taken as 100%. Error bars indicate standard deviation.

3.3.2.2 Effect of temperature

The chromate reductase was active over a very wide range of temperatures (Figure 3.13). The reductase activity increased rapidly as the reaction temperature was increased from 50 to 65°C. The optimum temperature for the chromate reductase was 65°C, which correlates well with the optimal temperature for growth (Kieft *et al*., 1999), but is less than the optimum temperature for chromate reduction by whole–cells under resting conditions. A gradual decline in activity is seen at elevated temperatures, but even at temperatures as high as 80°C, the chromate reductase was more than 70% active.

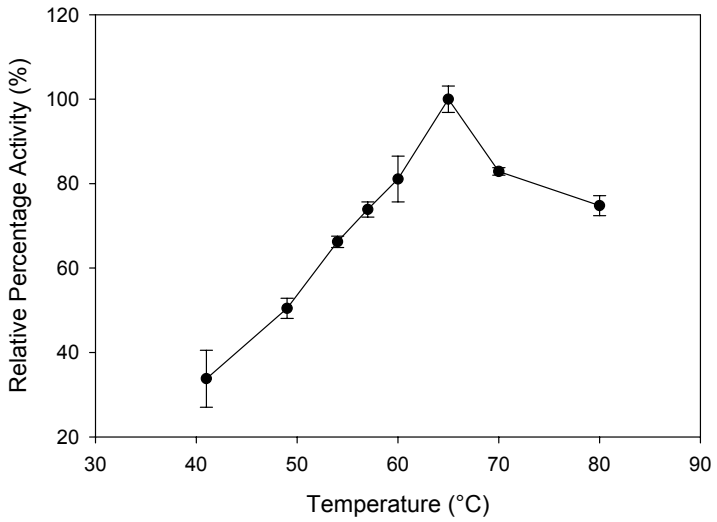

Figure 3.13: Optimum temperature of the purified *Thermus scotoductus* SA–01 chromate reductase. Activity at the optimum temperature (65°C) was taken as 100%. Error bars indicate standard deviation.

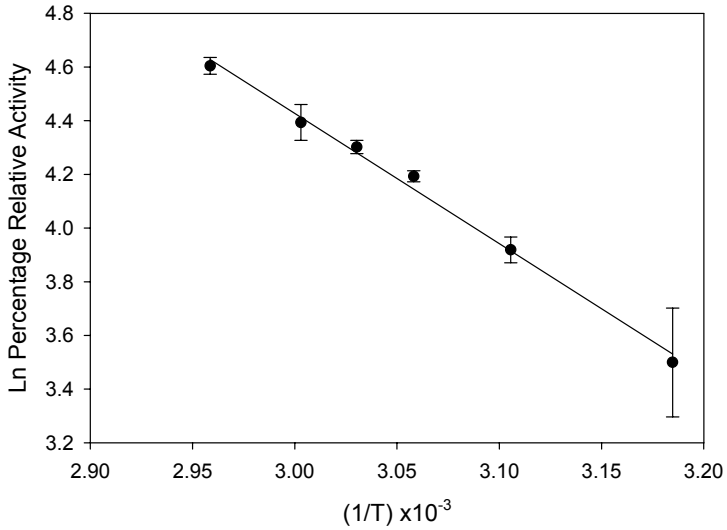

Figure 3.14: Arrhenius plot for the calculation of activation energy of the cytoplasmic chromate reductase.

The activation energy (E_a) of the chromate reductase was calculated to be 40.3 kJ.mol^{-1} over the temperature range of 40 – 65°C. The linear slope of the Arrhenius plot (Figure 3.14) also suggests that the functional conformation of the enzyme remains unchanged throughout this temperature range. The lower activity is thus probably as result of the higher rigidity of the protein at lower temperatures.

3.3.2.3 Effect of divalent metals and EDTA

Activity was dependent on the presence of the divalent metals Ca^{2+} or Mg^{2+} which increased the activity more than 4 fold, whereas Zn^{2+}, Mn^{2+} and EDTA inhibited the reaction (Table 3.3).

Table 3.3: The effect of divalent metals and EDTA on the specific activity of the chromate reductase.

Metal / EDTA	Specific Activity ± SD (μmol min^{-1} mg^{-1})
-	3.14 ± 0.53
Ca	14.52 ± 2.24
Mg	13.59 ± 0.73
Zn	0
Mn	1.5 ± 0.10
EDTA	0.98 ± 0.56

3.3.2.4 Steady–state kinetics

The cytoplasmic chromate reductase could accept electrons from both NADH and NADPH with a preference towards NADPH. Figure 3.15 shows the hyperbolic dependence of Cr(VI) concentration to specific activity. The apparent K_m values obtained for Cr(VI) was 3.5 ± 0.3 μM and 8.4 ± 1.1 μM when utilizing NADH and NADPH as electron donor respectively, with corresponding V_{max} values of 6.2 ± 0.2 μmol min^{-1} mg^{-1} and 16.0 ± 0.6 μmol min^{-1} mg^{-1} (Figure 3.15). At concentrations above 0.1 mM, NADPH showed substrate inhibition, but was still more efficient at these concentrations than NADH (Figure 3.16).

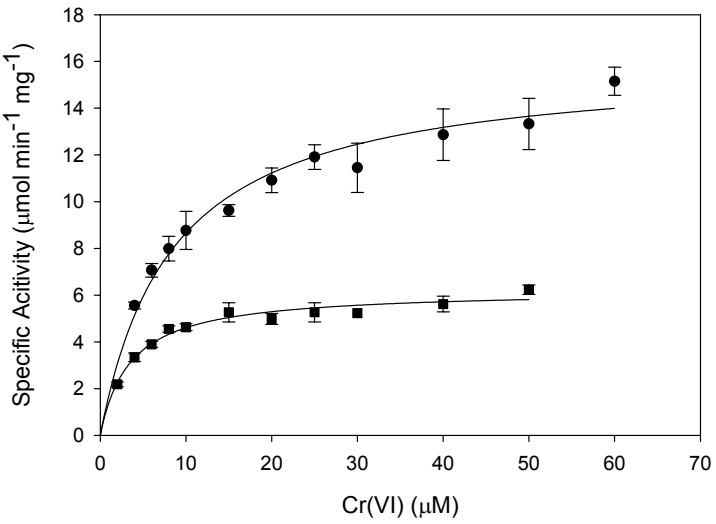

Figure 3.15: Substrate saturation curves (Michaelis–Menten plot) of the purified chromate reductase from *Thermus scotoductus* SA–01 for hexavalent chromium in the presence of 0.3 mM NADH (●) or 0.3 mM NADPH (■). Error bars indicate standard deviation.

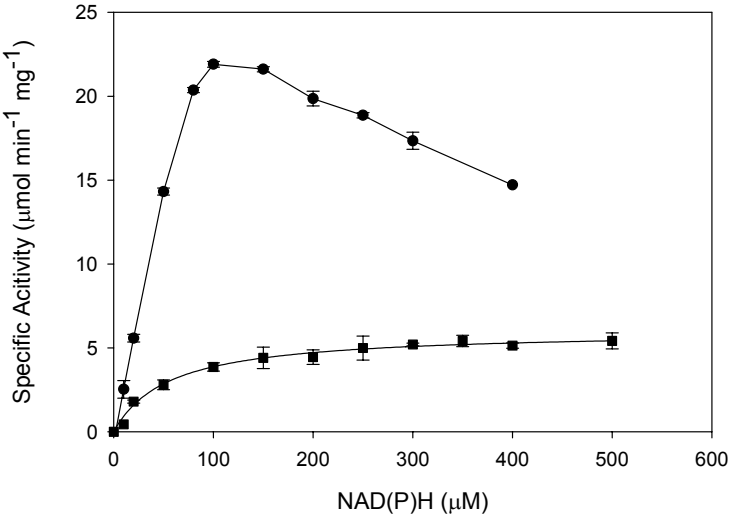

Figure 3.16: Substrate saturation curve (Michaelis–Menten plot) of the purified chromate reductase from *Thermus scotoductus* SA–01 for NADH (●) or NADPH (■) in the presence of 0.1 mM Cr(VI). Error bars indicate standard deviation.

Table 3.4: Comparison of kinetic parameters of various purified chromate reductases.

Organism (Enzyme)	V_{max} (µmol Cr(VI) min^{-1} mg^{-1} protein)	K_m (µM)	k_{cat} (s^{-1})	k_{cat}/K_m (M^{-1} s^{-1})	Reference
P. ambigua G-1	0.027	13	0.03	2.3×10^3	Suzuki *et al*., 1992
P. putida MK1	1.720	374	1.43	3.8×10^3	Park *et al*., 2000
V. harveyi (NfsA)	0.0107	5.4	0.009	1.65×10^3	Kwak *et al*., 2003
P. putida (ChrR)	8.800	260	5.8	2.2×10^4	Ackerley *et al*., 2004B
E. coli (YieF)	5.000	200	3.7	1.9×10^4	Ackerley *et al*., 2004B
E. coli (NfsA)	0.250	36	0.23	6.3×10^3	Ackerley *et al*., 2004A
T. scotoductus SA-01[a]	16.0	8.4	9.6	1.2×10^6	

[a] NADPH as electron donor

Substrate affinity (K_m) of the purified *Thermus scotoductus* SA–01 chromate reductase is relatively high (low K_m value) as compared to other Cr(VI) reductases (Table 3.4), with the exception of the *Pseudomonas ambigua* (13 µM) and the *Vibrio harveyi* (5.4 µM) chromate reductases.

Compared to other chromate reductase's catalytic constants (k_{cat}), the chromate reductase from SA–01 is the most rapid catalyst (Table 3.4). The catalytic efficiency of the chromate reductase with NADPH as electron donor (k_{cat}/K_m) was 1.2×10^6 M^{-1} s^{-1}, which is at least 180 fold more efficient than the NfsA proteins (Kwak *et al*., 2003; Ackerley *et al*., 2004A) and more than 50 fold more efficient than the ChrR proteins (Ackerley *et al*., 2004B).

3.3.2.5 Stoichiometric analysis of Cr(VI) reduction

NAD(P)H reduced chromate even in the absence of the chromate reductase. When the enzyme was added to the reaction mixture containing NAD(P)H and chromate, the NAD(P)H consumption rate increased, with a concomitant reduction of Cr(VI), suggesting that electrons move from NAD(P)H to chromate. Stoichiometric analysis relating NAD(P)H oxidation to Cr(VI) reduction, showed that 2.1 ± 0.1 mol NADH or 1.9 ± 0.2 mol NADPH is consumed per mol Cr(VI) reduced, indicating that Cr(III) was the end-product, as each NADH molecule donates two electrons, four electrons are consumed for Cr(VI) reduction. Complete Cr(VI) reduction to Cr(III) can however only utilize three of these electrons.

In 1990(A), Shi and Dalal reported that NAD(P)H–dependent flavoenzymes can catalyze one electron reduction of metal ions such as Cr(VI). During this enzymatic reduction, molecular oxygen is reduced to H_2O_2. A two–step catalysis model for enzymatic reduction of Cr(VI) to Cr(III) has been proposed (Suzuki *et al*., 1992) after stoichiometric analysis showed 3 mol of NADH were consumed during the reduction of 1 mol of Cr(VI) to Cr(III). Cr(VI) first accepts one electron from one NADH molecule and generates Cr(V) as an intermediate. Cr(V) then accepts two electrons from two molecules of the same coenzyme.

The soluble chromate reductases from *Pseudomonas putida* (ChrR) and *Escherichia coli* (YieF) are both flavoproteins with a dimeric structure (Ackerley *et al*., 2004B). Stoichiometric analysis of the YieF enzyme indicated an obligatory four–electron reduction of chromate, in which the enzyme simultaneously transfers three electrons to chromate and one electron to molecular oxygen (subsequently generating H_2O_2). The ChrR dimer however, generated a flavin semiquinone during chromate reduction, implying a nonsimultaneous transfer of electrons, which would generate Cr(V) transiently. More than 25% of the NADH electrons were transferred to reactive oxygen species (ROS). Ackerley and co–workers (2004A) termed these modes of enzyme–mediated electron transfer to chromate tight, semitight and single–electron, where tight describes the one step transfer of three electrons to Cr(VI) to generate Cr(III), semitight chromate reduction involving a one–electron (uni–valent) transfer component to form Cr(V) transiently followed by a two electron (di–valent) transfer step. Single–electron chromate reducers (Ackerley *et al*., 2004A; Shi & Dalal, 1990A) generate the highly unstable Cr(V) radical, which redox cycles, whereby Cr(V) is oxidized back to Cr(VI), giving its electron to molecular oxygen to generate reactive oxygen species (Figure 3.17). As the ratio of NAD(P)H:Cr(VI) is approximately 2:1, the cytoplasmic chromate reductase utilize either a tight or semi-tight transfer of electrons.

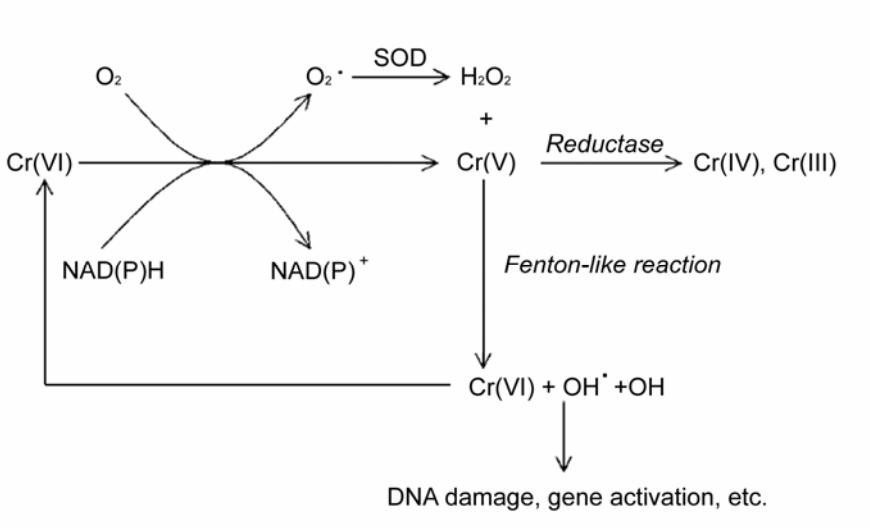

Figure 3.17: Cr(VI) reduction pathways and its related free radical generation (adapted from Liu & Shi, 2001).

3.3.2.6 Alternative substrates

NAD(P)H consumption with FMN and FAD as electron acceptor was determined due to sequence similarities of the chromate reductase (Chapter 5) with predicted NADH-dependent flavin oxidoreductases. Although an increase in NAD(P)H oxidation was observed with FAD and FMN as substrates, the reaction rates were significantly less than that observed for Cr(VI) (Table 3.5) and more comparable to the NAD(P)H oxidase rates were electrons are donated to oxygen, suggesting that the reactions are fortuitous.

Table 3.5: Comparison of the rate of NAD(P)H oxidation by different substrates.

Substrate	**Specific Activity ± SD (µmol min^{-1} mg^{-1})**	
	NADH	NADPH
Cr(VI)	12.00 ± 1.07	122.48 ± 13.03
FAD	1.04 ± 0.41	1.98 ± 0.02
FMN	1.77 ± 0.98	4.15 ± 1.40
Molecular oxygen	1.09 ± 0.31	0.97

3.3.2.7 N-terminal sequencing

The N-terminal sequence of the purified chromate reductase, determined through Edman degradation, was ALLFTPLELGG, and shows no similarity to the other proteins in literature characterized as chromate reductases. The mature protein did not have a N-terminal methionine residue, suggesting possible posttranslational modification.

3.4 CONCLUSIONS

The constitutively expressed cytoplasmic chromate reductase from *Thermus scotoductus* SA–01 was purified to electrophoretic homogeneity to a purification fold of approximately 450.

The cytoplasmic chromate reductase from *T. scotoductus* is a homodimeric enzyme with a monomer molecular mass of approximately 36 kDa containing a non-covalently bound FMN co-factor as well as the requirement of Ca^{2+} for activity. The chromate reductase was optimally active at 65°C and a pH of 6.3. The enzyme coupled the oxidation of NAD(P)H, with a preference for NADPH, to the reduction of Cr(VI), utilizing 2 mol of NAD(P)H per mol Cr(VI), suggesting the complete reduction to Cr(III). The chromate reductase activity was both dependent on chromate and NAD(P)H concentration, with an apparent V_{max} and k_m for chromate with NADPH as oxidant of 16.0 µmol.min^{-1}.mg^{-1} protein and 8.4 µM respectively. The catalytic efficiency of the chromate reductase with NADPH as electron donor (k_{cat}/K_m) was 1.14 x 10^6 M^{-1} s^{-1}, which is at least 180 fold more efficient than the NfsA proteins (Kwak *et al*., 2003; Ackerley *et al*., 2004A) and more than 50 fold more efficient than the ChrR proteins (Ackerley *et al*., 2004B). Low levels of NAD(P)H oxidase as well as flavin reductase activity were observed.

N-terminal sequencing of the chromate reductase gave only 11 amino acids residues of which the sequence showed no similarity to other enzymes with chromate reducing activity. The chromate reductase probably undergoes post-translational modification as indicated by the absence of a N-terminal methionine residue.

CHAPTER 4

PURIFICATION AND CHARACTERIZATION OF THE MEMBRANE-ASSOCIATED Cr(VI) REDUCTASE

4.1 INTRODUCTION

Chromate reductases are not limited to the cytoplasm of bacteria and have been found localized within the membranes (Myers *et al*., 2000; Wang *et al*., 1990) as well as the periplasm of bacteria (Ganguli & Tripathi, 2001).

Anaerobic Cr(VI) reduction is often mediated through membrane-associated reductases with some being able to utilize H_2 as an electron donor as well as the possibility of involving cytochromes (Wang & Shen, 1995). Under anaerobic conditions, Cr(VI) has also been shown to be able to serve as a terminal electron acceptor in the respiratory chains of *E. coli* (Shen & Wang, 1993), *Desulfovibrio vulgaris* (Lovley & Phillips, 1994) and *Thiobacillus ferroxidans* (QuiIntana *et al*., 2001).

Sub-cellular fractionation studies of *T. scotoductus* SA-01 have indicated the presence of more than one enzyme contributing to its Cr(VI) reducing ability. This chapter describes the purification and characterization of a membrane-associated chromate reductase.

4.2 MATERIALS AND METHODS

4.2.1 Bacterial strain and culture conditions

For protein purification *Thermus scotoductus* strain SA–01 was cultured aerobically in a complex organic medium, TYG (5 g tryptone [Biolab], 3 g yeast extract [Saarchem] and 1 g glucose in 1 L ddH_2O) at 65°C, pH 7.0, with aeration (200 rpm). SA–01 was cultured without added Cr(VI) until mid–exponential growth phase.

4.2.2 Preparation of subcellular fractions

Subcellular fractions were prepared using a modification of the method of Gaspard *et al*. (1998), as described by Kaufmann & Lovley in 2001 (section 2.2.6).

4.2.2.1. Peripherally-bound membrane protein extraction

Peripherally-bound membrane proteins were extracted using a high-ionic-strength salt buffer (Gaspard *et al.*, 1998). Membrane fractions were stirred for 2 h at room temperature in a high-ionic-strength buffer (20 mM MOPS-NaOH, 0.1 mM DTT, 0.5 M KCl, pH 7) in order to release the bound proteins. Following centrifugation at 100 000 x g for 2 h (4°C) the supernatant (peripherally-bound membrane proteins) was dialyzed overnight against a 20mM MOPS-NaOH (pH 7) buffer. The pellet containing the integral membrane proteins were resuspended in 20 mM MOPS-NaOH buffer (pH 7).

4.2.2.2 Total membrane protein extraction

Total membrane proteins (integral and peripherally-bound membrane proteins) were extracted through a combination of detergent mediated as well as high-ionic strength extraction. Membrane fractions were stirred for 1 h at room temperature in the high-ionic-strength buffer (section 4.2.2.1) containing 10 mM Triton X-100 to dissociate the membrane proteins. Membranes were removed through centrifugation (100 000 x g, 2 h at 4°C). The supernatant containing the extracted membrane proteins were dialyzed against 20 mM MOPS-NaOH (pH 7) buffer.

4.2.3 Purification of peripherally bound membrane Cr(VI) reductase

All purification steps were carried out at room temperature and enzyme preparations were stored at 4°C without any loss of activity. Purification to homogeneity entailed three chromatographic steps: anion–exchange, dye–affinity and size exclusion chromatography, using the ACTA Prime Purification System (Amersham Biosciences).

4.2.3.1 Anion exchange chromatography

The extracted peripherally-bound membrane proteins were dialyzed against 20 mM MOPS (pH 7.0) and precipitated proteins were removed through centrifugation (10 000 x g for 10 min).

The dialyzed fraction was applied to a DEAE–Toyopearl 650M column (6 x 2.5 cm; TOSOH Corporation) equilibrated with 20 mM MOPS–NaOH buffer (pH 7). Unbound proteins were eluted with the same buffer. Bound proteins were eluted with a linear gradient of 0 – 0.3 M NaCl (400 ml) in the same buffer (5 $ml.min^{-1}$ flow rate). Strongly bound proteins were eluted with the same buffer containing 1 M NaCl. Fractions (5 ml) containing the Cr(VI) reductase activity eluted at approximately 0.2 M NaCl. Fractions with Cr(VI) reduction activity were pooled and dialyzed against 20 mM MOPS (pH 7.0) and used in the subsequent purification step.

4.2.3.2 Dye-affinity chromatography

The dye-affinity chromatography step employed a Blue Sepharose CL–6B (Sigma–Aldrich) column (17 x 1.3 cm) equilibrated with 20 mM MOPS-NaOH (pH 7.0). After binding of the dialyzed sample, the column was washed sequentially with 70 ml 20 mM MOPS-NaOH, a 0 – 0.2 M NaCl gradient (100 ml) in the same buffer and lastly 1 M NaCl in the same buffer. Active fractions eluted at 0.1 M NaCl and were pooled and concentrated to 3 ml using ultrafiltration on a 10 kDa NMCO cellulose membrane Vivaspin column (VivaScience).

4.2.3.3 *Size-exclusion chromatography*

The final purification step was size–exclusion chromatography, whereby the native molecular weight (M_r) of the chromate reductase was also determined. The concentrate was loaded onto a Sephacryl S–200 HR column (2.6 x 63 cm; Sigma-Aldrich), equilibrated with 20 mM MOPS–NaOH (pH 7.0) containing 50 mM NaCl. Proteins were eluted with the same buffer at a flow rate of 0.5 ml.min^{-1}. Cytochrome c (12.4 kDa), chymotrypsin (25 kDa), bovine serum albumin (66 kDa) and alcohol dehydrogenase (148 kDa) were used as molecular weight standards.

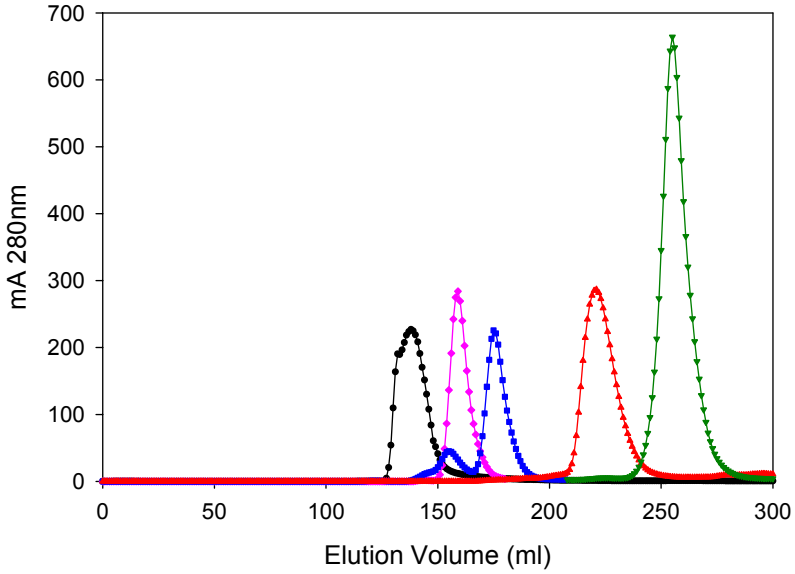

Figure 4.1: Elution profile from Sephacryl S200HR column calibration of Blue Dextran [2 000 kDa (●)], alcohol dehydrogenase [148 kDa (♦)], bovine serum albumin [66 kDa (■)], chymotrypsin [25 kDa (▲)] and cytochrome c [12.4 kDa (▼)].

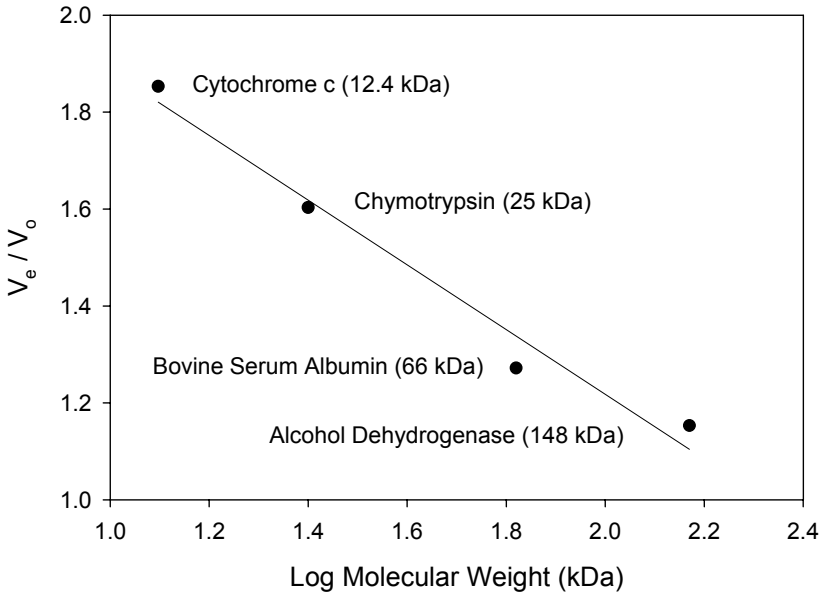

Figure 4.2: Calibration curve of Sephacryl S200HR relating molecular weight to elution volume. The void volume (V_o) was calculated using the elution volume of Blue Dextran (2 000 kDa).

4.2.4 Characterization of the purified enzyme

4.2.4.1 The effect of pH and temperature on the enzyme activity

The effect of pH as well as temperature on the activity of the purified chromate reductase was measured under standard conditions as described in section 3.2.4.1 and 3.2.4.2 respectively.

4.2.4.2 Steady state kinetics

Kinetic constants were determined at a pH of 6.5 and 65°C by measurement of initial velocities at various concentrations of Cr(VI) and NADH. The apparent kinetic parameters were determined from non–linear regressions of Michaelis–Menten plots using SigmaPlot 8.0 (SPSS Inc.).

4.2.5 Analytical techniques

4.2.5.1 Standard enzyme assay

Chromate reductase was determined by measuring the decrease of hexavalent chromium. Cr(VI) was analyzed by the *s*-diphenylcarbazide method as described in section 3.2.5.1. During purification the enzyme was assayed in 1 ml reaction mixtures containing 20 mM MOPS-NaOH buffer (pH 6.5), 5 mM EDTA, 0.1 mM CrO_3, 0.3 mM NADH and 0.05 ml of the enzyme preparation at 65°C. One Unit is defined as the amount of enzyme required to reduce 1 nmol of Cr(VI) per minute.

4.2.5.2 Protein assay

Protein concentrations were determined using the bicinchoninic acid (BCA) method as described in section 3.2.5.2.

4.2.5.3 Gel electrophoresis

SDS-PAGE and Native-PAGE analysis were according to the methods described by Laemmli (1970) as described in section 3.2.5.3.

4.2.5.4 Determination of flavin content

UV-visible spectra of the purified protein as well as the identification of the flavin co-factor were determined as described in section 3.2.5.4.

4.2.5.5 Determination of N-terminal amino acid sequence

N-terminal amino acid sequencing was performed using automated Edman-degradation as described in section 3.2.5.5.

4.3 RESULTS AND DISCUSSION

4.3.1 Purification of the peripherally-bound membrane chromate reductase

In addition to the aerobic cytoplasmic chromate reductase, anaerobic chromate reduction activity was also found within the membrane fraction of *Thermus scotoductus* SA-01. Total membrane-associated protein extraction using the nonionic detergent Triton X-100 gave two activity peaks eluting from the DEAE-Toyopearl anion-exchange resin (Figure 4.3), suggesting that two proteins are located within or associated with the membrane that are able to reduce Cr(VI).

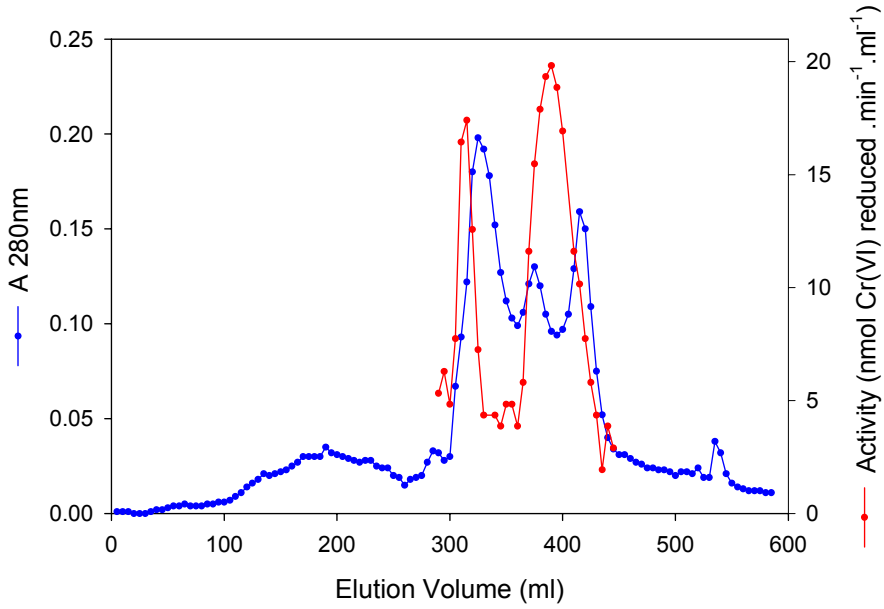

Figure 4.3: Typical elution profile of DEAE Toyopearl chromatographic column of total membrane protein extract eluted with a linear NaCl gradient. Only the binding fraction is shown, with A_{280nm} for protein estimation (●) and chromate reducing activity (●).

Dissociation of only the peripherally membrane bound proteins, gave a single peak of activity eluting from the same chromatographic column (Figure 4.4). The remaining membranes after extraction contain only the integral membrane proteins, which still had chromate reducing ability. This suggest that *T. scotoductus* SA-01, in addition to the

cytoplasmic chromate reductase also possess two membrane-associated enzymes able to reduce Cr(VI), of which one is integrally situated within the membrane and the other only peripherally-associated to the membrane. Interestingly, after extraction of the proteins from the membrane, the obligatory anaerobic conditions required for activity of the membrane-associated enzyme was no longer necessary, as the enzyme functioned equally well under aerobic conditions.

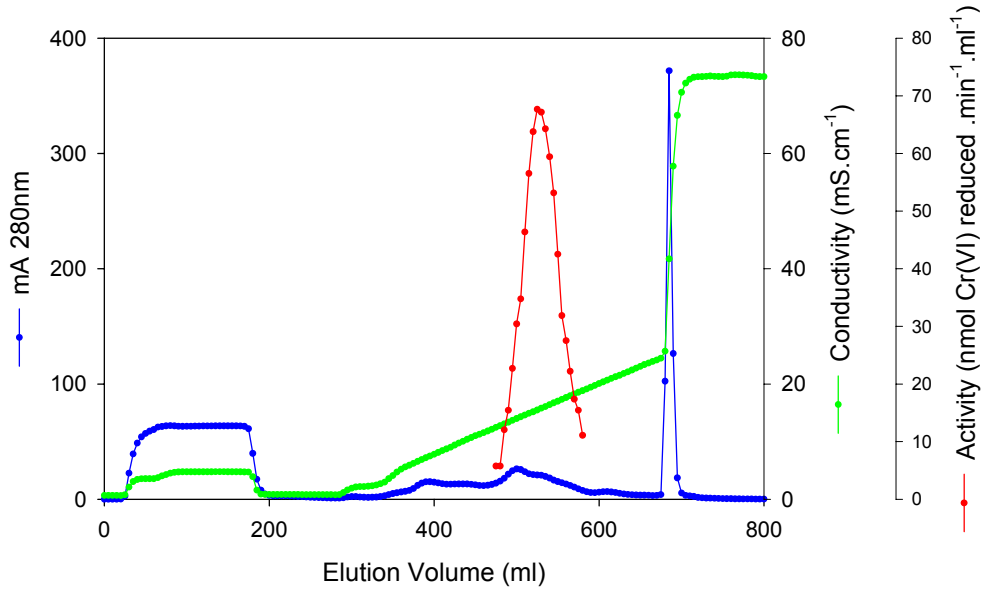

Figure 4.4: Typical elution profile of DEAE Toyopearl chromatographic column of peripherally-bound membrane protein extract eluted with a linear NaCl gradient. Both the non-binding and binding fractions are shown, with A_{280nm} for protein estimation (●), chromate reducing activity (●) and NaCl concentration (●).

The peripherally-bound membrane protein was further purified to homogeneity to a purification fold of approximately 31 and an overall yield of 27.9%. Purification parameters are summarized in Table 4.1.

The chromate reductase eluted from the DEAE-Toyopearl resin as a single symmetrical activity peak at approximately 0.15 M NaCl, suggesting an acidic native pI. The active fractions were pooled and bound to the dye-affinity column (Blue Sepharose CL-6B). The chromate reductase eluted without the addition of co-factor at a NaCl concentration of 0.1 M.

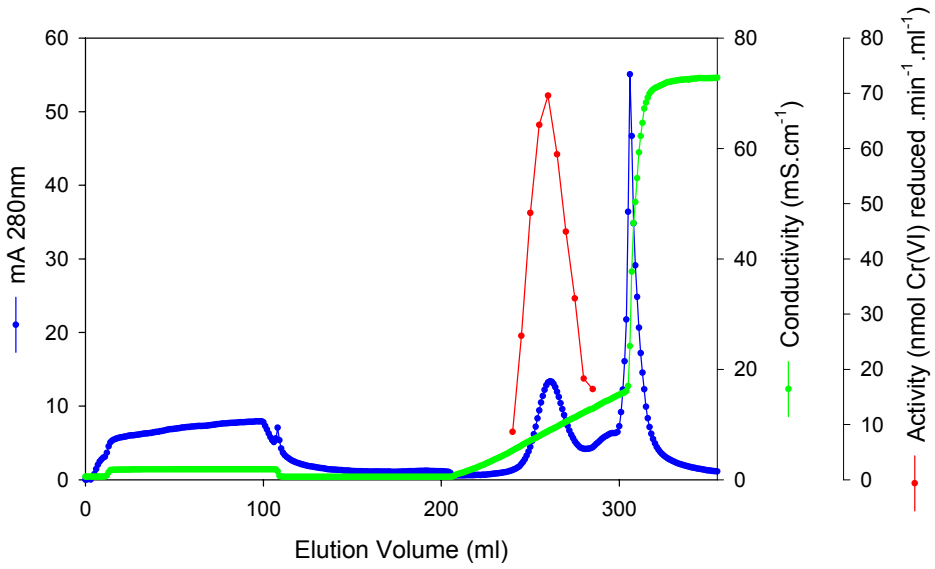

Figure 4.5: Typical elution profile of Blue Sepharose chromatographic column eluted with a linear NaCl gradient. Both the non-binding and binding fractions are shown, with A_{280nm} for protein estimation (●), chromate reducing activity (●) and NaCl concentration (●).

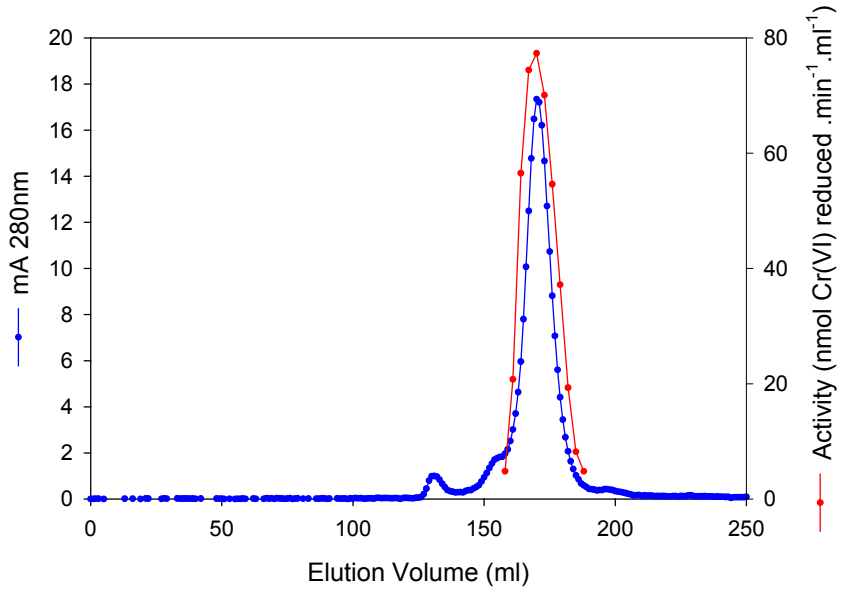

Figure 4.6: Typical elution profile of the Sephacryl S200HR size exclusion chromatographic column eluted with a 20 mM MOPS-NaOH (pH 7) containing 50 mM NaCl. A_{280nm} indicate protein estimation (●) with chromate reducing activity (●).

Table 4.1: Purification parameters of the peripherally-bound membrane chromate reductase.

Fraction	Volume	Activity	Total Activity	[Protein]	Total Protein	Specific Activity	Purification Fold	% Yield
	ml	Units.ml^{-1}	Units[a]	mg.ml^{-1}	mg	Units.mg^{-1}		
Crude KCl extract	150	35.7	5359	0.628	94.2	56.9	1.0	100.0
Dialyzed extract	150	26.5	3982	0.280	42.1	94.7	1.7	74.3
DEAE Toyopearl	78	59.4	4635	0.140	10.9	426.1	7.5	86.5
Dialysis	80	57.0	4560	0.131	10.5	436.5	7.7	85.1
Blue Sepharose	39	55.1	2148	0.033	1.3	1668.7	29.3	40.1
Sephacryl S-200HR	26	57.5	1495	0.033	0.86	1742.0	30.6	27.9

[a] Units are defined as amount of nmol Cr(VI) reduced . min^{-1}

The final purification step entailed size-exclusion chromatography which was also used to estimate the non-denature molecular weight of the native protein relative to known protein standards. The activity again eluted as a single peak, giving an estimated native molecular mass of 89.5 kDa. SDS-PAGE analysis of the purified chromate reductase gave a single band with an apparent monomer molecular weight of approximately 48.2 kDa (Figure 4.7). The chromate reductase is thus a functional dimer consisting of two identical subunits. Nonproportional movement of proteins in SDS-PAGE and gel filtration due to altered conformations and Stokes radii from possible bound cofactors as well as inter- or intrasubunit cross-linkages, often cause small discrepancies from calculated molecular weight (Smith, 1994).

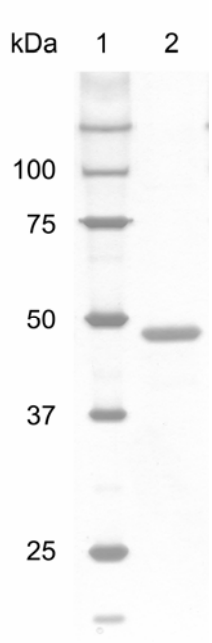

Figure 4.7: SDS-PAGE analysis of the purified chromate reductase from *Thermus scotoductus* SA-01. Lane 1, standard molecular weight marker, lane 2, purified protein (0.7 µg). Proteins were visualized by silver staining.

Similar to the cytoplasmic chromate reductase, activity corresponded to a light brown colour resistant to ultrafiltration. Near UV-visible absorption spectrum (Figure 4.8) typical of flavoproteins were obtained for the air-oxidized protein with absorption maxima at 370 nm and 455 nm and a shoulder at 480 nm. 1 mM NADH reduced the enzyme with a characteristic decrease in absorption in the 450 – 500 nm range. Treatment with 0.2 % SDS released the non-covalently bound FAD group, showing absorption maxima shifts

correlating to that of free FAD. Heat denaturation of the enzyme also resulted in dissociation of the flavin from the protein, which was identified by thin-layer chromatography to be FAD (Figure 4.9).

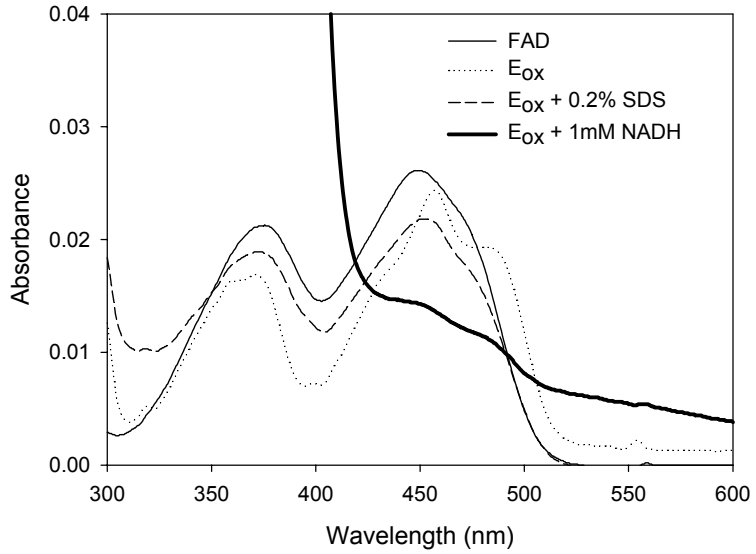

Figure 4.8: UV-visible absorbance spectra of purified oxidized chromate reductase (E_{ox}) from *Thermus scotoductus* SA-01 and free FAD. Enzyme was denatured through addition of 0.2 % SDS and reduced with 1 mM NADH.

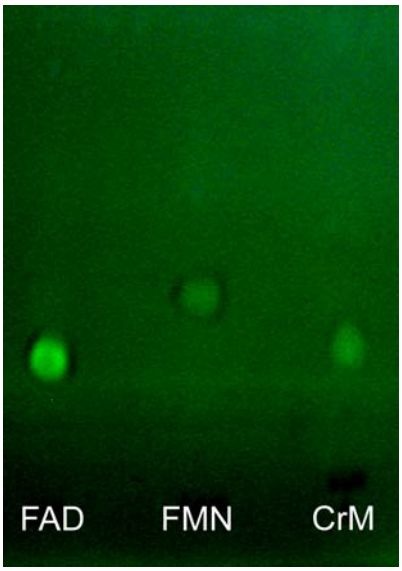

Figure 4.9: Thin layer chromatography (TLC) analysis of the non-covalently bound co-factor from the cytoplasmic chromate reductase through dissociation at high temperatures.

4.3.2 Characterization of the purified chromate reductase

4.3.2.1 Effect of pH and temperature

Chromate reduction activity was optimal between a pH of 6.1 and 6.5 (Figure 4.10), similar to that found for the cytoplasmic chromate reductase The enzyme was also active over a wide range of temperatures (Figure 4.11) and retained more than 50% of its activity between 50°C to 80°C, with the highest activity found at 65°C.

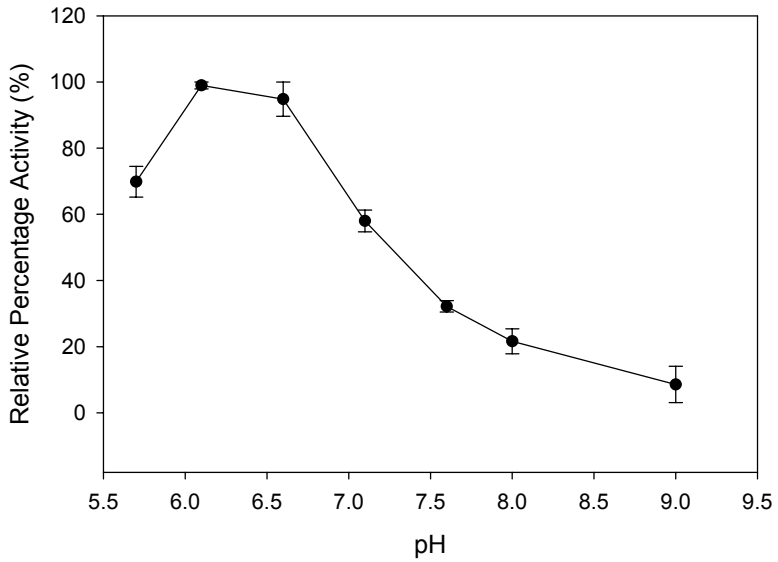

Figure 4.10: Effect of pH on the activity of the purified chromate reductase. Activity at pH 6.2 (optimum) was taken as 100%. Error bars indicate standard error.

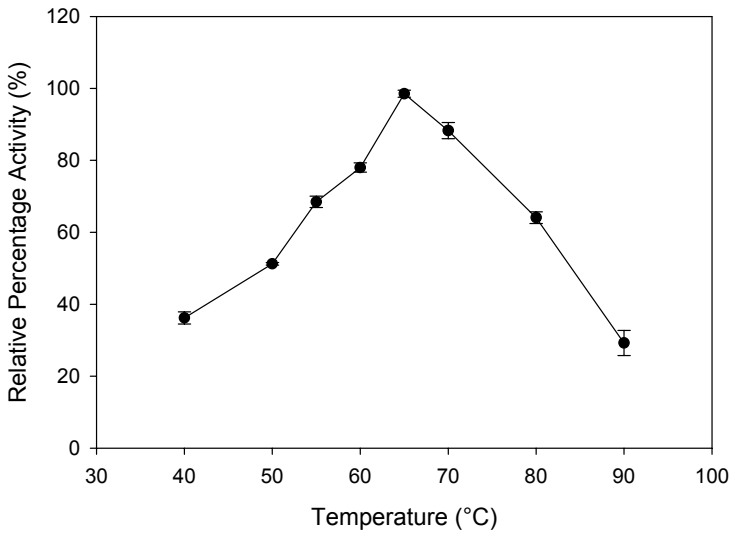

Figure 4.11: Effect of temperature on the activity of the purified chromate reductase. Activity at the optimum temperature (65°C) was taken as 100%. Error bars indicate standard error.

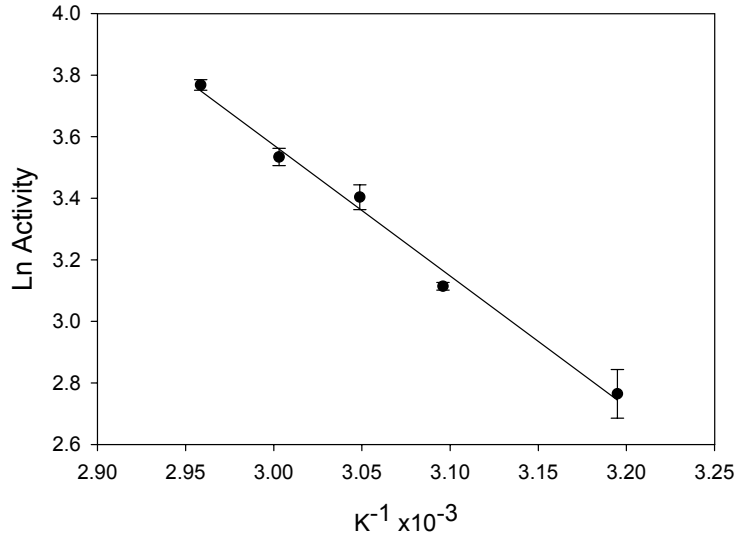

Figure 4.12: Arrhenius plot for the calculation of activation energy of the peripherally-bound chromate reductase. Error bars indicate standard error.

The activation energy was calculated at 35 kJ.mol^{-1}, which is very similar to that of the cytoplasmic chromate reductase.

4.3.2.2 Steady-state kinetics

The presence of an electron donor was absolutely required for Cr(VI) reducing activity and both NADH and NADPH could be utilized as an electron donor. The enzyme showed a preference towards NADH as NADPH only gave 37.3 % of the chromate reducing activity relative to the same concentration of NADH.

The enzyme showed substrate-saturation kinetics with both Cr(VI) and NADH (Figure 4.13), with apparent K_m values obtained for NADH and Cr(VI) 55.2 ± 2.0 µM and 55.5 ± 4.2 µM respectively, and corresponding V_{max} values of 1.7 ± 0.03 and 2.3 ± 0.09 µmol Cr(VI).min^{-1}.mg^{-1}. The affinity for Cr(VI) (K_m) of the peripherally-bound membrane chromate reductase was more than 6 times less that that of the cytoplasmic chromate reductase. Although the catalytic efficiency (k_{cat}/K_m) is comparable to the quinone reductases (ChrR), and more efficient than the nitroreductases (NfsA) (Table 4.2), it is more than 30 times less efficient than the cytoplasmic chromate reductase.

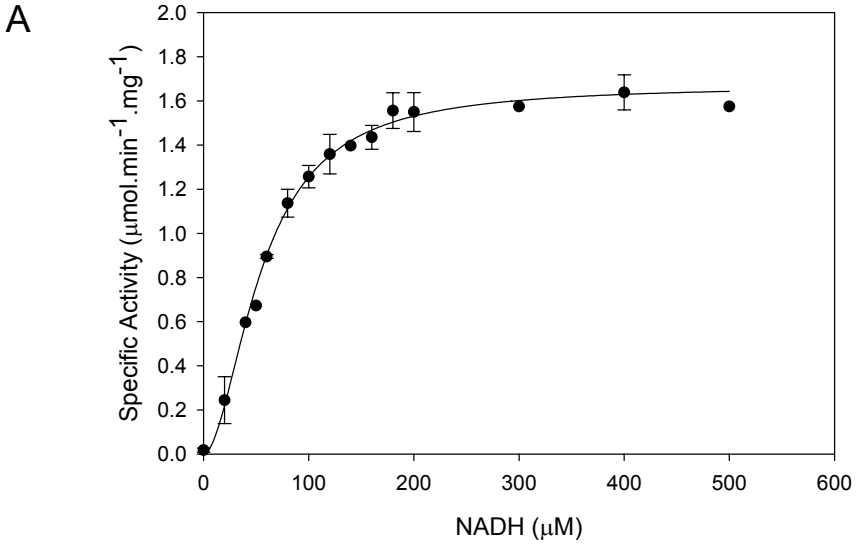

B

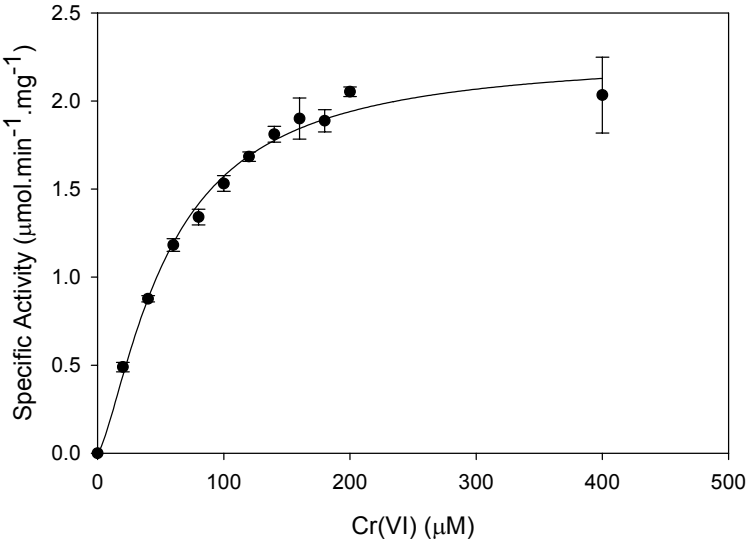

Figure 4.13: Steady-state kinetics of the purified chromate reductase illustrating the dependence of initial velocities against substrate concentrations. Reactions contained 20 mM MOPS-NaOH (pH 6.5), 5 mM EDTA, 0.1 mM Cr(VI) (A) and 0.3 mM NADH (B) and was performed at optimal conditions. Error bars indicate standard error.

Table 4.2: Comparison of kinetic parameters of various purified chromate reductases.

Organism (Enzyme)	V_{max} (μmol Cr(VI) min^{-1} mg^{-1} protein)	K_m (μM)	k_{cat} (s^{-1})	k_{cat}/K_m (M^{-1} s^{-1})	Reference
P. ambigua G-1	0.027	13	0.03	2.3×10^3	Suzuki *et al*., 1992
P. putida MK1	1.720	374	1.43	3.8×10^3	Park *et al*., 2000
V. harveyi (NfsA)	0.0107	5.4	0.009	1.65×10^3	Kwak *et al*., 2003
P. putida (ChrR)	8.800	260	5.8	2.2×10^4	Ackerley *et al*., 2004B
E. coli (YieF)	5.000	200	3.7	1.9×10^4	Ackerley *et al*., 2004B
E. coli (NfsA)	0.250	36	0.23	6.3×10^3	Ackerley *et al*., 2004A
T. scotoductus SA-01[a]	16.0	8.4	9.58	1.2×10^6	Chapter 3
T. scotoductus SA-01[b]	2.3	55.5	1.85	3.3×10^4	

[a] Cytoplasmic chromate reductase

[b] Peripherally-bound membrane chromate reductase

4.3.2.3 N-terminal sequencing

Edman degradation sequencing of the peripherally-bound chromate reductase N-terminal sequence identified the 14 amino acids MKTYDLIVIGTGPG, which was identical to the N-terminal sequence of a putative dihydrolipoamide dehydrogenase from *Thermus thermophilus* determined through whole-genome sequencing.

4.4 CONCLUSIONS

An additional chromate reductase, distinct from the previously described cytoplasmic chromate reductase, has been identified and purified from *T. scotoductus* SA-01.

This membrane-associated chromate reductase is a homodimer enzyme with a monomer molecular weight of approximately 48 kDa containing a non-covalently bound FAD co-factor and couple the reduction of Cr(VI) to NAD(P)H oxidation, with a preference towards NADH. The enzyme is optimally active at a pH of 6.5 and 65 °C with a K_m of 55.5 ± 4.2 µM and V_{max} of 2.3 ± 0.1 µmol Cr(VI) min^{-1} mg^{-1} protein. The affinity for Cr(VI) (K_m) of the membrane-associated chromate reductase was more than 6 times less that that of the cytoplasmic chromate and more than 30 times less catalytic efficient (k_{cat}/K_m) than the cytoplasmic chromate reductase. However, the catalytic efficiency (k_{cat}/K_m) of the enzyme was found to be comparable to that found for quinone reductases but more efficient than the nitroreductases.

N-terminal sequencing, yielding a sequence of 14 amino acids, confirmed the membrane-associated chromate reductase to be distinct from the cytoplasmic chromate reductase and is identical to the N-terminal sequence of a putative dihydrolipoamide dehydrogenase from *Thermus thermophilus*.

CHAPTER 5

IDENTIFICATION OF THE GENE SEQUENCES CODING THE CHROMATE REDUCTASES

5.1 INTRODUCTION

Although a variety of bacteria has been identified as having Cr(VI) reducing properties, very few of the responsible chromate reductases have been purified and characterized with respect to their gene sequence in order to elucidate their true function.

Most research has focused on soluble enzymes such as a group of cytoplasmic dimeric flavoproteins identified as chromate reductases from *Pseudomonas putida* and *Escherichia coli* (Park *et al*., 2000; Ackerley *et al*., 2004B). Sequence similarities however indicate these enzymes likely to be quinone reductases. A soluble homodimeric iron(III) reductase (FerB) with a noncovalently bound FAD coenzyme from *Paracoccus denitrificans* also shows high sequence homology with the chromate reductase from *P. putida* and flavin reductases (Fre) from *P. syringae*, and has furthermore been shown to be able to reduce Cr(VI) and quinones but not free flavins (Mazoch *et al*., 2004).

The chromate reductase purified from *Pseudomonas ambigua* showed high homology to nitroreductases (NfsA) from both *E. coli* and *Vibrio harveyi* which also have chromate reductase activity (Suzuki *et al*., 1992; Kwak *et al*., 2003; Ackerley *et al*., 2004A). A flavin reductase (Fre) system from *E. coli* also reduces Cr(VI) to a soluble Cr(III)-NAD^+ complex *via* unbound, highly active reduced flavins (Puzon *et al*., 2005). The close relatedness of the nitroreductases (NfsA) and flavin reductases has previously been shown by Zenno and co-workers when the NfsA from *E. coli* was transformed from a nitroreductase into a flavin reductase with activity comparable to that of the native flavin reductase of *Vibrio harveyi* (Zenno *et al*., 1998) through a single amino acid substitution within the active site.

This chapter describes the elucidation of the gene sequences coding for the chromate reductases identified from *T. scotoductus* SA-01 through their Cr(VI) reducing activity and describing their possible physiological functions.

5.2 MATERIALS AND METHODS

5.2.1 Construction of genomic DNA library

5.2.1.1 Total genomic DNA isolation

Total genomic DNA (gDNA) was isolated using a modified SDS-proteinase K treatment method of Towner (1991). Cells were harvested from mid-exponential phase using centrifugation (3000 x g, 10 min, 4°C) and washed in TE-buffer (10 mM Tris-HCl, 1 mM EDTA, pH 8). The cell pellet was finally resuspended in resuspension buffer [50 mM Tris-HCl (pH 8) containing 0.7 mM sucrose] in a 6.4 ml:1 g (wet weight) ratio. Lysozyme was added to a final concentration of 3.2 $mg.ml^{-1}$ and placed on ice for 5 min. Following the addition of EDTA and SDS to final concentrations of 68 mM and 1% respectively, the sample was mixed gently and again placed on ice for 5 min. 10 ml digestion buffer [1% SDS, 50 mM Tris-HCl (pH 9); 0.1 M EDTA; 0.2 M NaCl and 0.5 $mg.ml^{-1}$ proteinase K] was added to the mixture for every 0.5 g cells (wet weight). The suspension was incubated overnight at 55°C with mild shaking.

The volume was doubled using pH calibrated biophenol and incubated for 3 h at 25°C with gentle mixing, followed by centrifugation at 4000 x g for 10 min at 25°C. The supernatant was mixed with one volume phenol:chloroform:isoamylalcohol [25:24:1 (v/v/v)] and centrifuged at 3000 x g for 10 min at 25°C. The supernatant was mixed with one volume chloroform:isoamylalcohol [24:1 (v/v)] and centrifuged at 3000 x g for 10 min at 25°C. The supernatant was placed on ice for 5 min after which one-tenth the volume 5 M NaCl (pH 5.7) and 10 ml 100% ice cold ethanol was added. The precipitated DNA was spooled from suspension and centrifuged for 1 min at 4°C. The DNA pellet was washed using 70% ethanol and again centrifuged for 1 min at 4°C. The air dried pellet were resuspended in 50 mM Tris-HCl buffer (pH 8) and incubated for 1 h at 50°C where after RNase A was added to a final concentration of 20 $\mu g.ml^{-1}$ and incubated at 37°C for 1 h. DNA integrity was evaluated on a 0.8% agarose gel.

5.2.1.2 Partial restriction digest

Total gDNA was subjected to restriction digestion using the restriction endonuclease *Sau*3AI (New England BioLabs). A serial dilution of the enzyme was made to ensure a

range of DNA fragments (Table 5.1). The reaction mixtures contained gDNA, 1x NeBuffer *Sau*3AI, 100 µg.ml^{-1} BSA and *Sau*3AI, ranging from 250 U.ml^{-1} to 4.6 U.ml^{-1}.

Table 5.1: Partial restriction digest mixtures of total genomic DNA with *Sau*3AI.

	Reactions				
	A	**B**	**C**	**D**	**E**
DNA Mix	30 µl	20 µl	20 µl	20 µl	10 µl
1µl BSA 10µl buffer 89µl gDNA					
***Sau*3AI**	2 µl	10 µl of A	10 µl of B	10 µl of C	10 µl of D
	250 U.ml^{-1}	83 U.ml^{-1}	28 U.ml^{-1}	9 U.ml^{-1}	4.6 U.ml^{-1}

The reactions were incubated for 15 min at 37°C whereafter the enzyme was heat inactivated at 65°C for 20 min. The digested gDNA were separated on a 0.8% agarose gel (Fermentas TopVision LM GC) and fragments ranging from 3 to 6 kbp were excised and purified using the GFX PCR DNA and Gel Band Purification kit (Amersham Biosciences). DNA concentrations were determined using a BioPhotometer (Eppendorf).

5.2.1.3 Plasmid preparation

pTrueBlue (GenomicsOne) vector (Slilaty & Lebel, 1998) was used as cloning vector for genomic library construction. pTrueBlue was proliferated by transforming 2 µl into One Shot TOP10 *E. coli* competent cells (Invitrogen), according to the manufacturers instructions. Transformed cells were plated onto LB medium plates containing ampicillin (0.1 mg.ml^{-1}), isopropyl β-D-thiogalactoside (0.12 mg.ml^{-1}) and 5-bromo-4-chloro-3-indolyl β-D-galactoside (0.08 mg.ml^{-1}) and incubated overnight at 37°C. 100 ml of LB-medium supplemented with 0.1 mg.ml^{-1} ampicillin was inoculated with transformed *E. coli* cells and again grown overnight at 37°C. Plasmid purification was performed using Qiagen Plasmid Midi kit according to the manufacturer's instructions.

pTrueBlue was linearized using the restriction enzyme *Bam*HI (New England Biolabs). The reaction mixture (100 µl) consisted of 100 ng.µl^{-1} plasmid, 1x NEBuffer *Bam*HI, 100 µg.ml^{-1} BSA and 5µl *Bam*HI (100 U). The reaction mixture was incubated for 3 h at 37°C

whereafter the reaction was stopped by purification of the linearized plasmid using the GFX PCR DNA and Gel Band Purification kit (Amersham Biosciences). DNA was eluted with 50 µl ddH_2O.

Linearized pTrueBlue was dephosphorylated using Antarctic phosphatase (New England BioLabs). 13 µl Antarctic phosphatase (65 U) and 7 µl Antarctic phosphatase reaction buffer were added to the 50 µl linearized plasmid. The reaction was incubated at 37°C for 4 h whereafter the enzyme was heat inactivated at 65°C for 15 min. Again the plasmid was purified using the GFX PCR DNA and Gel Band Purification kit (Amersham Biosciences). Purified plasmid was evaluated by agarose gel electrophoresis (0.8%) and DNA concentrations were determined using the BioPhotometer (Eppendorf).

5.2.1.4 Ligation

Size fractionated DNA fragments were ligated into pTrueBlue in a 1:2 and 1:3 vector:insert ratio using an average insert size of 4.5 kb for conversion of molar ratios to mass ratios. The reaction mixtures (20 µl) contained 100 ng vector DNA, 310 ng or 465 ng insert DNA (1:2 and 1:3 vector:insert ratio respectively), 1x T4 DNA ligase buffer and T4 DNA ligase (New England BioLabs) (400 cohesive end ligation unit or 6 Weiss units). Ligations were performed overnight at 16°C.

5.2.1.5 Transformation

Ligation mixtures (5 µl and 10 µl) were transformed into One Shot TOP10 *E. coli* competent cells (Invitrogen) according to the manufacturer's recommendations. Transformed cells were plated onto LB medium plates (100 µl.plate^{-1}) containing ampicillin (0.1 mg.ml^{-1}), IPTG (0.12 mg.ml^{-1}) and X-Gal (0.08 mg.ml^{-1}), and incubated overnight at 37°C to verify DNA ligation using blue/white selection.

5.2.1.6 Evaluation of insert size

To evaluate the ligated insert sizes, 20 single white colonies were separately inoculated into 5 ml LB media containing ampicillin (0.1 mg.ml^{-1}) and incubated overnight at 37°C. Plasmids were isolated using the GeneJET Plasmid Miniprep Kit (Fermentas) as per manufacturer's instructions. Purified plasmids were subjected to double digestion with the restriction enzymes *Eco*RI and *Sal*I (Fermentas). 2 µl plasmid was incubated with 1 µl

Fermentas REase buffer O and 0.2 µl (2 U) of each restriction enzyme. The reaction mixture was made up to 10 µl with sterile ddH_2O and incubated for 1 h at 37°C after which the enzymes were heat inactivated at 65°C for 20 min. The restriction digestions were assessed by electrophoresis on a 0.8% agarose gel and analyzed using Quantity One V4.5 (Bio-Rad).

5.2.2 Screening of genomic DNA library

5.2.2.1 Oligonucleotide probe design

Oligonucleotide probes were designed from the N-terminal amino acid sequences of the cytoplasmic and peripheral-bound membrane chromate reductases. A codon usage table was constructed from four complete protein coding sequences (CDSs) available for *Thermus scotoductus* from the GenBank DNA sequence database. Codon preference was analyzed using Kazusa CountCodon (Nakamura *et al*., 2000).

5.2.2.2 Screening of genome library

Colony hybridization using digoxigenin (DIG) -labelled oligonucleotide probes was performed as described in the DIG Application Manual for Filter Hybridization (Roche). Agar plates containing overnight grown colonies were pre-cooled for 30 min at 4°C. Colonies were transferred to nylon membranes (Roche) by placing membrane discs (82 mm) onto the surface of the precooled plates for 1 min. Discs were removed and the bottom of the membranes were briefly blotted on dry sheets of filter paper. The discs (colonies facing up) were first soaked in 1 ml denaturation solution (0.5 M NaOH, 1.5 M NaCl) for 15 min, blotted on filter paper, and transferred to 1 ml neutralization buffer (1.5 M NaCl, 1 M Tris-HCl, pH 7.4) for 15 min and again blotted on filter paper. The membranes were transferred to 1 ml of 2x SSC solution for 10 min, followed by air-drying and crosslinking of DNA to the discs by UV light illumination (Bio-Rad GC Gene Linker, 150 mJ). Cell debris was removed by incubating the membranes in 1 ml of proteinase K (60 $U.ml^{-1}$) for 1 h at 37°C, followed by blotting the membranes (colonies facing down) onto pre-wetted filter paper.

Membrane discs were placed in sealable hybridization bags (Roche) and incubated with 60 ml DIG Easy Hyb solution (Roche) for 60 min at 41°C and 33°C for the ChrM and ChrS probes respectively. Membranes were hybridized for 4 h with 10 ml DIG Easy Hyb solution containing 25 $ng.ml^{-1}$ DIG-labeled DNA probe at their respective temperatures. Membranes were washed twice with Low Stringency wash buffer (2x SSC, 0.1% SDS) for 5 min at room temperature, followed by two washes with High Stringency wash buffer (1x SSC, 0.1% SDS) at their hybridization temperatures. Membranes were briefly washed in Wash buffer followed by Blocking solution for 30 min. Anti-digoxigenin antibodies conjugated with alkaline phosphatase (AP) were used for the detection of DIG-labelled oligonucleotide probes by incubating 150 $mU.ml^{-1}$ antibody in Blocking solution (20 $ml.disc^{-1}$) with the membranes for 30 min. Unbound antibody was removed by washing the membranes twice for 15 min in Wash buffer. The membranes were equilibrated in Detection buffer and incubated overnight with 4-nitro blue tetrazolium chloride (NBT; 0.34 $mg.ml^{-1}$) and 5-bromo-4-chloro-3-indolyl phosphate (BCIP; 0.175 $mg.ml^{-1}$) solution (4 $ml.disc^{-1}$), whereafter the reactions were stopped by incubating the membranes in TE buffer.

Positive clones were identified on the master plates and inoculated into 5 ml LB-medium supplemented with 0.1 $mg.ml^{-1}$ ampicillin and grown overnight at 37°C. Plasmid extractions were performed using the GeneJET Plasmid Miniprep Kit (Fermentas) as per manufacturer's instructions. Insert sizes were evaluated as previously described. Confirmation of positively identified clones were performed by applying 2 µl of the purified plasmid directly onto nylon membranes (dot blot), cross-linking, hybridization and detection as described above using their respective DIG-labelled oligonucleotide probes.

5.2.3 DNA sequencing

Plasmid inserts were sequenced by Inqaba Biotechnical Industries (South Africa) using a Spectrumedix SCE2410 genetic analysis system (SpectruMedix LLC). Sequencing reactions were performed using the BigDye (v3.1) dye terminator cycle sequencing kit (Applied Biosystems) with the universal T7 promoter primer and pTrueBlueRev (5' GGGATGCGCAGCTAATC 3'), which were located on the plasmid vector. A primer

walking strategy was used to design subsequent internal primers for sequencing. Sequences were analyzed using Vector NTI 9.0.0 (Informax).

Homology searches against the GenBank database were performed using the Basic Logical Alignment Search Tool (BLAST) (Altschul *et al.*, 1990). Multiple alignments were done using CLUSTAL W Multiple Sequence Alignment software (Thompson *et al.*, 1994), while secondary structure prediction was done using 3D-PSSM (Kelley *et al*., 2000).

5.2.4 Analytical techniques

DNA concentrations were determined using a NanoDrop spectrophotometer (NanoDrop Technologies) and a BioPhotometer (Eppendorf).

5.3 RESULTS AND DISCUSSION

5.3.1 Construction of genomic DNA (gDNA) library

Total genomic DNA was isolated from *Thermus scotoductus* SA-01 using a modified SDS-proteinase K method (Figure 5.1A).

gDNA was digested using a serial dilution of *Sau*3AI giving a variety of fragment sizes, where 28 $U.ml^{-1}$ *Sau*3AI gave DNA fragments of approximately 3 kbp to 10 kbp (Figure 5.1B). Digested 3 kbp to 6 kbp DNA fragments were excised from the agarose gel and purified for construction of the genomic library.

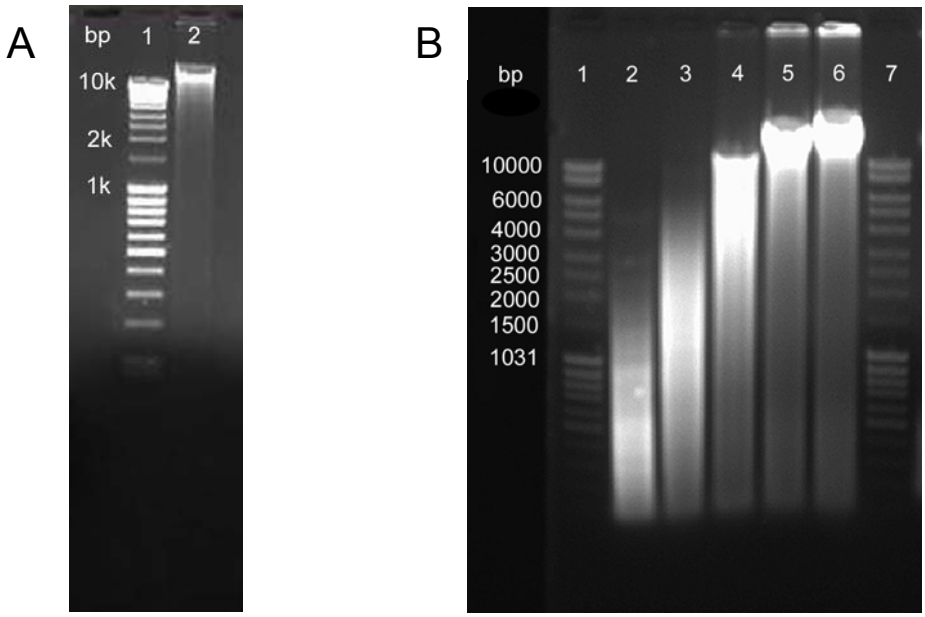

Figure 5.1: Total genomic DNA (lane 2) from *Thermus scotoductus* SA-01 (A). Partial restriction digestion of gDNA with *Sau*3AI using a serial dilution of restriction enzyme (lanes 2-6) (B). Lanes 1 and 7, molecular weight marker.

pTrueBlue plasmid were linearized with *Bam*HI to give compatible ends with the *Sau*3AI digested gDNA. The size fractionated DNA fragments were ligated into dephosphorylated linearized pTrueBlue vector in a 1:2 and 1:3 vector:insert ratio using an average insert size of 4.5 kb for conversion of molar ratios to mass ratios.

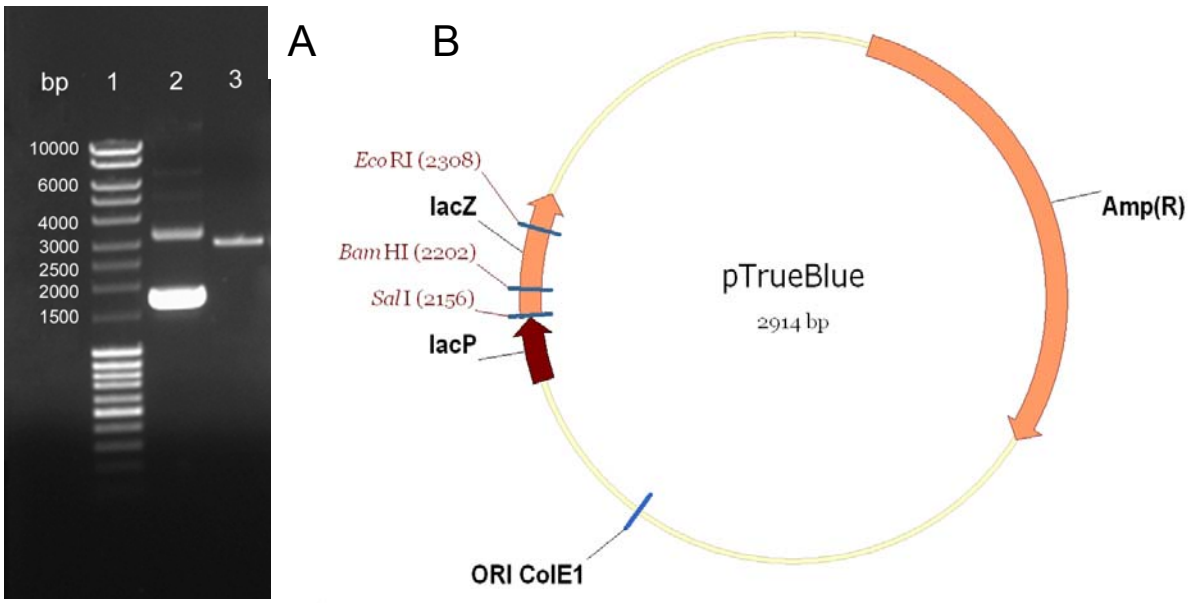

Figure 5.2: Supercoiled pTrueBlue plasmid (lane 2) and linearized plasmid using *Bam*HI (lane 3) (A). Lane 1, molecular weight marker. Vector map of pTrueBlue (B) indicating the ampicillin resistance gene, ColE1 origin of plasmid replication, *lac* promoter as well as the multiple cloning site within the *lac*Zα coding region.

The number of clones (N) required for a 99% probability (P) of the particular gene being represented in a library, was calculated using the Clarke and Carbon formula (Clarke & Carbon, 1976),

$$N = \frac{\ln(1-P)}{\ln(1-f)}$$

$$N = \frac{\ln(1-P)}{\ln\left(1-\frac{I}{GS}\right)}$$

where, N is the number of clones necessary to give a probability (P) of finding at least one clone for a give gene and f is the fraction of the genome (GS) represented by the average

insert size (I). In excess of 2000 clones were plated to ensure a one times redundancy gene library.

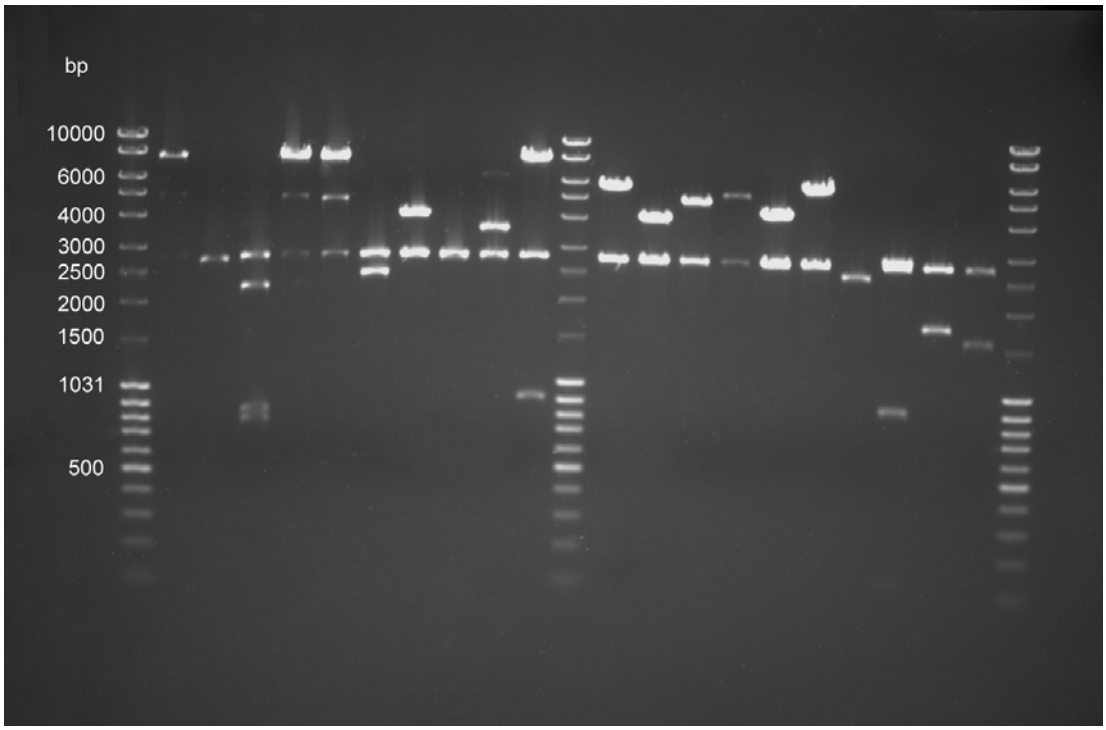

Figure 5.3: Double restriction digest of 20 clones with *Eco*RI and *Sal*I to evaluate the insert size of the genomic library.

Restriction digests of 20 clones indicated that 90% of the library consisted of recombinant clones, of which the majority contained inserts of the expected size range between 3 – 6 kbp (Figure 5.3).

5.3.2 Screening of genomic library

The oligonucleotide probes used for screening of the genomic library were designed from the N-terminal amino acid sequences of the chromate reductases. The first 14 (MKTYDLIVIGTGPG) and 9 (ALLFTPLEG) amino acids of the membrane-associated and cytoplasmic reductase were used respectively. Codon preferences of *Thermus scotoductus* was analyzed using the four complete protein coding sequences (CDSs) available from the GenBank DNA sequence database to design probable degenerate oligonucleotide probes.

Table 5.2: Sequences of the degenerate oligonucleotide probes representing the N-terminal sequences of the chromate reductases designed for screening of the genomic library.

Probe	Oligonucleotide sequence (5'-3')
ChrM	ATG AAG ACS TAC GAY CTS ATC GTS ATC GGS ACS GGS CCS GGS
ChrS	GGC CTS CTS TTY ACS CCC CTS GAD GGS

S = G/C, Y = C/T, D = A/G/T

Screening of the genomic library through colony hybridizations identified several positive clones (Figure 5.4A). Positive inserts were confirmed by dot blot hybridization with plasmid isolations of these clones with their respective DIG-labeled probes (Figure 5.4B). Four positive clones for the membrane-associated reductase and two positive clones for the cytoplasmic reductase were retained for further analysis.

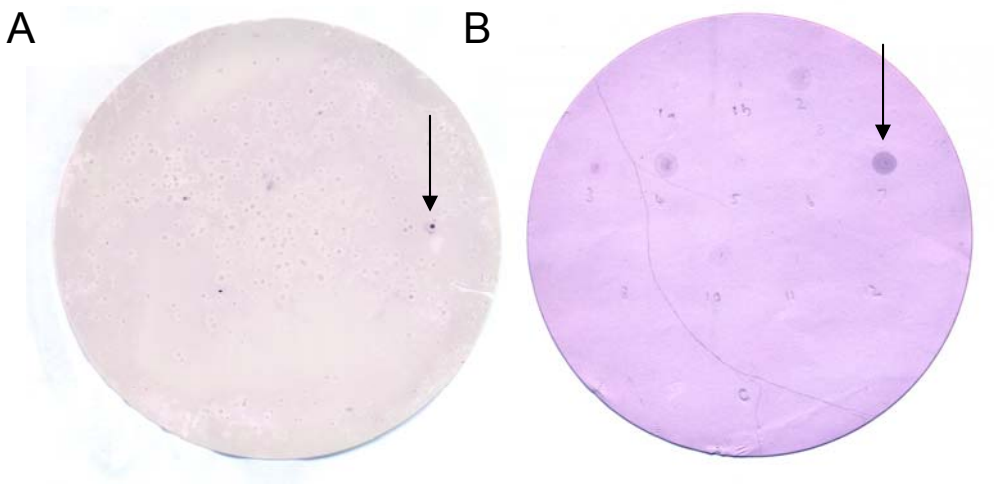

Figure 5.4: Representative colony (A) and dot-blot (B) hybridizations used for screening the genomic library for clones containing genes of interest using DIG-labeled probes and colorimetric detection. Positive colonies or plasmid are indicated.

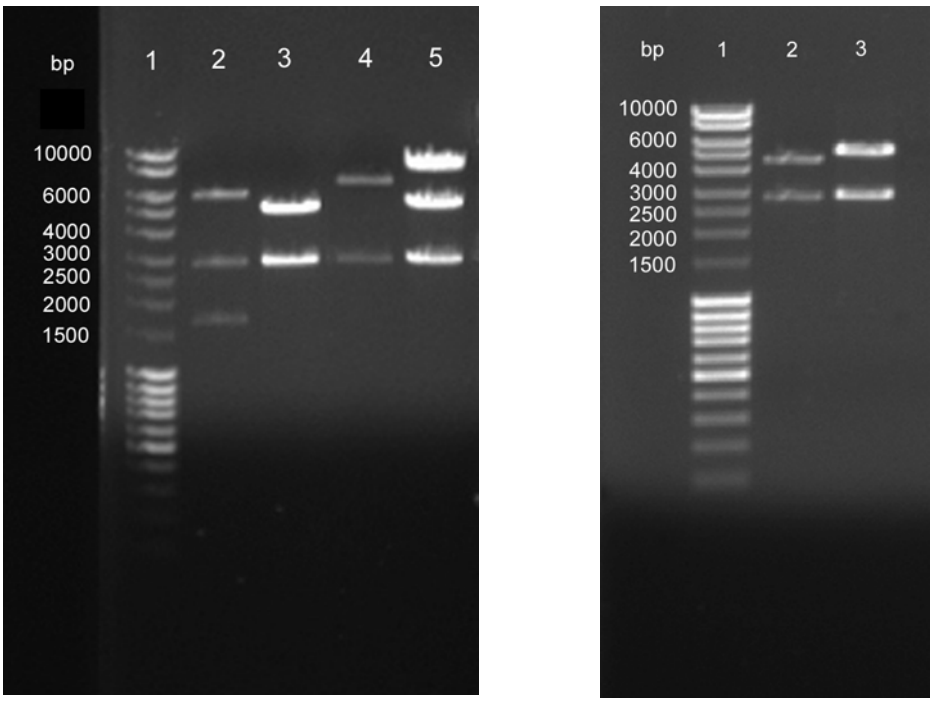

Figure 5.5: Double restriction digests of positive clones identified in genomic library screening for the peripherally bound membrane (lanes 2 – 5, A) and cytoplasmic (lanes 2 and 3, B) chromate reductase with *Eco*RI and *Sal*I to evaluate insert size. Lanes 1, molecular weight marker.

5.3.3 Sequence analysis

5.3.3.1 Cytoplasmic chromate reductase

Sequence analysis of the clones confirmed the presence of the oligonucleotide probe sequence and revealed an open reading frame (ORF) of 1050 bp. GenBank similarity search (blastn) showed the ORF to have the highest sequence identity to a probable NADH-dependent flavin oxidoreductases from *Thermus thermophilus* HB8 (86%), from whole-genome sequencing. Computational analysis of the chromate reductase gene showed it to encode a single protein of 349 amino acids with a predicted molecular mass of 37.98 kDa, consistent with the experimental molecular weight, and a theoretical pI of 7.83.

A putative ribosome binding site (GGAGG) was identified directly upstream of the ORF (Figure 5.6), but is uncharacteristically close to the start codon, with only one nt separation. The 5'-flanking region of the ORF also included putative -10 and -35 hexamer

promoter elements approximately 100 nt upstream of the translation initiation site, with the distance between these two hexamers being 18bp. The putative -35/-10 sequences are similar to the consensus *E. coli* sequences (TATAAT and TTGACA respectively) for the housekeeping σ^{70} factor (Hawley & McClure, 1983) as well as to promoters identified in *Thermus* species (Maseda & Hoshino, 1995).

A 9 bp inverted repeat was detected immediately downstream of the ORF indicating a putative transcription termination sequence (Figure 5.6).

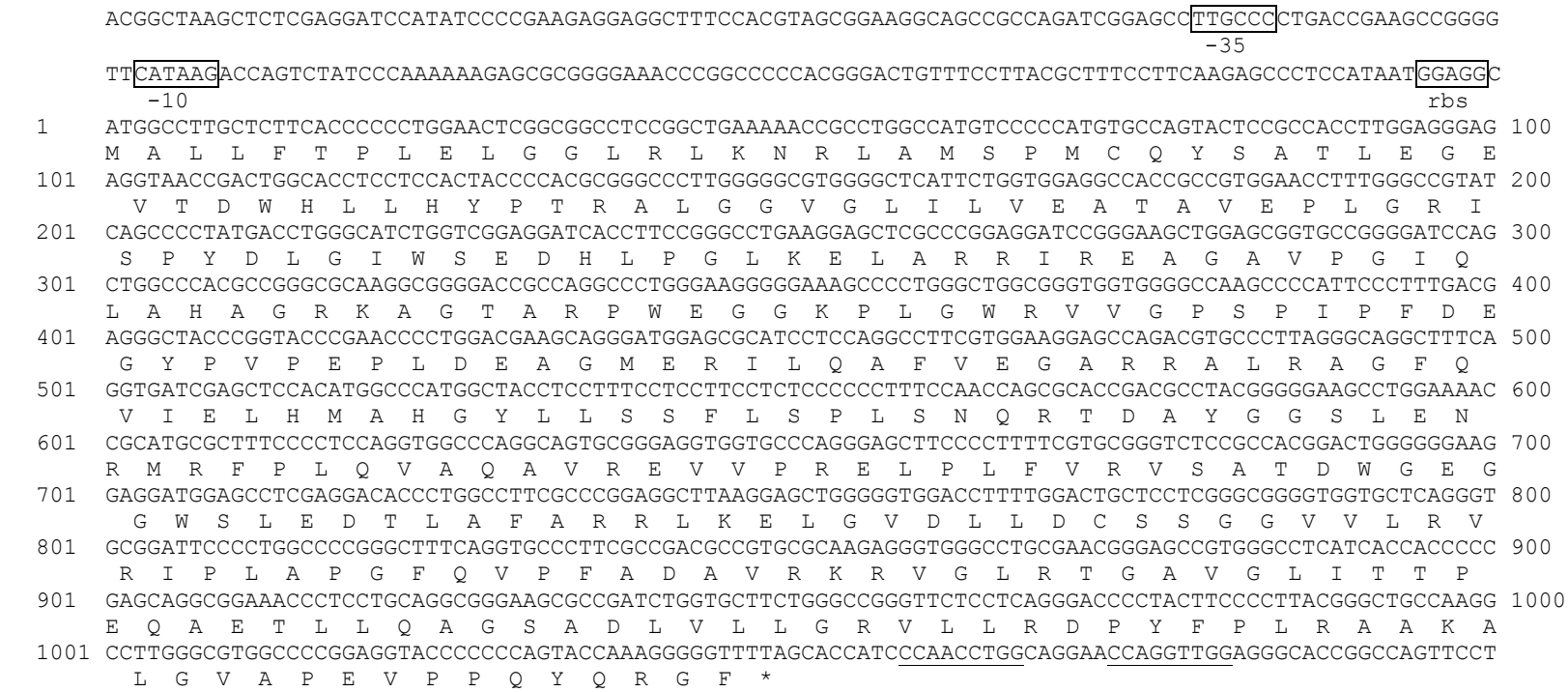

Figure 5.6: Nucleotide sequence of the chromate reductase of *Thermus scotoductus* SA-01 and deduced amino acid sequence. The putative -35 and -10 promoter regions and ribosome binding site (rbs) are boxed with the putative inverted termination sequences underlined.

Amino acid sequence comparison

BLAST analysis against the RCSB Protein Data Bank, of the predicted amino acid sequence, showed the highest homology (50% identity and 69% similarity) to be with an Old Yellow Enzyme homologue (YqjM) from *Bacillus subtilis* involved in the oxidative stress response through the reductive degradation of various xenobiotics (Fitzpatrick *et al*., 2003, Kitzing *et al*., 2005). High homology (45% identity and 60% similarity) with the xenobiotic reductase (XenA) from *Pseudomonas putida* 86, catalyzing the NAD(P)H-dependent reduction of electrophilic xenobiotics (Griese *et al*., 2006), was also found. Multiple alignments of the gene product with the predicted flavin oxidoreductases from *T. thermophilus* HB8 (NCBI:YP 143423), XenA from *P. putida* 86 (PDB:2H8X), YqjM from *B.* subtilis (PDB:1Z41A) and the predicted NADH:flavin oxidoreductase from *Geobacter metallireducens* (NCBI:YP 385521) are shown in Figure 5.7.

The *Bacillus* and *Pseudomonas* reductases have been shown to reduce a variety of xenobiotic substrates. Due to the broad substrate specificity of YqjM and other members of the family, as well as their involvement in the oxidative stress response, Fitzpatrick and co-workers (2003) speculate that it is unlikely that these enzymes have a single specific physiological substrate *in vivo* and that these enzymes could function in the maintenance of the cellular redox state. Reduction of Cr(VI) by cellular components to Cr(V) as well as transiently formed Cr(V) intermediate before complete reduction to Cr(III) by some flavoenzymes is thought to be a major cause of chromate oxidative stress and carcinogenesis through the formation of reactive oxygen species (ROS) (Shi & Dalal, 1990C; Liu & Shi, 2001). The NfsA (nitroreductase) from *E. coli*, has been shown to be able to pre-empt ROS generation and minimize oxidative stress during chromate reduction, protecting against chromate toxicity as well increasing Cr(VI) tolerance (Ackerley *et al*., 2004A).

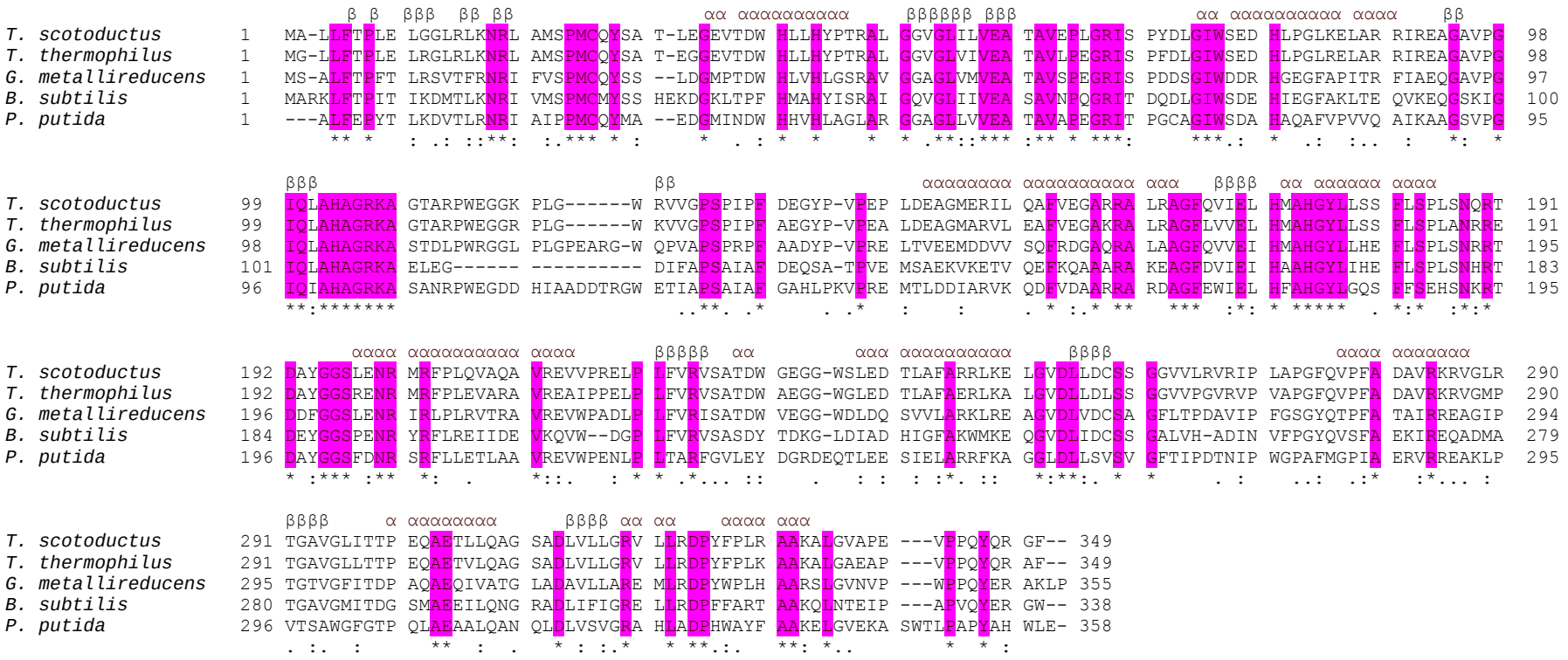

Figure 5.7: Multiple alignment (Clustal W) of the chromate reductase with the predicted NADH:flavin oxidoreductase from *Thermus thermophilus* (NCBI:YP 143423) and from *Geobacter metallireducens* (NCBI:YP 385521), with the xenobiotic reductase from *Pseudomonas putida* 86 (PDB:2H8X) and YqjM of *Bacillus subtilis* (PDB:1Z41A). Predicted secondary structure elements are indicated by α (helix) or β (sheet). Symbols indicate identical residues (*/purple), conserved substitutions (:) and semi-conserved substitutions (.).

The high degree of similarity between the chromate reductase and the Old Yellow Enzyme homologues suggests the characteristic $(\beta\alpha)_8$-barrel (TIM Barrel) fold. Secondary structure prediction also indicates 8 alternating β-sheets and α-helixes (Kelley *et al*., 2000). $(\beta\alpha)_8$-barrel folded proteins catalyze a variety of biochemical reactions and are amongst the most frequent folds observed (Nagano *et al*., 2002; Vega *et al*., 2003).

Multiple alignments of the chromate reductase with homologous enzymes (Figure 5.7) showed that the sequence identities corresponded to the functionally important amino acids identified in YqjM and XenA involved in lining the active-site and especially those involved in the interaction between the apoprotein and FMN. In YqjM, a sulphate ion from the crystallization solution occupied the catalytic site on the isoalloxazine ring of the FMN and in XenA, a sulphate ion could be modeled into the same position (Figure 5.8). The residues able to interact with the sulphate ion are also conserved in the chromate reductase (specifically His173, His176 and Tyr178) (Figure 5.7). The structural similarity between sulphate and chromate could be an indication as to how chromate binds as a substrate in the catalytic site. In addition, Kitzing and co-workers (2005) showed that the active site of YqjM is hydrophobic, wide open and easily accessible and that this huge substrate binding pocket allows the binding of a variety of different substrates (including the possibility of other proteins) to control the cellular redox state.

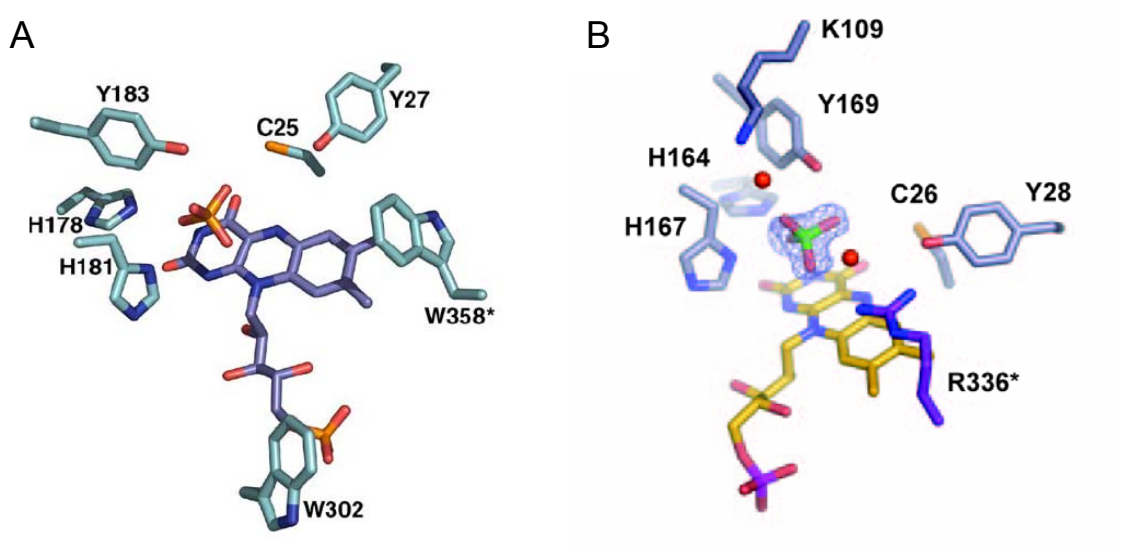

Figure 5.8: Substrate binding sites of the flavoproteins XenA from *Pseudomonas putida* (A; Kitzing *et al.*, 2005) and YqjM from *Bacillus subtilis* (B; Griese *et al.*, 2006) complexed with sulphate. An asterisk denotes a residue from the adjacent monomer extending into the catalytic site.

5.3.3.2 Peripherally bound membrane chromate reductase

Sequence analysis of the clones showed that the peripherally bound membrane enzyme is coded for by an open reading frame (ORF) of 1386 bp. GenBank similarity search (blastn) indicated the ORF had a 84% and 83% identity with the dihydrolipoamide dehydrogenase from *Thermus thermophilus* HB8 and HB27 respectively. The ORF encoded for a single protein of 461 amino acids with a calculated molecular mass of 48.5 kDa, which is similar to the experimental monomer molecular mass of 48.2 kDa determined by SDS-PAGE analysis. The deduced amino acid sequence also matches the sequence obtained from N-terminal sequencing of the reductase (Figure 5.9). No promoter nor Shine-Dalgarno sequences (ribosome binding site) could be identified directly upstream of the ORF. Upstream flanking regions identified the gene to be located within a probable pyruvate dehydrogenase operon, as is also seen in the *Thermus thermophilus* genome (Henne *et al.*, 2004). An additional translation initiation codon is located 9 bp upstream (in-frame) of the start codon identified by N-terminal sequencing. Whether translation proceeds from

the second start codon or if the protein undergoes post-translational cleavage to remove the additional Met-Asp-Pro is unknown.

Amino acid sequence comparison

The protein was identified as a pyridine nucleotide-disulphide oxidoreductases with a class I active site. The deduced amino acid sequence shows high homology (blastp) to other bacterial dihydrolipoamide dehydrogenase (LPD) primary structures. The highest amino acid sequence identity (85%) was found with the LPD of *Thermus thermophilus* HB27 deduced from genome sequencing. Multiple alignments of the gene product with LPDs of *Thermus thermophilus*, *E. coli*, *Geobacillus stearothermophilus*, *Deinococcus radiodurans*, *Shewanella oneidensis* and *Pseudomonas putida* showed very high homology within the conserved signature motifs of LPDs (Figure 5.9). These motifs include the NADH and FADH binding sites, the pyridine nucleotide-disulphide oxidoreductase class-I active site, the central domain region and the interface domain that surrounds the His-Glu active site diad (Carothers *et al*., 1989).

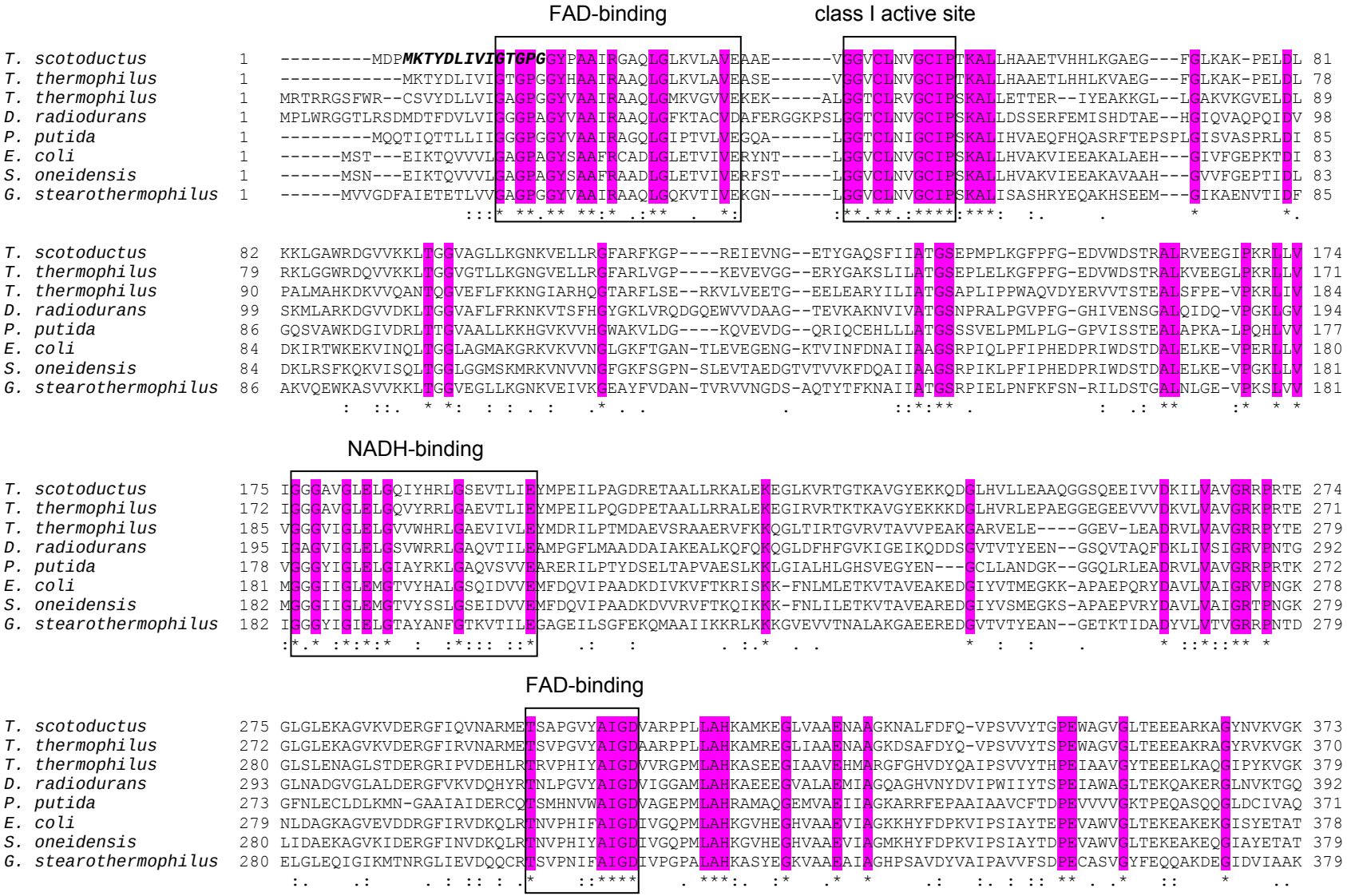
FAD-binding
class I active site
T. scotoductus 1 ---------MDPMKTYDLIVIGTGPGGYPAAIRGAQLGLKVLAVEAAE------VGGVCLNVGCIPTKALLHAAETVHHLKGAEG---FGLKAK-PELDL 81
T. thermophilus 1 ------------MKTYDLIVIGTGPGGYHAAIRAAQLGLKVLAVEASE------VGGVCLNVGCIPTKALLHAAETLHHLKVAEG---FGLKAK-PELDL 78
T. thermophilus 1 MRTRRGSFWR--CSVYDLLVIGAGPGGYVAAIRAAQLGMKVGVVEKEK-----ALGGTCLRVGCIPSKALLETTER--IYEAKKGL--LGAKVKGVELDL 89
D. radiodurans 1 MPLWRGGTLRSDMDTFDVLVIGGGPAGYVAAIRAAQLGFKTACVDAFERGGKPSLGGTCLNVGCIPSKALLDSSERFEMISHDTAE--HGIQVAQPQIDV 98
P. putida 1 ---------MQQTIQTTLLIIGGGPGGYVAAIRAGQLGIPTVLVEGQA------LGGTCLNIGCIPSKALIHVAEQFHQASRFTEPSPLGISVASPRLDI 85
E. coli 1 ------MST---EIKTQVVVLGAGPAGYSAAFRCADLGLETVIVERYNT-----LGGVCLNVGCIPSKALLHVAKVIEEAKALAEH---GIVFGEPKTDI 83
S. oneidensis 1 ------MSN---EIKTQVVVLGAGPAGYSAAFRAADLGLETVIVERFST-----LGGVCLNVGCIPSKALLHVAKVIEEAKAVAAH---GVVFGEPTIDL 83
G. stearothermophilus 1 ------MVVGDFAIETETLVVGAGPGGYVAAIRAAQLGQKVTIVEKGN------LGGVCLNVGCIPSKALISASHRYEQAKHSEEM---GIKAENVTIDF 85
T. scotoductus 82 KKLGAWRDGVVKKLTGGVAGLLKGNKVELLRGFARFKGP----REIEVNG--ETYGAQSFIIATGSEPMPLKGFPFG-EDVWDSTRALRVEEGIPKRLLV 174
T. thermophilus 79 RKLGGWRDQVVKKLTGGVGTLLKGNGVELLRGFARLVGP----KEVEVGG--ERYGAKSLILATGSEPLELKGFPFG-EDVWDSTRALKVEEGLPKRLLV 171
T. thermophilus 90 PALMAHKDKVVQANTQGVEFLFKKNGIARHQGTARFLSE--RKVLVEETG--EELEARYILIATGSAPLIPPWAQVDYERVVTSTEALSFPE-VPKRLIV 184
D. radiodurans 99 SKMLARKDGVVDKLTGGVAFLFRKNKVTSFHGYGKLVRQDGQEWVVDAAG--TEVKAKNVIVATGSNPRALPGVPFG-GHIVENSGALQIDQ-VPGKLGV 194
P. putida 86 GQSVAWKDGIVDRLTTGVAALLKKHGVKVVHGWAKVLDG----KQVEVDG--QRIQCEHLLLATGSSSVELPMLPLG-GPVISSTEALAPKA-LPQHLVV 177
E. coli 84 DKIRTWKEKVINQLTGGLAGMAKGRKVKVVNGLGKFTGAN-TLEVEGENG-KTVINFDNAIIAAGSRPIQLPFIPHEDPRIWDSTDALELKE-VPERLLV 180
S. oneidensis 84 DKLRSFKQKVISQLTGGLGGMSKMRKVNVVNGFGKFSGPN-SLEVTAEDGTVTVVKFDQAIIAAGSRPIKLPFIPHEDPRIWDSTDALELKE-VPGKLLV 181
G. stearothermophilus 86 AKVQEWKASVVKKLTGGVEGLLKGNKVEIVKGEAYFVDAN-TVRVVNGDS-AQTYTFKNAIIATGSRPIELPNFKFSN-RILDSTGALNLGE-VPKSLVV 181
NADH-binding
T. scotoductus 175 IGGGAVGLELGQIYHRLGSEVTLIEYMPEILPAGDRETAALLRKALEKEGLKVRTGTKAVGYEKKQDGLHVLLEAAQGGSQEEIVVDKILVAVGRRPRTE 274
T. thermophilus 172 IGGGAVGLELGQVYRRLGAEVTLIEYMPEILPQGDPETAALLRRALEKEGIRVRTKTKAVGYEKKKDGLHVRLEPAEGGEGEEVVVDKVLVAVGRKPRTE 271
T. thermophilus 185 VGGGVIGLELGVVWHRLGAEVIVLEYMDRILPTMDAEVSRAAERVFKKQGLTIRTGVRVTAVVPEAKGARVELE----GGEV-LEADRVLVAVGRRPYTE 279
D. radiodurans 195 IGAGVIGLELGSVWRRLGAQVTILEAMPGFLMAADDAIAKEALKQFQKQGLDFHFGVKIGEIKQDDSGVTVTYEEN--GSQVTAQFDKLIVSIGRVPNTG 292
P. putida 178 VGGGYIGLELGIAYRKLGAQVSVVEARERILPTYDSELTAPVAESLKKLGIALHLGHSVEGYEN---GCLLANDGK--GGQLRLEADRVLVAVGRRPRTK 272
E. coli 181 MGGGIIGLEMGTVYHALGSQIDVVEMFDQVIPAADKDIVKVFTKRISKK-FNLMLETKVTAVEAKEDGIYVTMEGKK-APAEPQRYDAVLVAIGRVPNGK 278
S. oneidensis 182 MGGGIIGLEMGTVYSSLGSEIDVVEMFDQVIPAADKDVVRVFTKQIKKK-FNLILETKVTAVEAREDGIYVSMEGKS-APAEPVRYDAVLVAIGRTPNGK 279
G. stearothermophilus 182 IGGGYIGIELGTAYANFGTKVTILEGAGEILSGFEKQMAAIIKKRLKKKGVEVVTNALAKGAEEREDGVTVTYEAN--GETKTIDADYVLVTVGRRPNTD 279
FAD-binding
T. scotoductus 275 GLGLEKAGVKVDERGFIQVNARMETSAPGVYAIGDVARPPLLAHKAMKEGLVAAENAAGKNALFDFQ-VPSVVYTGPEWAGVGLTEEEARKACYNVKVGK 373
T. thermophilus 272 GLGLEKAGVKVDERGFIRVNARMETSVPGVYAIGDAARPPLLAHKAMREGLIAAENAAGKDSAFDYQ-VPSVVYTSPEWAGVGLTEEEAKRAGYRVKVGK 370
T. thermophilus 280 GLSLENAGLSTDERGRIPVDEHLRTRVPHIYAIGDVVRGPMLAHKASEEGIAAVEHMARGFGHVDYQAIPSVVYTHPEIAAVGYTEEELKAQGIPYKVGK 379
D. radiodurans 293 GLNADGVGLALDERGFVKVDQHYRTNLPGVYAIGDVIGGAMLAHKAEEEGVALAEMIAGQAGHVNYDVIPWIIYTSPEIAWAGLTEKQAKERGLNVKTGQ 392
P. putida 273 GFNLECLDLKMN-GAAIAIDERCQTSMHNVWAIGDVAGEPMLAHRAMAQGEMVAEIIAGKARRFEPAAIAAVCFTDPEVVVVGKTPEQASQQGLDCIVAQ 371
E. coli 279 NLDAGKAGVEVDDRGFIRVDKQLRTNVPHIFAIGDIVGQPMLAHKGVHEGHVAAEVIAGKKHYFDPKVIPSIAYTEPEVAWVGLTEKEAKEKGISYETAT 378
S. oneidensis 280 LIDAEKAGVKIDERGFINVDKQLRTNVPHIYAIGDIVGQPMLAHKGVHEGHVAAEVIAGMKHYFDPKVIPSIAYTDPEVAWVGLTEKEAKEQGIAYETAT 379
G. stearothermophilus 280 ELGLEQIGIKMTNRGLIEVDQQCRTSVPNIFAIGDIVPGPALAHKASYEGKVAAEAIAGHPSAVDYVAIPAVVFSDPECASVGYFEQQAKDEGIDVIAAK 379

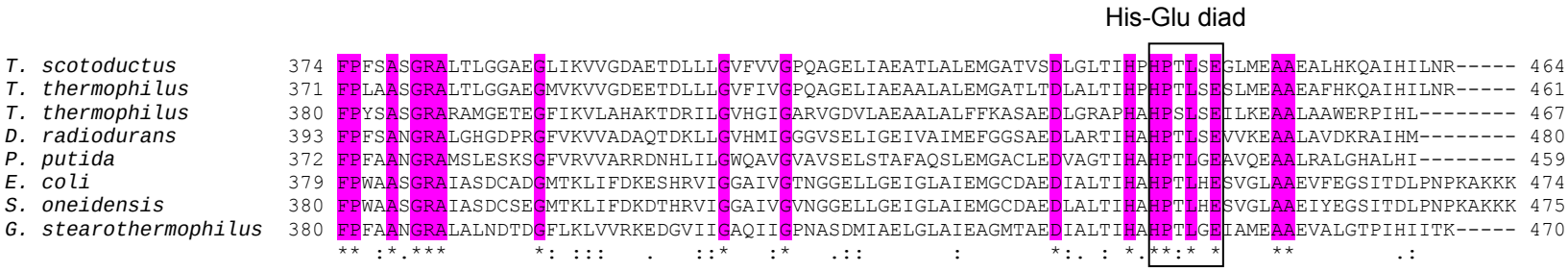

Figure 5.9: Multiple alignment (Clustal W) of the deduced amino acid sequence of the dihydrolipoamide dehydrogenase (LPD) from *Thermus scotoductus* SA-01 with the LPD counterparts in *Thermus thermophilus* HB27 (YP005722 & YP005669), *Deinococcus radiodurans* R1 (NP296246), *Pseudomonas putida* PpG2 (AAA65618), *Escherichia coli* CFT073 (NP752095), *Shewanella oneidensis* MR-1 (NP 716063) and *Geobacillus stearothermophilus* NCA 1503 (CAA37631). Boxed sequences show the FAD-binding, disulphide from the active site, NADH-binding and His-Glu active site diad domains. Sequence determined by Edman degradation shown in italics. Symbols indicate identical residues (*/purple), conserved substitutions (:) and semi-conserved substitutions (.).

Dihydrolipoamide dehydrogenases are part of the multisubunit pyruvate dehydrogenase complex (PDH), ubiquitously found in aerobic bacteria, where it catalyzes the conversion of pyruvate to acetyl-CoA. Bacterial pyruvate dehydrogenase complexes consist of multiple copies of the enzymes pyruvate dehydrogenase/decarboxylase (E1), dihydrolipoamide transacetylase (E2) and dihydrolipoamide dehydrogenase (E3) (De Kok *et al.*, 1998; Neveling *et al.*, 1998). Lehmacher and Bisswanger (1988) isolated the LPD from *Thermus flavus*, showing that it occurred as an uncomplexed homodimer in higher amounts than found associated with the PDH complex at reduced temperatures. The destabilizing effects of the high-ionic strength buffer used for extraction in this study as well as the decreased hydrophobic interactions between subunits due to lower temperatures could have dissociated the LPD from the PDH complex as well as the membranes, as sequencing of the upstream flanking regions indicate the protein within a probable PDH operon. The predicted subcellular location of the protein however was determined to be cytoplasmic in Gram negative bacteria [PSORTb (Gardy *et al.*, 2005)] and no transmembrane regions were detected with Kyte and Doolittle hydrophobicity plots (data not shown). Only the C-terminal and N-terminal regions showed higher hydrophobicity and correspond to the interface domain surrounding the active site residues.

Dihydrolipoamide dehydrogenases belong to the family of pyridine nucleotide-disulphide oxidoreductases (class I active site) which also includes glutathione reductase, mercuric reductase and trypanothione reductases and are identifiable by the consensus pattern GGXC[LIVA]XXGC[LIVM]P (PROSITE database PS00076) that surrounds the two redox-active cysteine residues located near the N-terminus (Argyrou & Blanchard, 2004). Additional highly conserved functional motifs of LPDs identified include the βαβ-structures (GXGXXGXXXGXXXXXXG and GXGXXGXXXAXXXXXXG) involved in NAD and FAD binding (Wierenga *et al*., 1986; Eggink *et al*., 1990) and an essential His-Glu diad at the C-terminus of the protein (Benen *et al.*, 1992).

The protein was purified as a functional homodimer (chapter 4) with a monomer molecular weight of approximately 48 kDa and a non-covalently bounded FAD cofactor. LPDs form homodimers with two identical active sites at the subunit interface. Each active site consists of the redox-active disulphide and cofactor binding domain of one subunit and the

His-Glu diad from the second monomer subunit, resulting in the native dimeric form of the enzyme being active (De Kok *et al.*, 1998; Argyrou & Blanchard, 2004). Electron transfer from NADH to Cr(VI) was mediated *via* the reduction of a bound FAD as could be observed through characteristic UV-visible spectra changes. The overall mechanism of LPDs can be divided into reductive and oxidative phases. During the reductive half-reaction, NAD(P)H binds to the oxidized enzyme (E_{ox}) and reduces the tightly bound FAD molecule to the transiently reduced flavin ($FADH_2$) intermediate. The electrons are then transferred to the redox-active disulphide (EH_2). In the oxidative half-reaction the substrate binds to the enzyme and the electrons are transferred *via* a general-acid catalysis by the His-Glu diad (Argyrou & Blanchard, 2004).

An additional four-electron-reduced state has, however, been demonstrated for LPDs. Since both the FAD and disulphide can accept electrons, an EH_4 reduction state, where both the flavin and the disulphide is reduced can exist (Argyrou *et al*., 2002; Argyrou *et al*., 2003). Dihydrolipoamide dehydrogenase was originally termed diaphorase because of its efficiency in catalyzing the NADH-dependent reduction of redox dyes, ferricyanide as well as quinones (Argyrou & Blanchard, 2004). Although the EH_4 state is not catalytically active towards lipoamide, diaphorase activity occurs at the EH_4 level (Argyrou *et al*., 2003). Reduction of quinones by pyridine nucleotide disulphide oxidoreductases is thought to proceed through one- or two electron transfers from the reduced flavin to the quinone substrate and that under steady-state conditions, the enzyme cycles between the EH_2 and EH_4 states (Argyrou *et al*., 2003; Argyrou & Blanchard, 2004). Whether Cr(VI) receives electrons directly from the reduced FAD is still under investigation. Reduction to the EH_4 level has also been proposed to promote the dissociation of the LPD into the monomeric subunits which could also mediate interaction with membranes (Argyrou & Blanchard, 2004).

Although LPD is a key enzyme between glycolysis and the citric acid cycle, its catalytic promiscuity could suggest that it might have additional physiological functions. Catalyzing diverse reactions including the reduction of quinones and Cr(VI) could prove advantageous in defense as a detoxification method. Interestingly, two probable LPDs (*lpdA* and *lpdB*) from *Mycobacterium tuberculosis* have been identified based on sequence

homology to other LPDs but lack some of the catalytic residues. Although unable to reduce lipoamide, the diaphorase activity is still present (Argyrou & Blanchard, 2001).

5.4 CONCLUSIONS

The cytoplasmic chromate reductase was identified to be encoded for by an ORF of 1050 bp, encoding a single protein of 38 kDa under the regulation of an *E. coli* σ^{70}-like promoter. Sequence analysis shows the chromate reductase to be related to the Old Yellow Enzyme (OYE) family, in particular the xenobiotic reductases (XenA) from *Pseudomonas putida* and YgjM from *Bacillus subtilis* involved in the oxidative stress response which has been speculated to be involved in the maintenance of cellular redox states. OYE was the first flavin oxidoreductase identified (Warburg & Christian, 1933) but despite over 70 years of research, the physiological reductants of most of the OYEs are still unknown (Williams & Bruce, 2002). However, the involvement of many of the OYE homologues in the oxidative stress response, as well as the broad range of electrophilic substrates (Kohli & Massey, 1998; Kitzing *et al*., 2005; Griese *et al*., 2006; Fitzpatrick *et al*., 2007) could suggest a general detoxification enzyme.

The membrane-associated chromate reductase was found to be encoded for by an ORF of 1386 bp, homologous to the dihydrolipoamide dehydrogenase genes. The ORF also encodes for a single protein of approximately 48 kDa located within a probable pyruvate dehydrogenase operon.

Several researchers have proposed that chromate reductases might be due to the serendipitous activity of enzymes with other primary physiological functions, as these fortuitous reactions are often carried out by constitutive enzymes. A general feature of these enzymes capable of Cr(VI) reduction is the presence of bound flavins or reduction mediated *via* unbound flavins (Ackerley *et al*., 2004A; Ackerley *et al*., 2004B; Puzon *et al*., 2005) and together with their comparable affinity for Cr(VI), suggests a similar catalytic mechanism. In contrast to the quinone reductases (ChrR), the nitroreductases (NfsA) and the cytoplasmic chromate reductase, the LPD contains a non-covalently bound FAD instead of FMN as well as the presence of a redox active disulfide. Thermodynamically, the reduction of Cr(VI) by flavins such as $FADH_2$ is very favourable due to the low standard electrochemical potential (E_0) of the $FADH_2$/FAD couple (E^0 < 0.2 V) compared to the redox potential of most Cr(VI)/Cr(III) couples (E^0 > 1.2 V) (Ball & Nordstrom, 1998; Petrat *et al*., 2003).

CHAPTER 6

HETEROLOGOUS EXPRESSION OF THE CHROMATE REDUCTASES IN *E. COLI* AND *T. THERMOPHILUS*

6.1 INTRODUCTION

The overproduction of enzymes from thermophiles are usually produced in mesophilic hosts such as *E. coli* (Bruins *et al*., 2001), which allows for its rapid purification through the thermal denaturation of the host's mesophilic enzymes. Several thermozymes have however been shown to be inactive when expressed in these mesophilic surrogates (Moreno *et al*., 2005; Hidalgo *et al*., 2004), due to the requirement of cofactors, inappropriate posttranslational modifications or incorrect multisubunit assembly. The high-level overproduction of recombinant proteins in *E. coli* also often results in misfolded proteins and in aggregation into inclusion bodies or in degradation (Thomas *et al*., 1997). *In vivo* protein folding is dependent on molecular chaperones and folding catalysts that facilitate proper folding (Thomas *et al*., 1997).

The recent development of gene expression vectors for *Thermus thermophilus* (Lasa *et al*., 1992; de Grado *et al*., 1999; Moreno *et al*., 2003; Moreno *et al*., 2005) has allowed the production of biotechnologically important thermozymes through the use of a homologous thermophilic host, circumventing many of the problems associated with heterologous expression in mesophilic hosts.

This chapter describes the heterologous expression of the chromate reductases, identified in *T. scotoductus*, in both the mesophile *E. coli* and thermophile *T. thermophilus*, and characterization of the recombinant enzymes with respect to activity as well as structural differences.

6.2 MATERIALS AND METHODS

6.2.1 Bacterial strains, plasmids and growth conditions

All bacterial strains and plasmids used in this study are listed in Table 6.1. *Thermus scotoductus* was cultured in TYG medium as described in section 2.2.1. *Thermus thermophilus* HB8 (ATCC 27634) was used as a host for expression at 65°C and was kindly provided by Dr. J. Berenguer (Universidad Autónoma de Madrid, Spain). HB8 was routinely cultured in TB medium (de Grado *et al*., 1999) consisting of 8 $g.L^{-1}$ tryptone, 4 $g.L^{-1}$ yeast extract and 3 $g.L^{-1}$ NaCl dissolved in mineral water (pH 7.5) with shaking (200 rpm). For plasmid selection, 30 $\mu g.ml^{-1}$ kanamycin was added to the TB medium plates solidified with 15 $g.L^{-1}$ agar.

Escherichia coli strains TOP10 (Invitrogen) and BL21(DE3) (Lucigen) were used as hosts for genetic manipulation and expression of proteins respectively. *E. coli* strains were grown in Luria-Bertani (LB) medium at 37°C with shaking (200 rpm). Kanamycin (30 $\mu g.ml^{-1}$) or ampicillin (100 $\mu g.ml^{-1}$) was added when required.

Plasmids pET-22b(+) and pET-28b(+) (Novagen) were used for expression of the proteins in *E. coli* BL21(DE3). For expression in *T. thermophilus* HB8, the bifunctional *E. coli-Thermus* sp. vector pMK18 (de Grado *et al.*, 1999) was used.

Table 6.1: Bacterial strains and plasmids used in this study.

Strain or plasmid	Description	Reference
Thermus scotoductus SA-01		ATCC 700910
Thermus thermophilus HB8		ATCC 27634
Escherichia coli TOP10	One Shot TOP10 chemically competent cells	Invitrogen
	F⁻ *mcr*A Δ(*mrr-hsd*RMS-*mcr*BC) Φ80*lac*ZΔM15 Δ*lac*X74 *rec*A1 *ara*D139 Δ(*ara-leu*)7697	
	*gal*U *gal*K *rps*L (Str^R) *end*A1 *nup*G	
Escherichia coli BL21(DE3)	*E.cloni* EXPRESS BL21(DE3) chemically competent cells	Lucigen
	F⁻ *ompT* $hsdS_B$ (r_{B-} m_B^-) *gal dcm* (DE3)	
pGEM-T Easy	Amp^r, T7 and SP6 promoter, *Lac*Z, ori	Promega
pET-22b(+)	Amp^r, T7 promoter, *Lac*I, ori	Novagen
pET-28b(+)	Kan^r, T7 promoter, *Lac*I, N-terminal His-Tag and Thrombin configuration, ori	Novagen
pMK18	Kan^r, PslpA promoter, RepA, ori	de Grado *et al*., 1999

6.2.2 Construction of expression plasmids

6.2.2.1 PCR amplification of chromate reductases

The complete chromate reductase genes were amplified by PCR from genomic DNA using the Expand High Fidelity PCR System (Roche). PCR reactions were performed in a total reaction volume of 50 µl using a Thermal Cycler (PxE 0.2, Thermo Electron Corporation). Reaction mixtures consisted of 10X Expand High Fidelity Buffer with 15 mM $MgCl_2$ (5 µl), dNTP's (0.8 mM), Expand High Fidelity Enzyme mix (1 µl), 50 ng of gDNA and 0.2 µM of both the forward and reverse primers. Primer sets for each product are given in Table 6.2. Reaction conditions consisted of an initial denaturing step at 95°C for 5 min, followed by 25 cycles of denaturing at 95°C (30 sec), annealing at 65°C (40 sec) and elongation at 72°C (1.5 min). A final elongation step of 10 min at 72°C was added to ensure complete elongation of amplified products.

Table 6.2: Primer sequences used for PCR amplification of the chromate reductases.

Amplicon / Primer	Sequence	T_m
CrS_F_Nde	5' CAT ATG GCC TTG CTC TTC ACC CCC CTG GAA CTC 3'	67.1°C
CrS_R_Eco	5' GAA TTC CTA AAA CCC CCT TTG GTA CTG GGG GGG TAC 3'	66.0°C
CrM_F1_Nde	5' CAT ATG GAC CCC ATG AAG ACC TAC GAC CTC ATC 3'	63.4°C
CrM_R_Eco	5' GAA TTC TCA ACG GTT CAG GAT GTG GAT GGC CTG TTT 3'	65.2°C
CrM_F2_Nde	5' CAT ATG AAG ACC TAC GAC CTC ATC GTG ATC GGC 3'	63.5°C
CrM_R_Eco	5' GAA TTC TCA ACG GTT CAG GAT GTG GAT GGC CTG TTT 3'	65.2°C

Underlined sequences indicate introduced restriction sites for *Nde*I and *Eco*RI

CrS_F/R – Cytoplasmic chromate reductase

CrM_F1/R – Membrane-associated chromate reductase from 1st predicted start codon

CrM_F2/R – Membrane-associated chromate reductase from 2nd start codon as identified from N-terminal sequencing of native protein

PCR products were purified from TopVision LM GQ (low melting point) agarose gel through excision of the gel bands and extraction using the GFX PCR DNA and Gel Band Purification Kit (Amersham Biosciences) according to the manufacturer's instructions.

6.2.2.2 Constructs for expression in E. coli

The purified PCR products were ligated into pGEM-T Easy vector using a 1:1 molar ratio overnight at 4°C according to the manufacturer's instructions and proliferated in One Shot TOP10 *E. coli* competent cells (Invitrogen) according to the manufacturer's instructions. Plasmids were isolated using the GeneJet MiniPrep kit (Fermentas). Plasmids containing inserts were double digested with the restriction enzymes *Nde*I (0.5 $U.\mu l^{-1}$, Fermentas) and *Eco*RI (0.5 $U.\mu l^{-1}$, Fermentas) at 37°C (Buffer O, 3 h) for ligation into the pET22b(+) and pET28b(+) similarly digested. Inserts and digested pET22b(+) and pET28b(+) vectors were cleaned from a low melting point agarose gel using the GFX PCR DNA and Gel Band Purification Kit. Cohesive end ligations were performed in a 1:1 molar ratio using 40 ng of vector. Ligations were performed in 20 µl reaction volumes overnight at 4°C with 1.5 Weiss $U.\mu l^{-1}$ T4 DNA ligase (New England Biolabs). Ligation mixtures were again transformed into TOP10 *E. coli* and positive clones were identified through plasmid isolation and restriction digestion as described above.

6.2.2.3 Constructs for expression in T. thermophilus

As the pMK18 bifunctional *E.coli-Thermus* sp. does not contain a ribosome binding site (RBS) upstream of the multiple cloning site, the RBS of the pET-vectors was utilized. Inserts together with the RBS of pET22b(+)/pET28b(+) were restriction digested from the constructed *E. coli* expression vectors through double digesting with *Xba*I and *Eco*RI. Reaction mixtures (50 µl) consisted of 2X Tango buffer (Fermentas), 40 U *Xba*I (Fermentas), 20 U *Eco*RI (Fermentas), and approximately 0.8 - 1 µg plasmid. Products were cleaned from an agarose gel for ligation into pMK18, similarly restriction digested.

Ligations were performed as described above in a 1:1 molar ratio using 60 ng of pMK18 vector overnight at 4°C. Ligation mixtures were transformed into TOP10 *E. coli*, and positive clones identified through plasmid isolation and restriction digestion as described above.

6.2.3 Expression of the chromate reductases

The pET22/28-chromate reductase constructs were transformed into *E. coli* BL21(DE3) competent cells (Lucigen) for expression. Positive clones were identified through selection on LB-plates containing 30 $\mu g.ml^{-1}$ kanamycin or 100 $\mu g.ml^{-1}$ ampicillin and inoculated into LB-medium also containing the appropriate antibiotic pressure. Cells were incubated with shaking (200 rpm) until an OD_{600nm} of approximately 0.8 – 1 was reached. IPTG was added as inducer to a final concentration of 1 mM and cells grown for an additional 4 h. Cells were harvested through centrifugation (8 000 x g, 10 min) and washed using 20 mM MOPS-NaOH (pH 7).

For expression in *T. thermophilus*, pMK18-chromate reductase constructs were transformed into *T. thermophilus* HB8 through its natural competency. *T. thermophilus* was grown in TB medium [8 $g.L^{-1}$ tryptone (Biolab), 4 $g.L^{-1}$ yeast extract (Biolab) and 3 $g.L^{-1}$ NaCl in mineral water, pH 7.5] until late exponential growth (OD_{600nm} of approximately 0.8) at 65°C with aeration (200 rpm). 0.8 ml of culture was added to approximately 0.5 µg plasmid and grown for an additional 4 h where after the transformation mixture were plated onto TB-plates containing 30 $\mu g.ml^{-1}$ kanamycin. Positive transformants were selected and inoculated into TB-medium containing 30 $\mu g.ml^{-1}$ kanamycin and grown until late exponential growth phase. Cells were harvested through centrifugation (8 000 x g, 10 min) and washed using 20 mM MOPS-NaOH (pH 7).

6.2.4 Purification of recombinant chromate reductases

Harvested cells were resuspended in 20 mM MOPS (pH 7.4) containing 50 mM imidazole and 0.5 M NaCl [approximately 1 g cells (wet weight) in 10 ml]. Cells were broken by ultrasonic treatment for 5 min (100 W), whereafter unbroken cells and debris were removed through centrifugation (8 000 x g for 10 min). The soluble fraction (cytoplasm) was separated from the insoluble fraction (membranes) through ultracentrifugation (100 000 x g, 90 min).

6.2.4.1 Purification of the cytoplasmic chromate reductase

The recombinant cytoplasmic chromate reductase was purified through immobilized metal-affinity chromatography (IMAC), hydrophobic interaction chromatography and size-exclusion chromatography.

The cytoplasmic fraction was loaded onto a HisTrap FF column (5 ml, Amersham Biosciences) and unbound proteins eluted (5 $ml.min^{-1}$) using 20 mM MOPS (pH 7.4) containing 50 mM imidazole and 0.5 M NaCl. Bound proteins were then eluted in the same buffer using a linear gradient (100 ml) of imidazole up to 0.5 M. Fractions containing activity were pooled for subsequent purification step.

Ammonium sulphate was added to the sample to a final concentration of 0.4 M and bound to a Phenyl-Toyopearl column (10 x 2.5 cm, Tosohaas). Unbound proteins were eluted using 20 mM MOPS (pH 7) containing 0.4 M $(NH_4)_2SO_4$ and 0.5 M NaCl, where after the bound proteins were eluted using a negative linear gradient of ammonium sulphate and NaCl to 0 M over 200 ml. Active fractions were pooled and concentrated on an Amicon stirrer cell through a 10 kDa MWCO membrane (Osmonics Inc.).

To ensure complete saturation of the apoprotein with FMN, 0.5 mg of FMN was added to the sample before size-exclusion chromatography. The 4 ml concentrated sample was loaded onto a Sephacryl S-100HR column (65 x 2.5 cm, Sigma) equilibrated with 10 mM Tris-H_2SO_4 (pH 7). Proteins were eluted using the same buffer at a flow speed of 0.5 $ml.min^{-1}$.

6.2.4.2 Purification of the membrane-associated chromate reductase

The recombinant membrane-associated chromate reductase was also located within the cytoplasmic fraction and was purified through immobilized metal-affinity chromatography (IMAC) and size-exclusion chromatography.

The cytoplasmic fraction was loaded onto a HisTrap FF column (5 ml, Amersham Biosciences) and unbound proteins eluted (5 $ml.min^{-1}$) using 20 mM MOPS (pH 7.4) containing 50 mM imidazole and 0.5 M NaCl. Bound proteins were then eluted in the same buffer using a linear gradient (100 ml) of imidazole up to 0.5 M. Active fractions

were pooled and concentrated on an Amicon stirrer cell through a 10 kDa MWCO membrane (Osmonics Inc.).

To ensure complete saturation of the apoprotein with FAD, 0.5 mg of FAD was added to the sample before size-exclusion chromatography. The 4 ml concentrated sample was loaded onto a Sephacryl S-200HR column (63 x 2.5 cm, Sigma) equilibrated with 20 mM MOPS-NaOH (pH 7) containing 50 mM NaCl. Proteins were eluted using the same buffer at a flow speed of 0.5 $ml.min^{-1}$.

6.2.5 Characterization of the recombinant proteins

6.2.5.1 Co-factor (flavin) content

UV-visible absorption spectra of the recombinant cytoplasmic chromate reductases were obtained at room temperature in 10 mM Tris-H_2SO_4 buffer (pH 7) in a Beckmann Coulter DU-800 spectrophotometer in a quartz cuvette. 20 mM MOPS-NaOH buffer (pH 7) was used for the recombinant membrane-associated chromate reductase.

6.2.5.2 SDS-PAGE analysis

SDS-PAGE analysis was performed as described in section 3.2.5.3.

6.2.5.3 Steady-state kinetics

Kinetic parameters of the recombinant reductases were obtained as described in sections 3.2.4.4 and 4.2.4.2.

6.2.5.4 Circular Dichroism Spectroscopy

Circular Dichroism (CD) spectra were recorded on a Jasco J-710 spectropolarimeter in a jacketed cuvette connected to a circulating water-system for temperature control. Spectra were recorded in a circular quartz cuvette with a 0.2 cm path-length in the range of 190 – 300 nm. Spectra were acquired at a scan speed of 200 $nm.min^{-1}$, with a 1 nm bandwidth and 0.25 s response time. Each spectrum was an accumulation of 10 consecutive scans and corrected for buffer signal. Protein concentration was approximately 100 $\mu g.ml^{-1}$.

For urea-induced unfolding, samples were incubated for 4 h at 25°C in the presence of various concentrations of urea. Unfolding of secondary structural elements were monitored through circular dichroism in the far-UV region.

6.2.5.5 Protein Concentration

Protein concentrations were determined using the BCA-method as described in sections 2.2.7.3 and 3.2.5.2.

6.3 RESULTS AND DISCUSSION

6.3.1 Construction of the expression vectors

The complete ORFs of both the cytoplasmic chromate reductase and membrane-associated reductase (from the first identified and second start codon as observed through N-terminal sequencing) were PCR amplified from total genomic DNA, yielding single products of the expected sizes (Figure 6.1). The primers were designed to incorporate a *Nde*I restriction site at the 5' end and an *Eco*RI restriction site at the 3' end for directional cloning (Table 6.2) into the pET-vectors.

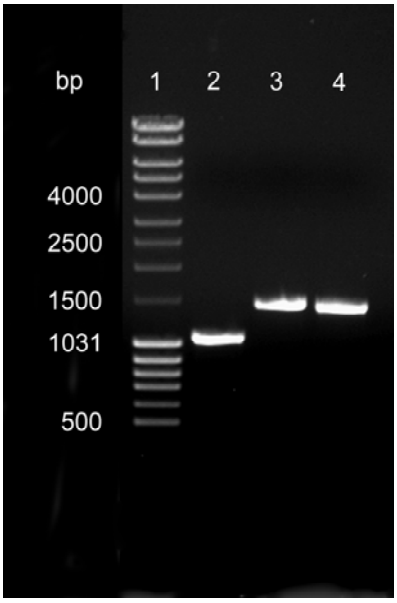

Figure 6.1: Agarose gel electrophoresis of the PCR amplified chromate reductases. Lane 1, Molecular weight marker; lane 2, cytoplasmic chromate reductase; lane 3, membrane-associated chromate reductase from 1st start codon; lane 4, membrane-associated chromate reductase from 2nd start codon.

The PCR amplified products were ligated into pGEM-T Easy vector, whereafter the inserts were again restriction digested from the plasmid using *Nde*I and *Eco*RI. pET-22b(+) and pET-28b(+) were digested with the same restriction enzyme combination to yield compatible cohesive ends and the reductases cloned into the expression vectors.

pET-22b(+) (Figure 6.2) would yield an unmodified proteins when introduced, whereas pET-28b(+) would result in a poly(6)histidine tag and a thrombin cleavage site fused to the N-terminus (Figure 6.3) of an introduced protein.

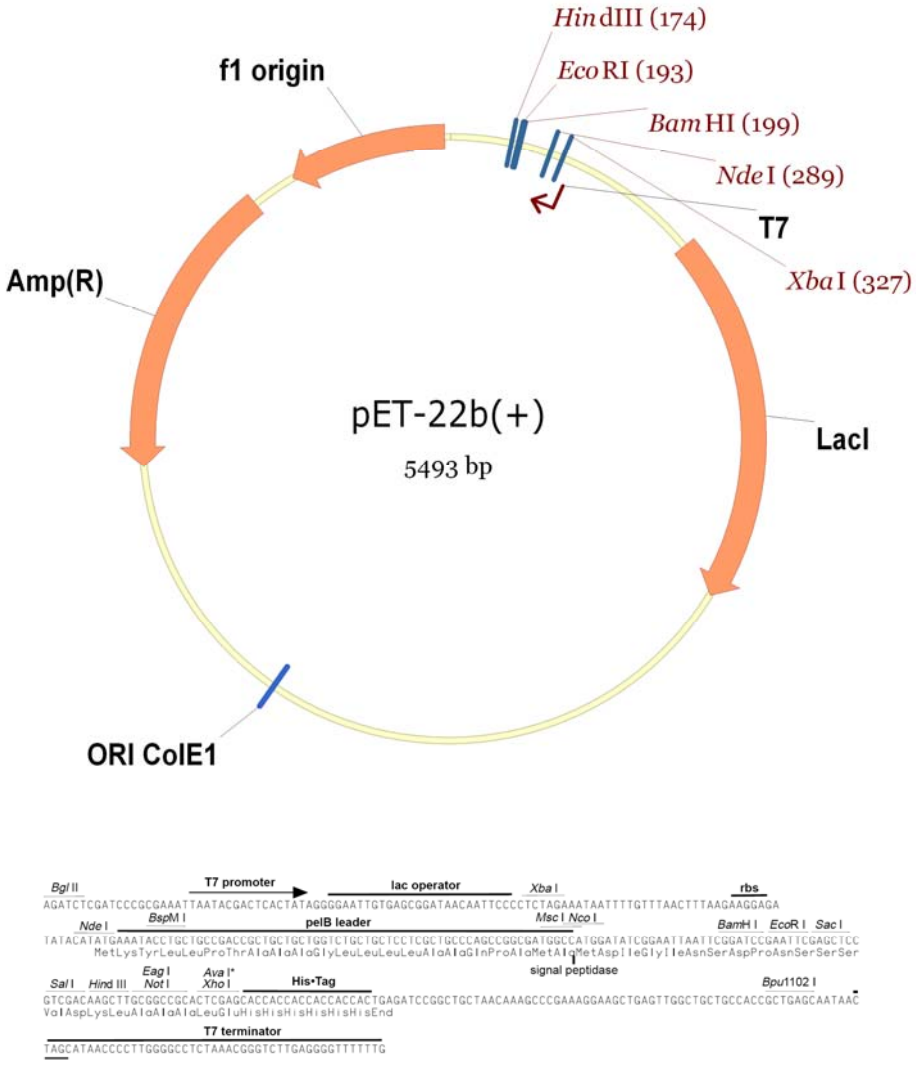

Figure 6.2: Vector map of pET-22b(+) indicating the ampicillin resistance gene, ColE1 origin of plasmid replication, *lacI* coding sequence and the multiple cloning site under the T7 promoter.

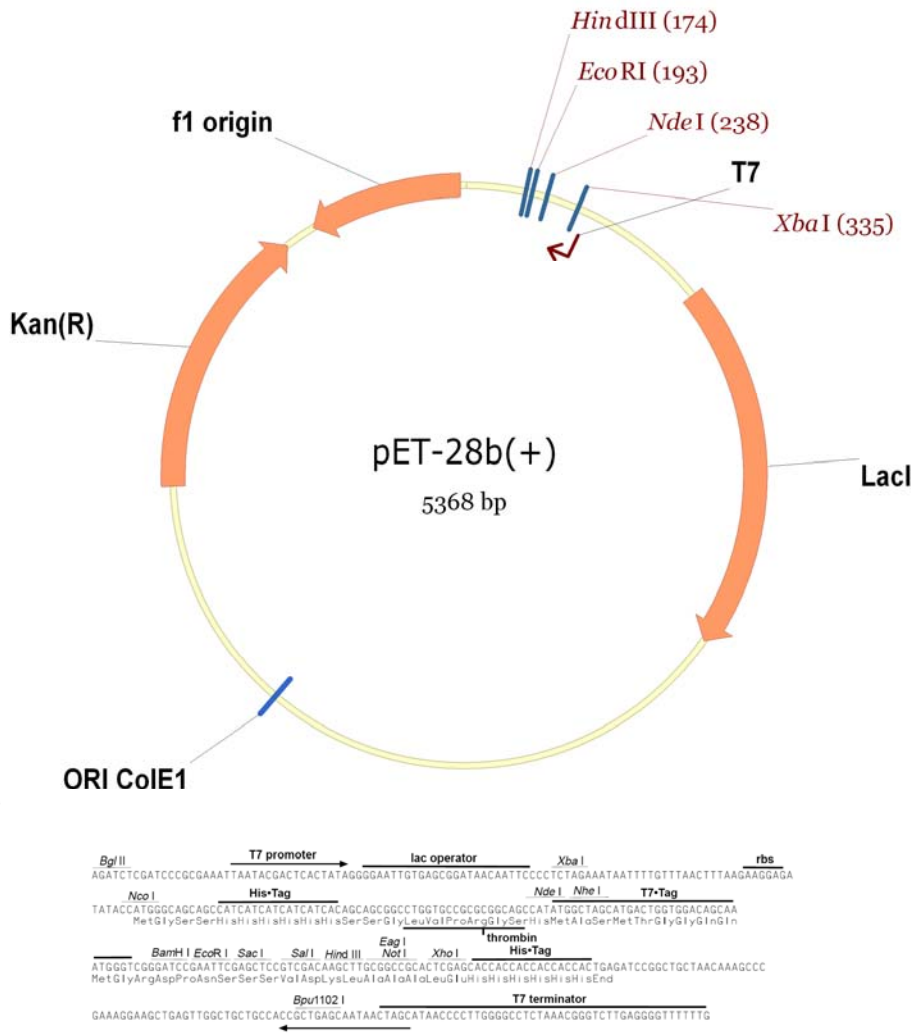

Figure 6.3: Vector map of pET-28b(+) indicating the kanamycin resistance gene, ColE1 origin of plasmid replication, *lacI* coding sequence and the multiple cloning site under the T7 promoter. Sequence of the pET-28b(+) cloning region showing the ribosome binding site and configuration for the N-terminal His-Tag and thrombin cleavage site fusion.

Cloned inserts were verified using restriction digestion with *Xba*I and *Eco*RI (Figure 6.4) yielding the plasmid backbone of approximately 5 kbp and the cytoplasmic (1 kbp) and membrane-associated (1.5 kbp) chromate reductase genes respectively.

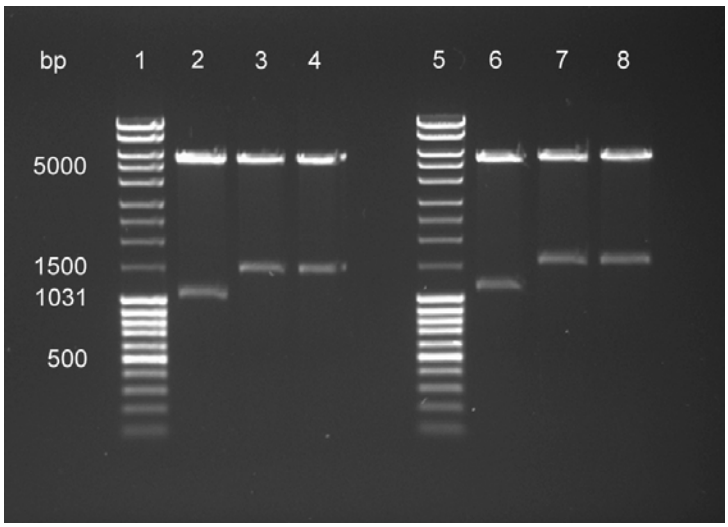

Figure 6.4: Double restriction digest of pET22 and pET28 vectors containing CrS (lanes 2 and 6 respectively), CrM from the first start codon (lanes 3 and 7 respectively) and from the second start codon (lanes 4 and 8 respectively). Lanes 1 and 5, molecular weight marker.

For expression in *T. thermophilus*, the pMK18 bifunctional *E.coli-Thermus* sp. vector (Figure 6.5) was used (de Grado *et al*., 1999). This vector confers resistance against kanamycin at both 37°C (*E. coli*) and 65°C (*T. thermophilus*), while expression of the cloned insert is under the constitutive PslpA promoter that also allows the expression of the kanamycin resistance gene. The multiple cloning site of the vector does not contain a ribosome binding site and therefore a ribosome binding site had to be introduced upstream of the cloned gene to allow translation of the desired protein.

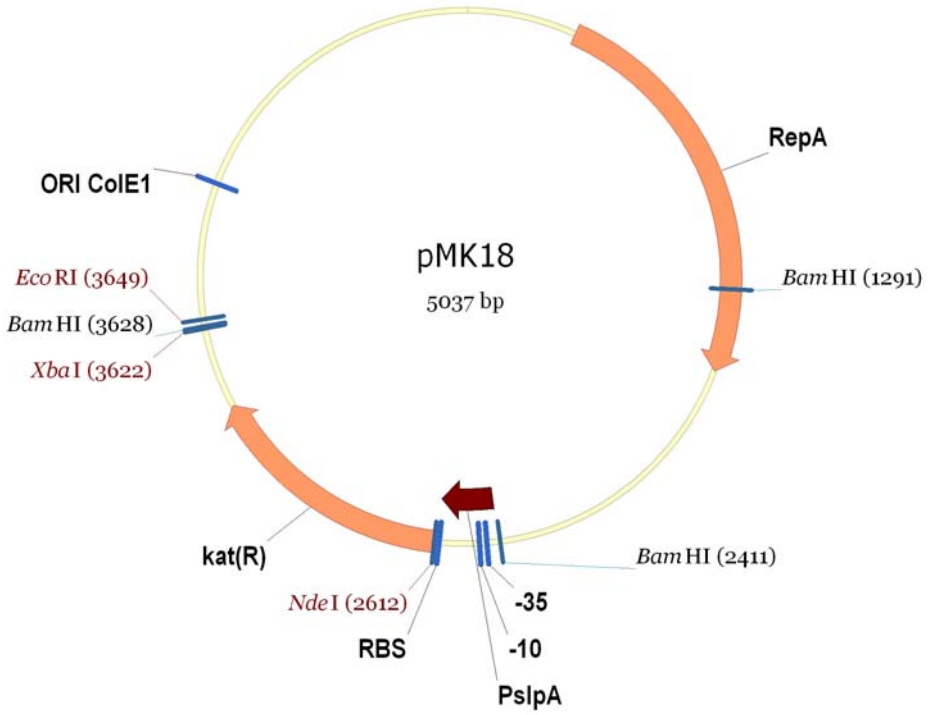

Figure 6.5: Vector map of the pMK18 bi-functional *E. coli-Thermus* sp. vector indicating the thermostable kanamycin resistance gene (kat), minimal replicon (RepA) for replication in *Thermus* sp., ColE1 origin of replication in *E. coli* and the multiple cloning site.

Restriction digestion of the pET-22 vector, containing the reductases, with *Xba*I and *Eco*RI allowed for the shuttling of the reductase genes together with the ribosome binding sites to the pMK18 vector. Similarly, the N-terminal poly-histidine (His-Tag) and the thrombin cleavage site were also shuttled from the pET-28 vectors. This allowed for the production of unmodified as well as His-Tagged chromate reductases in *T. thermophilus* (Figure 6.6).

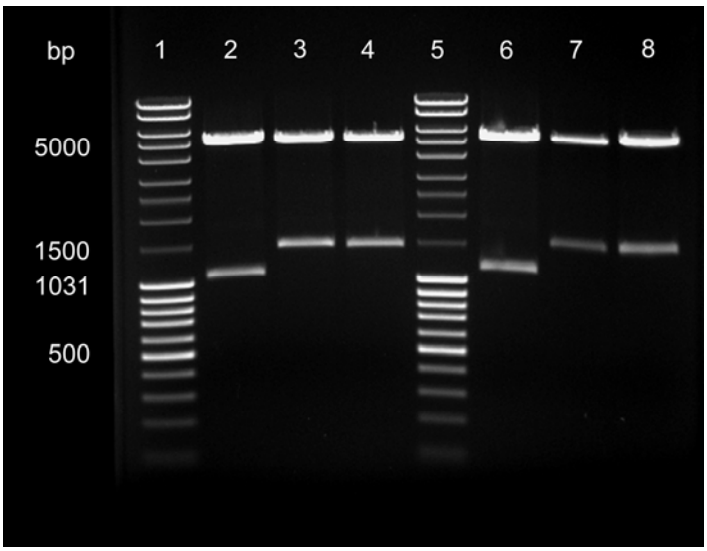

Figure 6.6: Double restriction digest of pMK18 vector containing CrS [lanes 2 (unmodified) and 6 (poly-His tag)], CrM from the first start codon [lanes 3 (unmodified) and 7 (poly-His tag)] and from the second start codon [lanes 4 (unmodified) and 8 (poly-His tag)]. Lanes 1 and 5, molecular weight marker.

6.3.2 Expression of the recombinant chromate reductases

The Cr(VI) reductases were over-expressed in *E. coli* BL21(DE3) at 37°C by induction through the addition of 1 mM IPTG to exponentially growing cells, and subsequent growth for another 4 h. SDS-PAGE analysis shows the accumulation of a major protein band of the expected size of approximately 37 kDa in the soluble fraction of *E. coli* (Figure 6.7A) for the recombinant CrS and a 49 kDa band for the recombinant CrM .

As expression in *T. thermophilus* was constitutive from the PslpA promoter, transformed cells were harvested at late exponential phase without any induction. Increased chromate reducing activity was also found within the cytoplasm of *T. thermophilus* for all the recombinant strains (Figure 6.7), although Coomassie blue staining of the SDS-PAGE analysis could not distinguish the production of any additional proteins of the expected size.

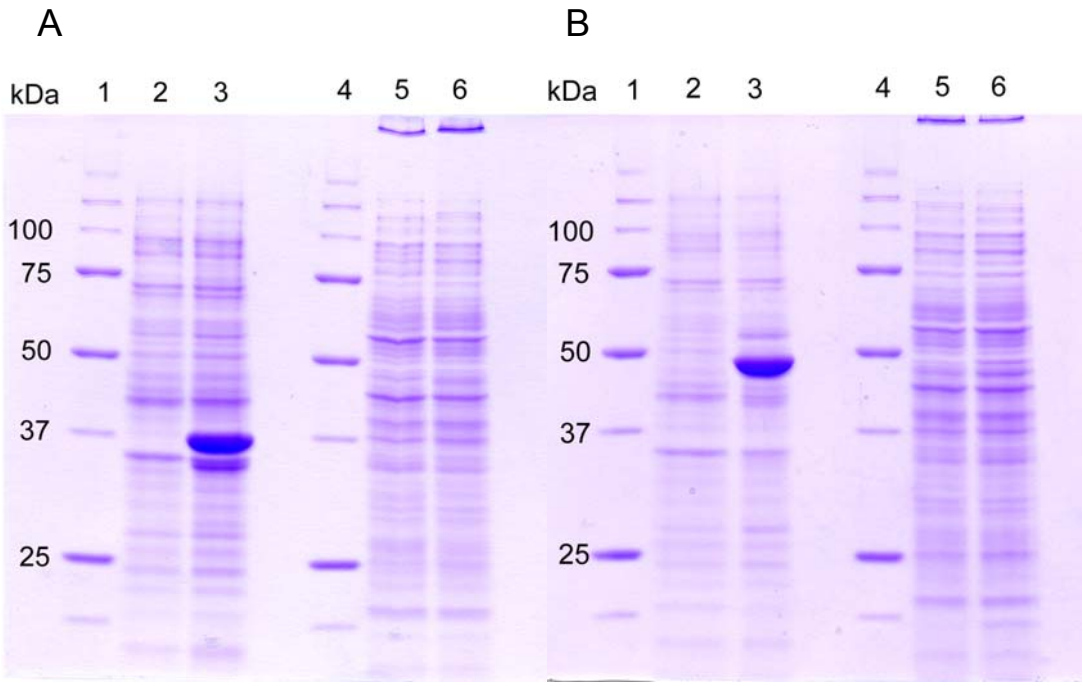

Figure 6.7: Overproduction of the cytoplasmic (A) and membrane-associated (B) chromate reductases in *E. coli* (lane 3) and *T. thermophilus* (lane 6). Lanes 2 and 5 represent the crude-extracts of *E. coli* and *T. thermophilus* transformed with plasmid (pET-28b(+) and pMK18 respectively) not containing any inserts. Lanes 1 and 4, molecular weight marker.

No chromate reducing activity could be detected in the *E. coli* cells transformed with only pET-22/28 vectors without inserts, whereas the recombinant strains expressing the CrS and CrM proteins showed varying amounts of chromate reductase activity (Figure 6.8A). Both the unmodified CrS (expression in pET22) as well as the poly(6)-His tag fused CrS recombinant proteins (expression in pET28) showed activity. The total activity for the unmodified protein was more than two times higher than that seen for the expression of the poly(6)-His tag fused CrS, but could be due to higher expression levels from the pET22 vector. The total activity found for the CrM proteins expressed in *E. coli* was nearly the same irrespective of whether from the first or second start codon, or unmodified or N-terminal fusion with the poly(6)-His tag.

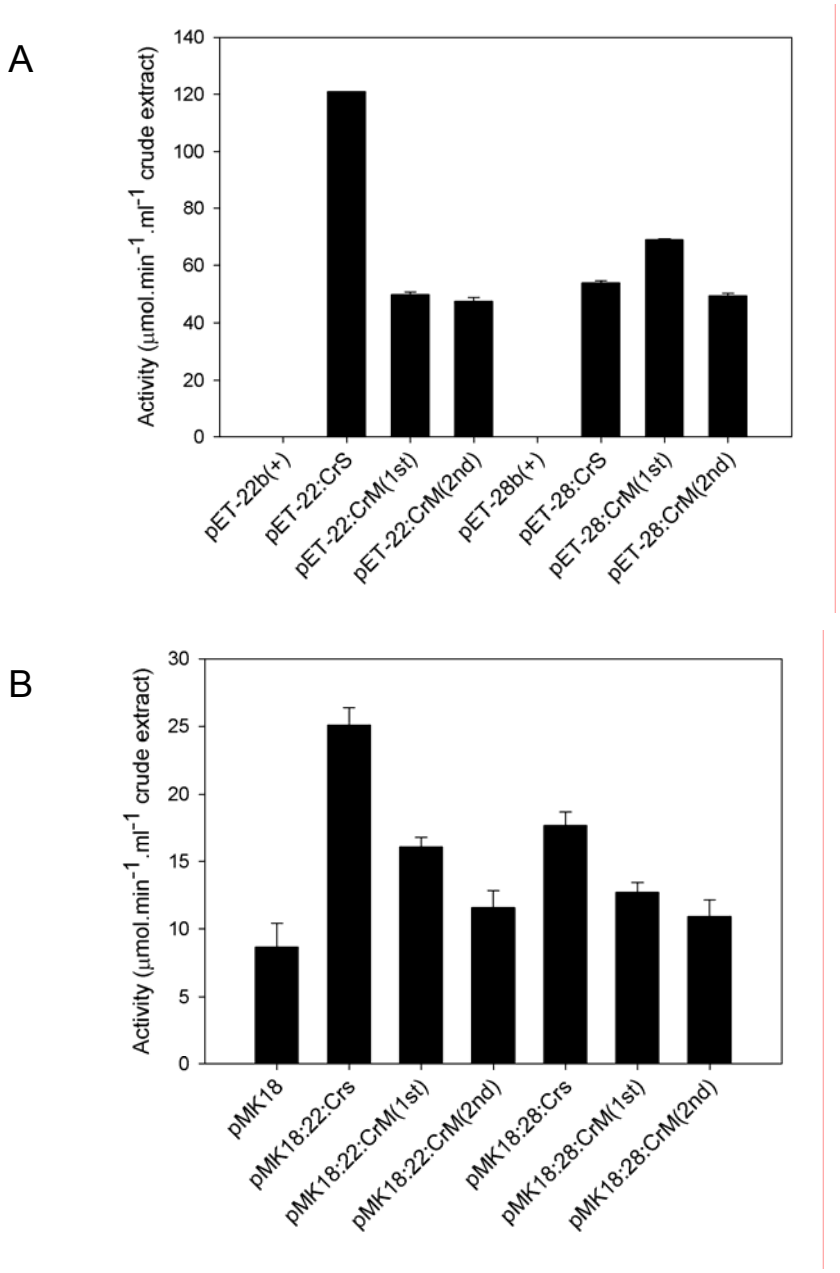

Figure 6.8: Chromate reducing activity of the crude extracts of the recombinant *E. coli* (A) and *T. thermophilus* (B) strains.

The cytoplasmic fractions of *T. thermophilus* showed chromate reducing activity at 65°C when transformed with the pMK18 vector without inserts. This activity could be attributed to the enzymes in *T. thermophilus* homologous to the chromate reductases in *T. scotoductus* (chapter 5). As seen with *E. coli*, all the recombinant *T. thermophilus* strains containing the *T. scotoductus* chromate reductase genes showed increased chromate reduction activity, indicating the active expression of both the modified and unmodified cytoplasmic and membrane-associated chromate reductases. The total activity was

however significantly lower than that seen for the recombinant *E. coli* strains, but is probably due to the weaker PslpA promoter as compared to the strong T7 promoter system in *E. coli*. The unmodified cytoplasmic chromate reductase was again approximately twice as active compared to the poly(6)-His tag modified protein.

6.3.3 Purification of the recombinant chromate reductases

6.3.3.1 Recombinant cytoplasmic chromate reductase (His-Tag)

The recombinant cytoplasmic chromate reductase was purified from the soluble fraction of both *E. coli* and *T. thermophilus* to near electrophoretic homogeneity (Figure 6.11A) through the use of immobilized metal affinity chromatography (IMAC), hydrophobic interaction chromatography and size-exclusion chromatography.

The recombinant proteins were firstly purified by taking advantage of the N-terminal poly(6)-histidine tag using Ni-affinity (Ni-NTA) chromatography. The chromate reductases eluted as single activity peaks (Figures 6.9A & 6.10A) from the His-Trap FF (Amersham Biosciences) column through the use of linear imidazole concentration gradients. Activity was also found within the non-binding fraction of the His-Trap FF column of *T. thermophilus* cytoplasm (data not shown) due to native proteins of *T. thermophilus* possessing chromate reducing activity as was seen with the *T. thermophilus* crude extracts transformed with pMK18 vector containing no inserts (Figure 6.8B).

Fractions containing activity were pooled and ammonium sulphate added to a final concentration of 0.4 M. Proteins were bound to a Phenyl-Toyopearl hydrophobic interaction column and bound proteins eluted with a linear negative gradient to no-salt buffer. Again the proteins eluted as a single peaks of chromate reducing activity (Figures 6.9B & 6.10B).

To ensure that all the apoproteins were saturated with FMN, the enzyme preparation was incubated with an excess amount of FMN (0.5 mg). The final purification step entailed size exclusion chromatography through the Sephacryl S-100HR (Sigma) column, whereby unbound FMN was removed as well as buffer exchange for subsequent circular dichroism

analysis. The proteins were eluted using a 10 mM Tris-H_2SO_4 (pH 7) buffer and were estimated to be in their native dimeric oligomeric states (Figures 6.9C & 6.10C).

The recombinant cytoplasmic chromate reductase denatured monomer molecular weights were estimated on SDS-PAGE analysis to be approximately 37 kDa (Figure 6.11A).

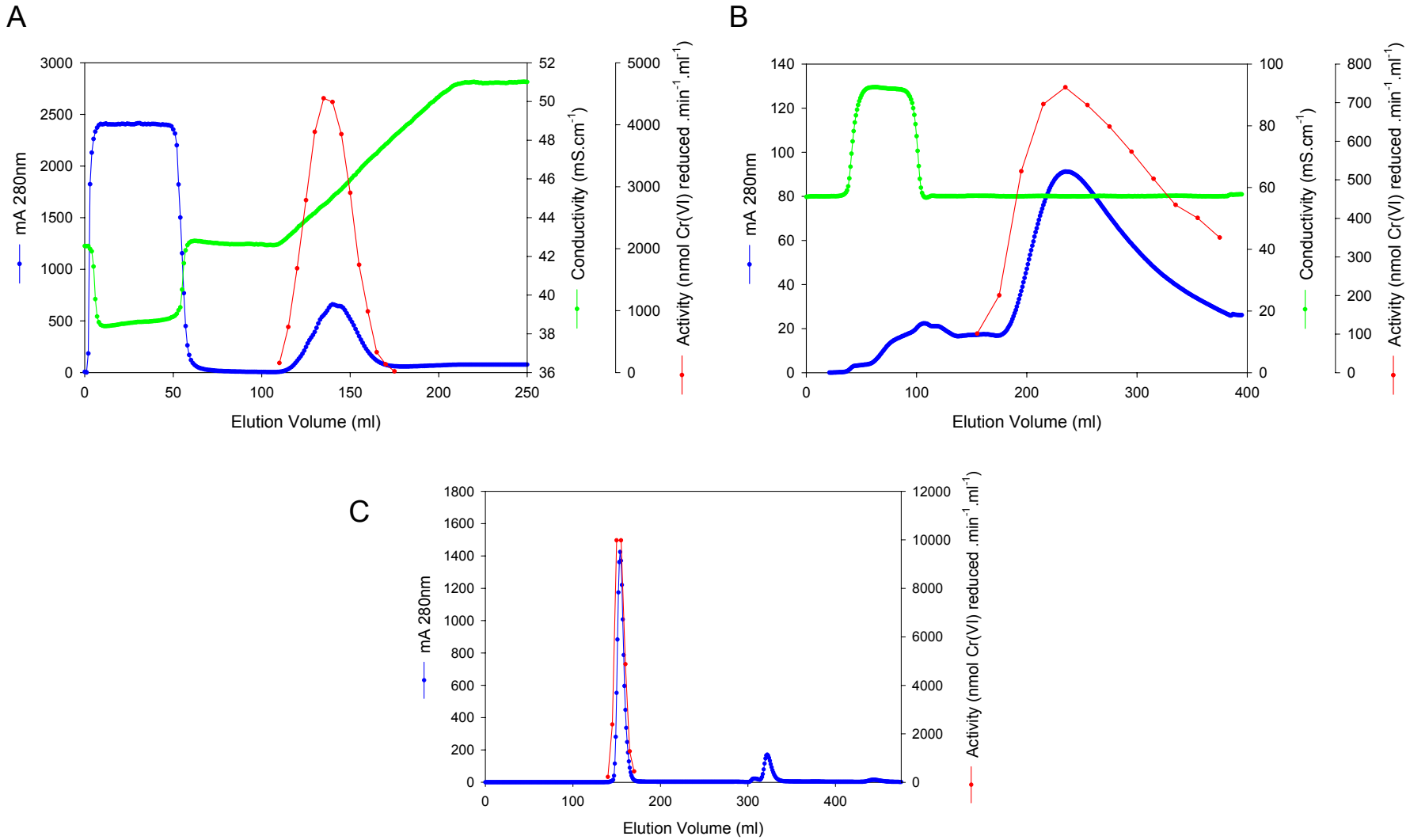

Figure 6.9: Purification of the recombinant cytoplasmic chromate reductase (CrS) overproduced in *E. coli* through Ni-affinity (A), hydrophobic interaction (B) and size exclusion (C) chromatography.

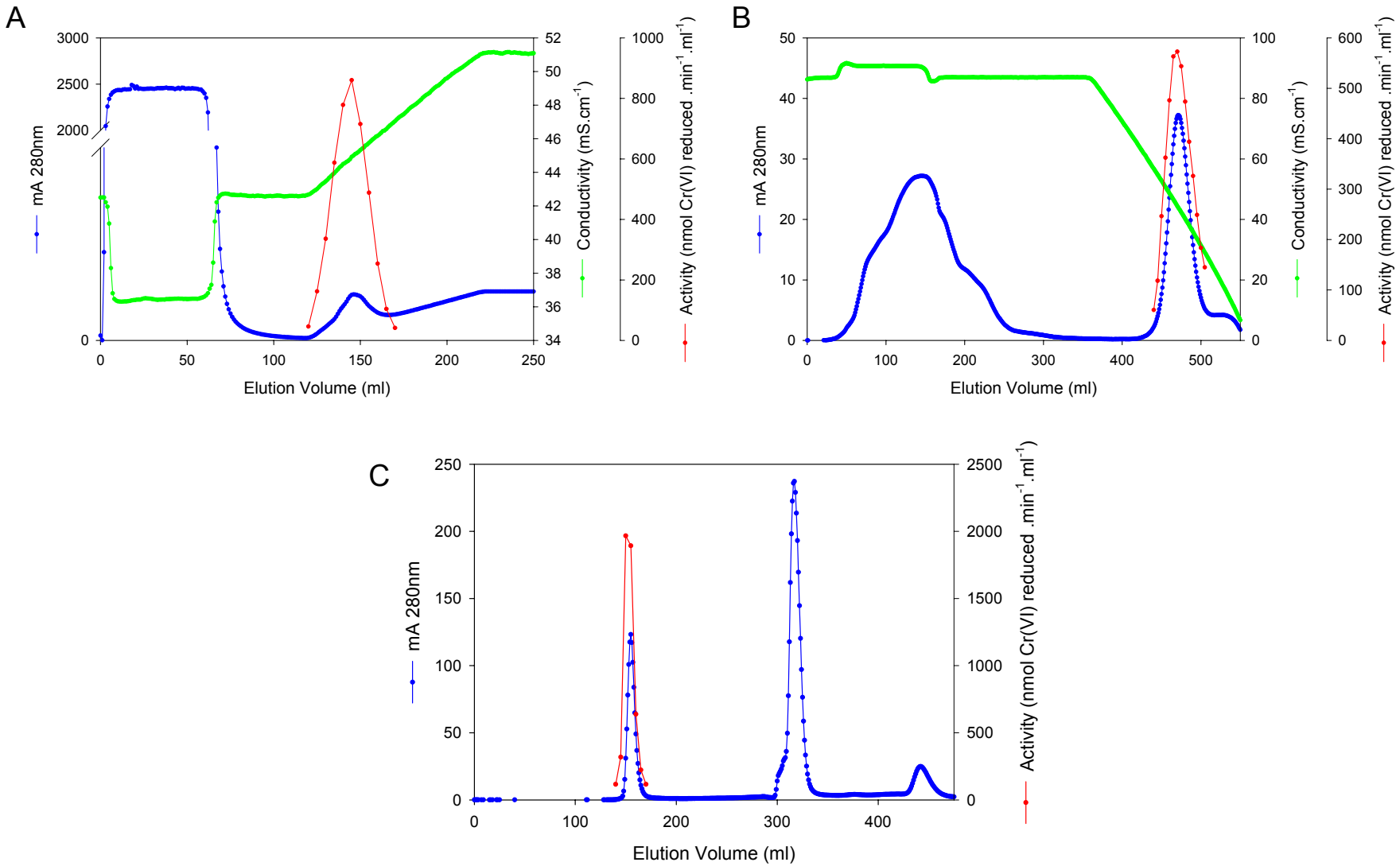

Figure 6.10: Purification of the recombinant cytoplasmic chromate reductase (CrS) overproduced in *T. thermophilus* through Ni-affinity (A), hydrophobic interaction (B) and size exclusion (C) chromatography.

6.3.3.2 Recombinant membrane-associated chromate reductase (His-Tag)

Similar to the recombinant cytoplasmic chromate reductase, the recombinant membrane-associated chromate reductase was purified from the soluble fraction of both *E. coli* and *T. thermophilus* to near electrophoretic homogeneity (Figure 6.11B) through the use of immobilized metal affinity chromatography (IMAC) and size-exclusion chromatography (data not shown).

The active fractions pooled after the Ni-affinity chromatography step, were also incubated with an excess amount of FAD to ensure saturation of all apoprotein. Size-exclusion chromatography again showed the proteins to be in their native dimeric states with estimated monomer molecular mass of approximately 49 kDa (Fig 6.11B).

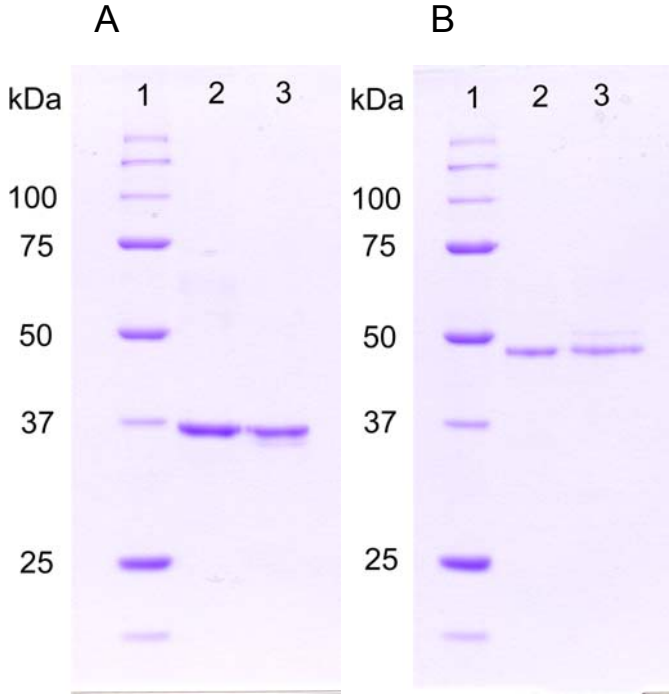

Figure 6.11: SDS-PAGE analysis of the purified recombinant cytoplasmic chromate reductases (A) and membrane-associated chromate reductase (B) when expressed in *E. coli* (lanes 2) and *T. thermophilus* (lanes 3). Lanes 1, standard molecular weight marker. Proteins were visualized through Coomassie-Blue staining.

6.3.4 Characterization of the recombinant chromate reductases

6.3.4.1 Catalytic parameters

The recombinant chromate reductases were compared with respect to their catalytic efficiency. Both the recombinant cytoplasmic and membrane-associated chromate reductases showed hyperbolic saturation kinetics but with higher specific activity when expressed in *T. thermophilus* as compared to the *E. coli*-expressed recombinant enzymes (Figure 6.12).

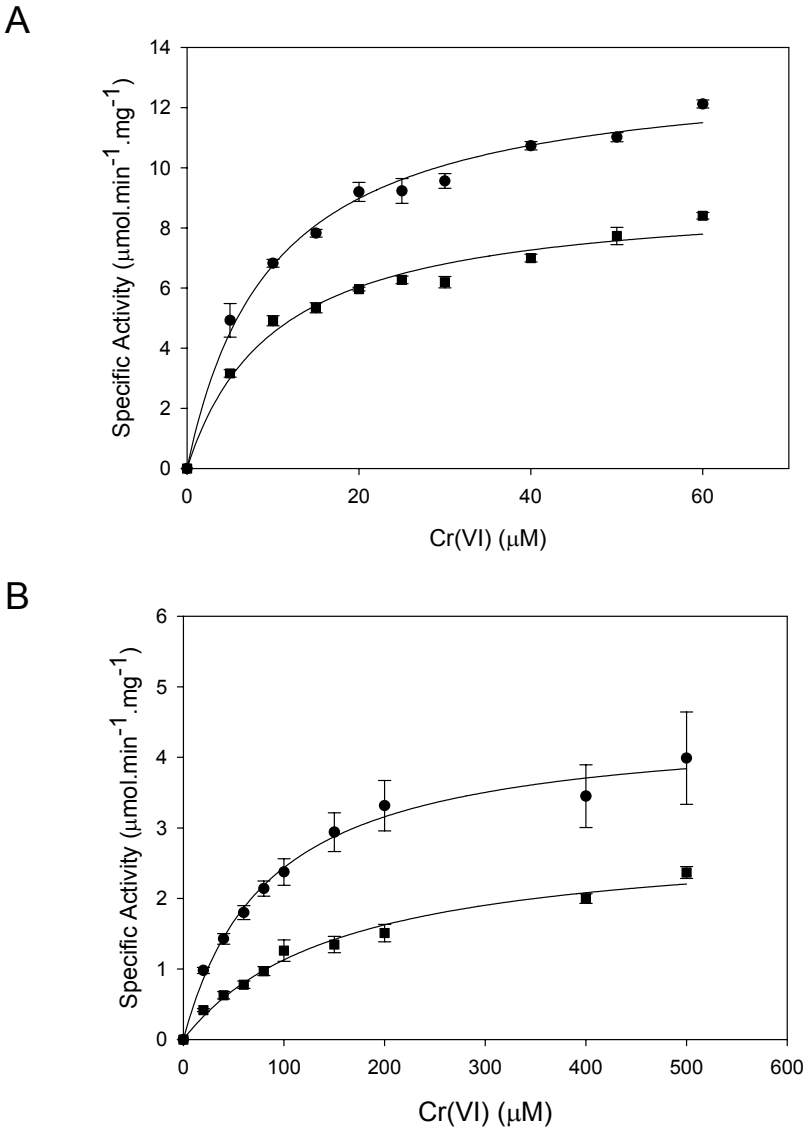

Figure 6.12: Steady-state kinetics of the purified recombinant CrS (A) and CrM (B) chromate reductases overproduced in *E. coli* (■) and *T. thermophilus* (●).

The recombinant cytoplasmic chromate reductases had comparable substrate affinities (K_m) but marginally lower than that found for the native *T. scotoductus* CrS (Table 6.3). Although the catalytic efficiencies (k_{cat}/K_m) for both recombinant cytoplasmic chromate reductases were lower than that of the native reductase, the reductase expressed in *T. thermophilus* were approximately 1.5 times more efficient than its counterpart expressed in *E. coli*.

More pronounced differences were found for the recombinant membrane-associated chromate reductases (Table 6.3). The recombinant CrM expressed in *E. coli* showed approximately 3 fold less substrate affinity towards the Cr(VI) as compared to the native CrM, whereas the *T. thermophilus*-recombinant CrM had a comparable substrate affinity for Cr(VI) relative to the native CrM. k_{cat}/K_m values obtained showed the catalytic efficiency of the *Thermus*-expressed recombinant CrM to be approximately 3 fold more efficient than its *E. coli*-expressed counterpart, with the *Thermus*-recombinant CrM even more efficient than the native CrM.

Table 6.3: Comparison of the kinetic parameters of the chromate reductases from different expression hosts. Reactions were performed under optimal conditions.

Enzyme / Expression Host	V_{max} (µmol Cr(VI) min^{-1} mg^{-1} protein)	K_m (µM)	k_{cat} (s^{-1})	k_{cat}/K_m (M^{-1} s^{-1})
Cytoplasmic chromate reductase				
T. scotoductus (native)	16.0	8.4	9.6[a]	1.1 x 10^6
E. coli	9.1	10.2	6.2[b]	0.6 x 10^6
T. thermophilus	13.4	9.8	9.1[b]	0.9 x 10^6
Membrane-associated chromate reductase				
T. scotoductus (native)	2.3	55.5	1.9[a]	3.3 x 10^4
E. coli	2.9	155.8	2.5[b]	1.6 x 10^4
T. thermophilus	4.5	84.1	38[b]	4.5 x 10^4

[a] Calculated from experimental monomer molecular mass determined through SDS-PAGE analysis

[b] Calculated from the theoretical monomer molecular mass including the N-terminal fusion as well as the bound co-factor

6.3.4.2 *Structural characterization*

The recombinant cytoplasmic chromate reductases expressed in *E. coli* and *T. thermophilus* were compared through comparison of their secondary structure elements and their co-factor incorporation through circular dichroism and UV-vis spectroscopy respectively.

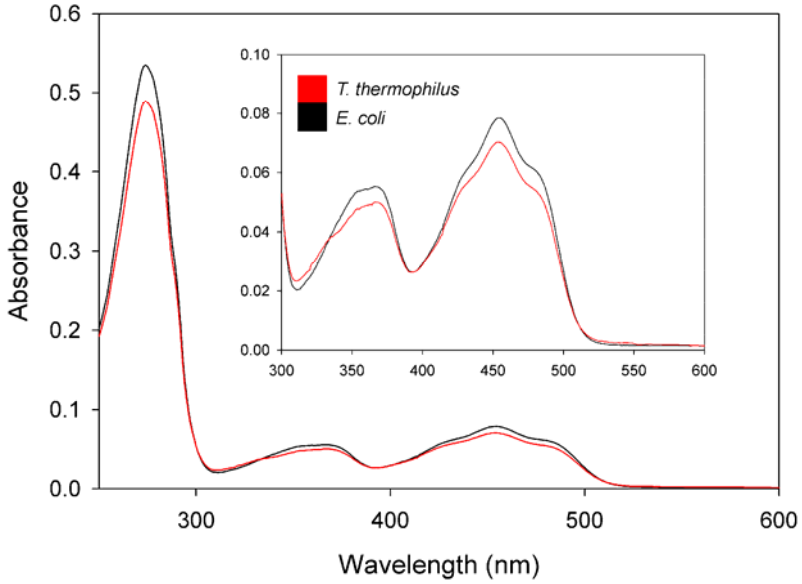

Figure 6.13: UV-vis spectroscopy of the recombinant cytoplasmic chromate reductase expressed in *E. coli* (black; 0.23 mg.ml^{-1}) and *T. thermophilus* (red; 0.22 mg.ml^{-1}).

The co-factor contents of the recombinant proteins were evaluated through UV-vis spectroscopy (Figure 6.13). Both the recombinant CrS enzymes produced typical flavoprotein spectra with A_{280}:A_{455} ratios of 6.3 and 6.5 for the *E. coli* and *T. thermophilus* expressed proteins respectively, suggesting both recombinant CrS enzymes had similar FMN incorporation and that the lower catalytic efficiency of the *E. coli* expressed CrS was not due to inadequate incorporation of FMN and subsequent inactive apoprotein.

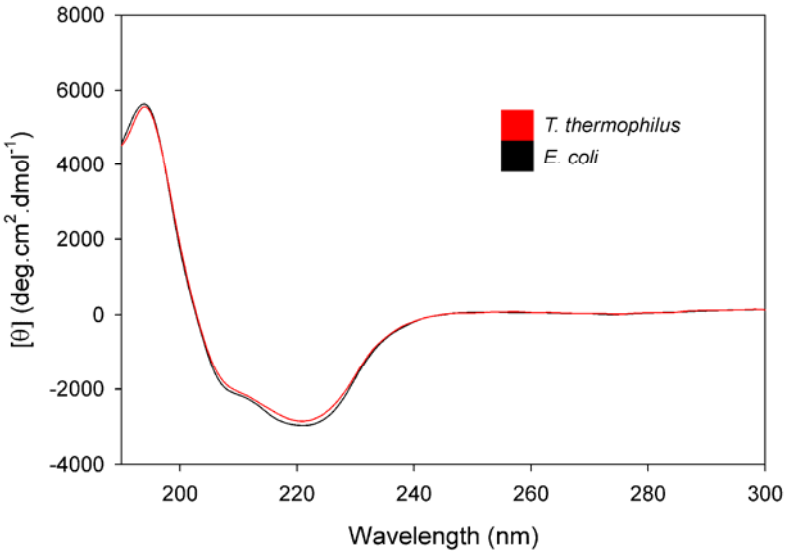

Figure 6.14: CD spectra of the recombinant cytoplasmic chromate reductases (~0.1 $mg.ml^{-1}$) expressed in *E. coli* (black) and *T. thermophilus* (red).

Far-UV circular dichroism spectra of the recombinant cytoplasmic chromate reductases show the enzymes to have very similar secondary structure composition (Figure 6.14) and both the reductases were stable with no significant denaturation at temperatures as high as 90°C (Figure 6.15).

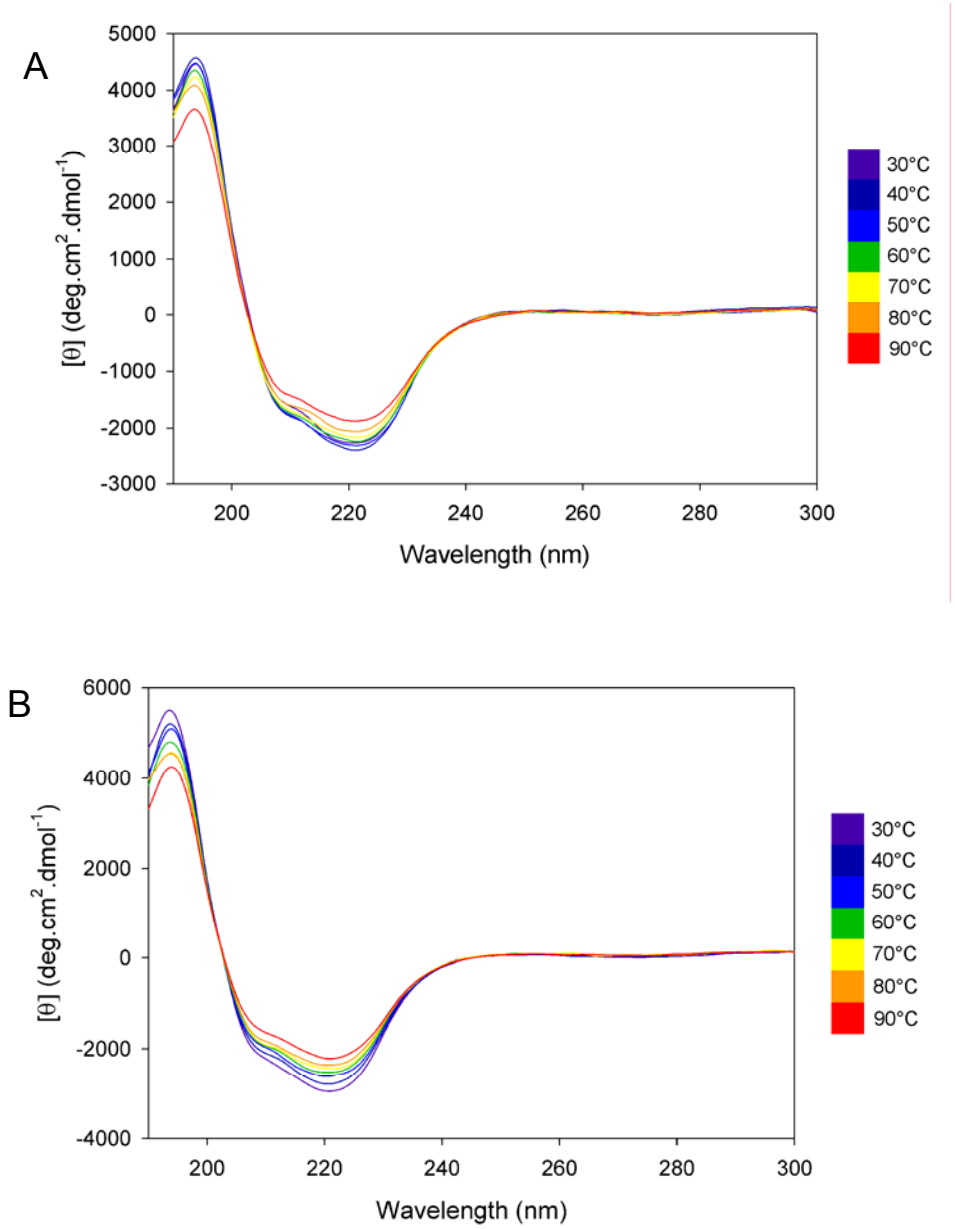

Figure 6.15: Temperature-induced unfolding of the recombinant cytoplasmic chromate reductases expressed in *E. coli* (A) and *T. thermophilus* (B) over a temperature range of 30 - 90°C followed through changes in the far-UV CD spectra.

Further structural stability was investigated through the reductases' conformational stability in various concentrations of urea. Again both reductases showed no significant changes in their secondary structure compositions in up to 5 M urea concentrations (Figure 6.16).

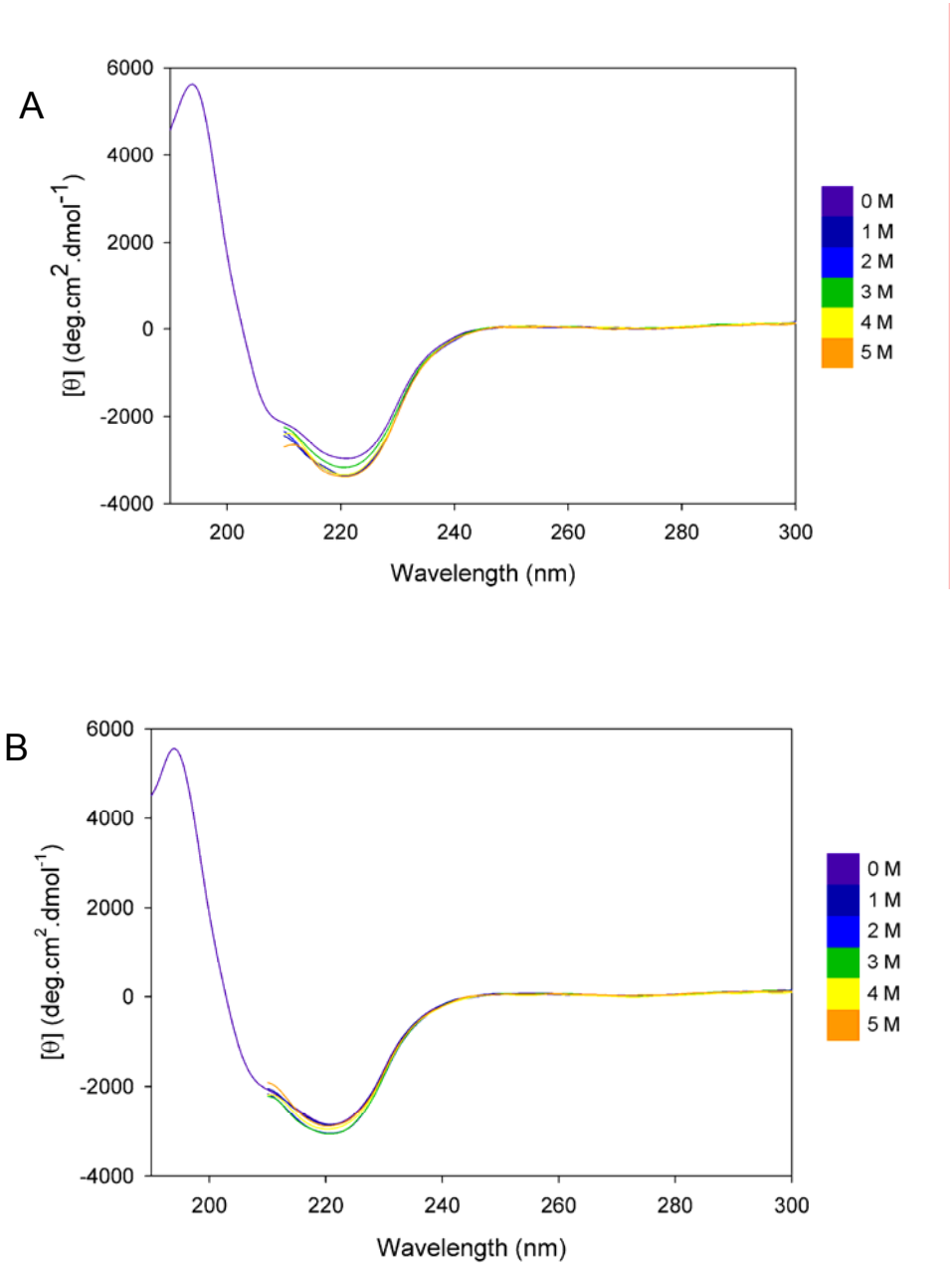

Figure 6.16: Urea-induced unfolding of the recombinant cytoplasmic chromate reductases expressed in *E. coli* (A) and *T. thermophilus* (B) followed through changes in the far-UV CD spectra.

Finally, samples incubated overnight in approximately 5 M urea were again subjected to a temperature gradient up to 90°C. Both proteins were structurally stable up to 80°C, however at 90°C, significant decrease in secondary structure elements were observed (Figure 6.17) for both recombinant reductases.

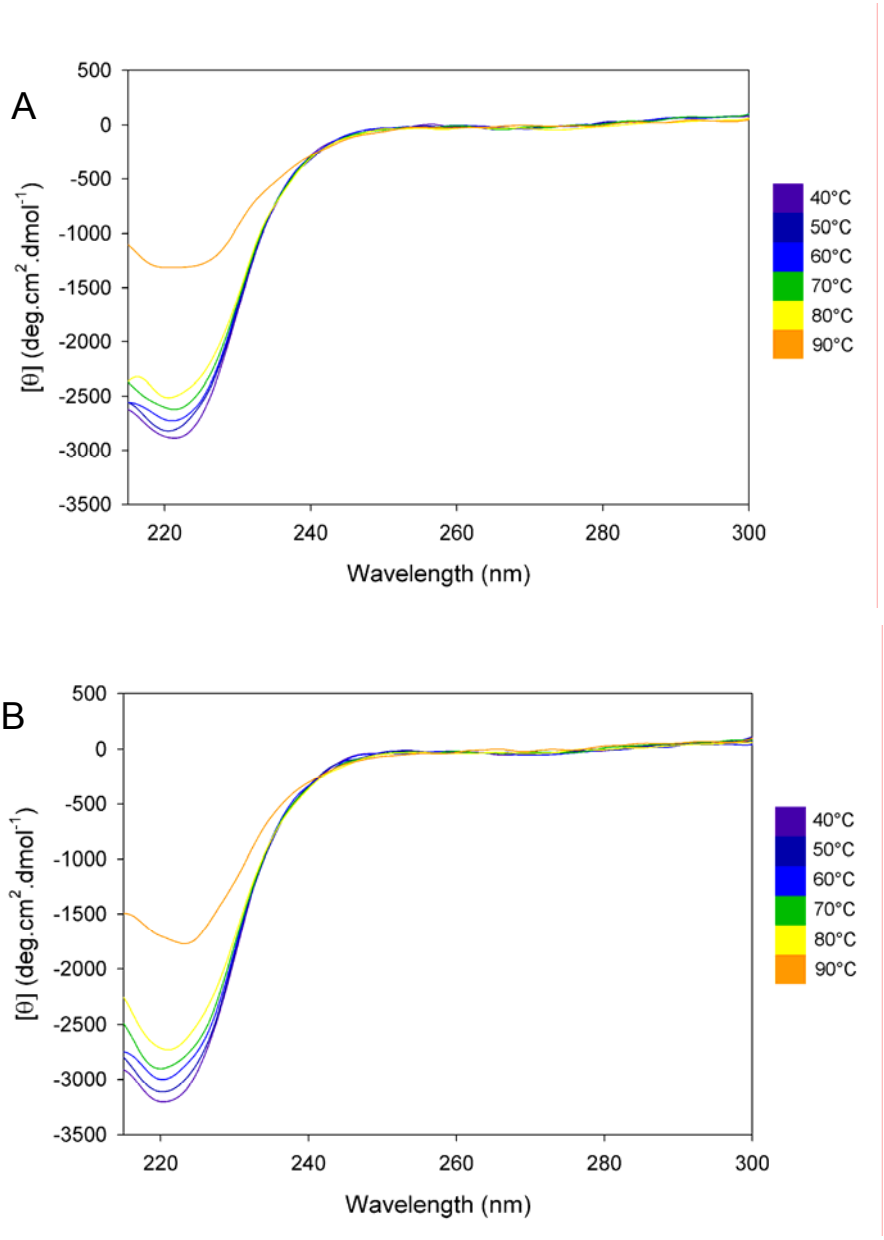

Figure 6.17: Temperature and urea-induced unfolding of the recombinant cytoplasmic chromate reductases expressed in *E. coli* (A) and *T. thermophilus* (B) over a temperature range of 40 - 90°C in the presence of approximately 5 M urea followed through changes in the far-UV CD spectra.

The rate of unfolding observed through the decrease in elepticity at 222 nm in 5 M urea and 90°C was used as a measure of the thermal stability of the two recombinant reductases. Both reductases showed rapid unfolding of their secondary structural elements. The CrS expressed in *E. coli* decrease at a rate of 189.5 deg.cm^2.dmol^{-1}.min^{-1},

whereas the CrS expressed in *T. thermophilus* only decreased at a rate of 127.1 $deg.cm^2.dmol^{-1}.min^{-1}$ (Figure 6.18).

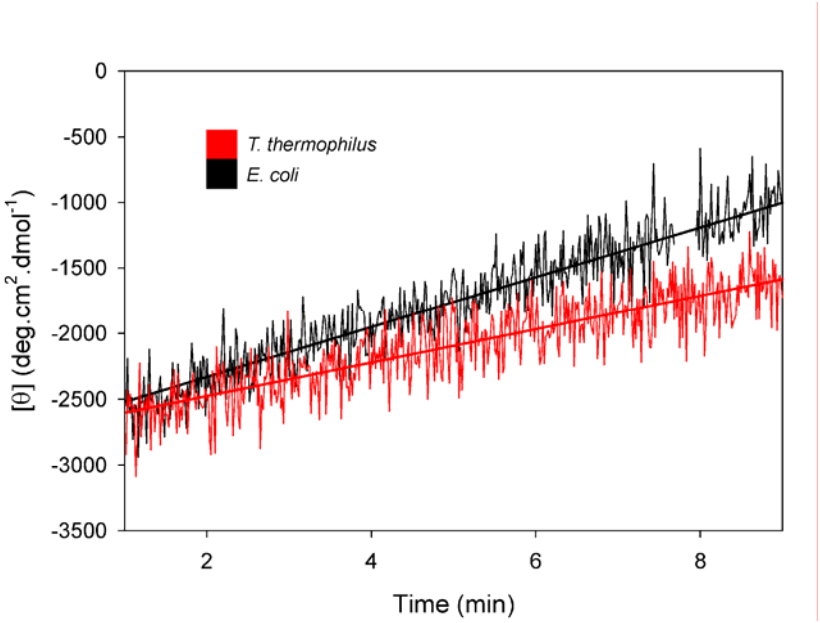

Figure 6.18: Temperature and urea-induced unfolding rates of the recombinant cytoplasmic chromate reductases expressed in *E. coli* (black) and *T. thermophilus* (red) at 90°C in the presence of approximately 5 M urea followed through changes in circular dichroism at 222 nm.

Although structurally overall the two recombinant cytoplasmic reductases were observed to be nearly identical, the thermal stability of the *T. thermophilus* expressed CrS proved to be approximately 30% more stable than its expressed counterpart in *E. coli*.

6.4 CONCLUSIONS

Both the cytoplasmic and membrane-associated chromate reductases were heterologously overproduced in *E. coli* and *T. thermophilus* as soluble, active enzymes as both unmodified as well as modified products through N-terminal poly-histidine fusion.

Purification of the poly(6)-his tagged proteins and subsequently comparison of their catalytic parameters indicated that the recombinant chromate reductases expressed in *T. thermophilus* were catalytically superior to their recombinant counterparts expressed in *E. coli.* Whereas the *E. coli* and *T. thermophilus* expressed recombinant cytoplasmic chromate reductase (CrS) had comparable affinities towards Cr(VI), the recombinant membrane-associated chromate reductase (CrM) expressed in *T. thermophilus* had approximately twice the affinity towards Cr(VI) as substrate compared to the *E. coli* expressed CrM. Although both the *E. coli* and *T. thermophilus* expressed CrS had catalytic efficiencies lower than that observed for the native *T. scotoductus* CrS, the reductase expressed in *T. thermophilus* was approximately 1.5 times more efficient than the *E. coli* expressed CrS. Similarly, the recombinant CrM expressed in *T. thermophilus* were approximately 3 times more efficient at Cr(VI) reduction than that of the *E. coli* expressed CrM. Surprisingly, the *T. thermophilus* expressed CrM was more efficient than the native *T. scotoductus* CrM.

Structural characterization through UV-vis and CD-spectroscopy showed no differences in either co-factor incorporation efficiency or secondary structural element composition of the recombinant CrS enzymes. The *T. thermophilus* expressed CrS were however slightly more structurally stable under chemical and thermal denaturization conditions.

SUMMARY

Recent contamination of the environment with Cr(VI) through various industrial activities is becoming an increasing problem to which microbial Cr(VI) reduction could prove an important alternative solution compared to currently available chemical and physical treatment options. Cr(VI) is highly toxic and has been shown to be a mutagen and carcinogen, whereas Cr(III) is considered relatively innocuous.

A variety of Cr(VI)-resistant and reducing bacteria have been isolated from diverse environments both contaminated and uncontaminated with Cr(VI). In 1999, Kieft and co-workers isolated a *Thermus scotoductus* strain from groundwater of a South African gold mine at a depth of 3.2 km. This thermophilic bacteria was shown to be able to readily reduce a variety of metals including Fe(III), Mn(IV), Co(III)-EDTA, U(VI) and Cr(VI). This ubiquitous nature of Cr(VI) reducing bacteria and the fact that Cr(VI) rarely occurs naturally in the environment, has led several researches to proposed that these chromate reducing properties is the serendipitous activity of enzymes with other primary physiological functions.

Thermus scotoductus SA-01 has the ability to tolerate up to 0.5 mM Cr(VI) during growth in a complex organic medium and reduce Cr(VI) under growth and non-growth conditions. The rate of chromate reduction is dependent on pH, temperature, initial Cr(VI) concentration and is abolished by metabolic inhibiters. Chromate reduction was catalyzed by cellular extracts using NADH as an electron donor indicating the chromate reduction mechanisms to be enzymatic.

Subcellular fractionation studies indicated that *Thermus scotoductus* SA-01 possesses more than one chromate reduction mechanisms. A novel cytoplasmic chromate reductase was purified to homogeneity and shown to couple the oxidation of NAD(P)H to the reduction of Cr(VI). This homodimeric protein consisted of monomers of approximately 36 kDa with a non-covalently bound FMN and required the divalent metal Ca^{2+} for activity. The enzyme was optimally active at 65°C and a pH of 6.3, reducing 2 mol of NAD(P)H per

mol Cr(VI), suggesting a mixed one- and two-electron transfer mechanism. N-terminal sequencing and screening of a genomic library of *T. scotoductus* SA-01 using a DIG-labelled DNA probe, revealed the cytoplasmic chromate reductase to be encoded for by an ORF of 1050 bp under the regulation of an *E. coli* σ^{70}-like promoter. Sequence analysis showed the chromate reductase to be related to the Old Yellow Enzyme (OYE) family and in particular some xenobiotic reductases.

The membrane-associated chromate reductase was also purified to homogeneity and shown to be distinct from the above mentioned cytoplasmic chromate reductase. The membrane-assocated reductase appears to be peripherally-associated with the membrane of *T. scotoductus* and consists of two identical subunits of approximately 48 kDa. The chromate reductase contained a non-covalently bound FAD co-factor and was optimally active at 65°C and a pH of 6.5. Through N-terminal sequencing and screening of a genomic library, the membrane-associated chromate reductase was identified as homologous to the dihydrolipoamide dehydrogenase gene, encoded for by a 1386 bp ORF and located within a probable pyruvate dehydrogenase operon.

Although neither of these enzymes are dedicated physiological chromate reductases, their catalytic efficiency toward Cr(VI) as substrate proved to be superior than that found for other chromate reductases described in literature, which include the nitroreductases and quinone reductases isolated from *Pseudomonas putida* and *Escherichia coli*

Both the cytoplasmic and membrane-associated chromate reductases were heterologously overproduced in *E. coli* and *T. thermophilus* as active, soluble enzymes. Kinetic studies of the recombinant proteins showed that the recombinant chromate reductases expressed in *T. thermophilus* were more catalytic efficient than their *E. coli*-expressed counterparts. Although structurally no differences could be observed using UV-vis and circular dichroism spectroscopy, the *T. thermophilus*-expressed recombinant cytoplasmic chromate reductase proved to be more stable under extreme chemical and thermal conditions.

OPSOMMING

Kontaminasie van die omgewing met Cr(VI) deur verskeie industriële aktiwiteite word 'n toenemende probleem waarvan mikrobiese Cr(VI) reduksie 'n belangrike alternatief tot die huidige beskikbare chemiese en fisiese behandeling opsies is. Cr(VI) is hoogs toksies en is bewys om mutagenies en karsinogenies te wees, teenoor Cr(III) wat beskou word as relatief onskadelik.

'n Verskeidenheid Cr(VI)-tolerante en reduserende bakterieë is geïsoleer vanaf diverse omgewings wat beide gekontamineer en ongekontamineer is met Cr(VI). In 1999, het Kieft en medewerkers 'n *Thermus scotoductus* spesie geïsoleer vanuit grondwater afkomstig vanaf 'n Suid Afrikaanse goud myn, 3.2 km onder die grond. Daar is bewys dat hierdie termofiliese bakterieë 'n verskeidenheid metale insluitende Fe(III), Mn(IV), Co(III)-EDTA, U(VI) en Cr(VI) kan reduseer. Die algemene voorkoms van Cr(VI) reduserende bakterieë en die feit dat Cr(VI) nie natuurlik in die omgewing voorkom nie, het daartoe gelei dat verskeie navorsers voorgestel het dat hierdie Cr(VI) reduserende eienskap 'n nie spesifieke reaksie is deur ensieme met ander primêre fisiologiese funksies.

Thermus scotoductus SA-01 het die vermoë om 0.5 mM Cr(VI) te weerstaan tydens groei in 'n komplekse organiese medium en reduseer Cr(VI) tydens groei en nie-groei kondisies. Die tempo van chromaat reduksie is afhanklik van pH, temperatuur asook aanvanklike Cr(VI) konsentrasie en word geïnhibeer deur metaboliese inhibitors. Chromaat reduksie word gekataliseer deur sellulêre ekstrakte en maak gebruik van NADH as elektron donor wat wys dat die chromaat reduksie ensimaties is.

Subsellulêre fraksionering wys dat *Thermus scotoductus* SA-01 het meer as een chromaat reduserende meganismes. 'n Eiesoortige sitoplasmiese chromaat reduktase was gesuiwer en daar is gewys dat die oksidasie van NAD(P)H verbind kan word met die reduksie van Cr(VI). Hierdie dimeriese proteïen bestaan uit twee identiese monomere van ongeveer 36 kDa met 'n nie-kovalente gebinde FMN en benodig die divalente metaal Ca^{2+} vir aktiwiteit.

Die ensiem was optimaal aktief by 65°C met ’n pH van 6.3. Twee mol NAD(P)H word gereduseer per mol Cr(VI) wat ’n gemengde een- en twee-elektron oordrag meganisme voorstel. N-terminale aminosuuropeenvolging bepaling en evaluering van ’n genomiese biblioteek van *T. scotoductus* SA-01, deur gebruik te maak van ‘n DIG-gemerkte DNS priemstuk, het gewys dat die sitoplasmiese chromaat reduktase gekodeer word deur ’n leesraam van 1050 bp wat onder die regulering van ’n E. coli σ^{70}-tiepe promotor is. Basispaaropeenvolging analise wys dat die chromaat reduktase verwant is aan die Ou Geel Ensiem (OGE) familie, meer spesifiek die xenobiotiese reduktases.

Die membraan-geassosieerde chromaat reduktase is ook gesuiwer as ’n homogeniese preparaat en dit is bewys om anders as die bogenoemde sitoplasmiese chromaat reduktase te wees. Die membraan-geassosieerde reduktase blyk periferaal-geassosieerd te wees en bestaan uit twee identiese subeenhede van ongeveer 48 kDa. Die chromaat reduktase bevat ‘n nie-kovalent gebinde FAD kofaktor en was optimaal aktief by 65°C by ‘n pH van 6.5. Deur N-terminaal aminosuuropeenvolging bepaling en evaluering van ’n genomiese biblioteek is die membraan-geassosieerde chromaat reduktase geen geïdentifiseer as ’n homoloog van die dihidrolipoamied dehidrogenase geen, wat gekodeer word deur ’n leesraam van 1386 bp en vorm deel van ’n moontlike piruvaat dehidrogenase operon.

Alhoewel nie een van die ensieme ’n egte fisiologiese chromaat reduktase is nie, is bewys dat beide se katalitiese effektiwiteit tot Cr(VI) as substraat beter is as ander chromaat reductases beskryf in literatuur, wat insluit die nitroreduktases en die quinien reduktase vanaf *Pseudomonas putida* en *Escherichia coli*.

Beide die sitoplasmiese en membraan-geassosieerde chromaat reduktases was uitgedruk in *E. coli* en *T. thermophilus* as aktiewe, oplosbare ensieme. Kinetiese studies van die rekombinante proteïene wys dat die chromaat reduktases uitgedruk in *T. thermophilus* meer katalities effektief was as proteïene uitgedruk in *E. coli.* Alhoewel daar geen strukturele verskille waargeneem is met UV-vis en sirkulêre dichroisme spektrofotografie nie, was die *T. thermophilus* uitgedrukte sitoplasmiese chromaat reduktase meer stabiel onder ekstreme chemiese en termiese toestande.

REFERENCES

Ackerley, D.F., Gonzalez, C.F., Keyhan, M., Blake II, R. and Matin, A. (2004A) Mechanisms of chromate reduction by the *Escherichia coli* protein, NfsA, and the role of different chromate reductases in minimizing oxidative stress during chromate reduction. *Environmental Microbiology* **6**:851–860.

Ackerley, D.F., Gonzalez, C.F., Park, C.H., Blake II, R., Keyhan, M. and Matin, A. (2004B) Chromate–reducing properties of soluble flavoproteins from *Pseudomonas putida* and *Escherichia coli*. *Applied and Environmental Microbiology* **70**:873–882.

Ackerley, D.F., Barak, Y., Lynch, S.V., Curtin, J. and Matin, A. (2006) Effects of chromate stress on *Escherichia coli* K-12. *Journal of Bacteriology* **188**:3371-3381.

Adams, M.W.W., Perler, F.B. and Kelly, R.M. (1995) Extremozymes: Expanding the limits of biocatalysis. *Biotechnology* **13**:662-668.

Altschul, S.F., Gish, W., Miller, W., Myers, E.W. and Lipman, D.J. (1990) Basic local alignment search tool. *The Journal of Molecular Biology* **215**:403-410.

Alvarez, A.H., Morenzo-Sánchez, R. and Cervantes, C. (1999) Chromate efflux by means of the ChrA chromate resistance protein from *Pseudomonas aeruginosa.* *Journal of Bacteriology* **181**:7398-7400.

Argyrou, A. and Blanchard, J.S. (2001) *Mycobacterium tuberculosis* lipoamide dehydrogenase is encoded by Rv0462 and not by the *lpdA* or *lpdB* genes. *Biochemistry* **40**:11353-11363.

Argyrou, A. and Blanchard, J.S. (2004) Flavoprotein disulfide reductases: Advances in chemistry and function. *Progress in Nucleic Acid Research and Molecular Biology* **78**:89-142.

Argyrou, A., Blanchard, J.S. and Palfey, B.A. (2002) The lipoamide dehydrogenase from *Mycobacterium tuberculosis* permits the direct observation of flavin intermediates in catalysis. *Biochemistry* **41**:14580-14590.

Argyrou, A., Sun, G., Palfey, B.A. and Blanchard, J.S. (2003) Catalysis of diaphorase reactions by *Mycobacterium tuberculosis* lipoamide dehydrogenase occurs at the EH_4 level. *Biochemistry* **42**:2218-2228.

Bader, J.L., Gonzalez, G., Goodell, P.C., Ali, A.S. and Pillai, S.D. (1999) Chromium-resistant bacterial populations from a site heavily contaminated with hexavalent chromium. *Water, Air and Soil Pollution* **109**:263-276.

Bae, W-C., Lee, H-K., Choe, Y-C., Jahng, D-J., Lee, S-H., Kim, S-J., Lee, J-H. and Jeong, B-C. (2005) Purification and characterization of NADPH-dependent Cr(VI) reductase from *Escherichia coli* ATCC 33456. *Journal of Microbiology* **43**:21-27.

Balkwill, D.L. (1993) DOE makes subsurface cultures available. *ASM News* **59**:504–506.

Balkwill, D.L., Kieft, T.L., Tsukuda, T., Kostandarithes, H.M., Onstott, T.C., Macnaughton, S., Bownas, J. and Fredrickson, J.K. (2004) Identification of iron–reducing *Thermus* strains as *Thermus scotoductus*. *Extremophiles* **8**:37–44.

Ball, J.W. and Nordstrom, D.K. (1998) Critical evaluation and selection of standard state thermodynamic properties of chromium metal and its aqueous ions, hydrolysis species, oxides and hydroxides. *Journal of Chemical and Engineering Data* **43**:895-918.

Benen, J., van Berkel, W., Dieteren, N., Arscott, D., Williams Jr, C., Veeger, C. and de Kok, A. (1992) Lipoamide dehydrogenase from *Azotobacter vinelandii*: site-directed mutagenesis of the His450-Glu455 diad. Kinetics of wild-type and mutated enzymes. *European Journal of Biochemistry* **207**:487-497.

Boe, I.N. and Lovrien, R.E. (1990) Energy reserves and storage polymers in intact bacteria analyzed by metabolic calorimetry. *Thermochim Acta* **172**:115–122.

Bopp, L.H., Chakrabarty, A.M. and Ehrlich, H.L. (1983) Chromate resistance plasmid in *Pseudomonas fluorescens. Journal of Bacteriology* **155**:1105-1109.

Bopp, L.H. and Ehrlich, H.L. (1988) Chromate resistance and reduction in *Pseudomonas fluorescens* strain LB300. *Archives of Microbiology* **150**:426-431.

Bruins, M.E., Janssen, A.E.M. and Boom, R.M. (2001) Thermozymes and their applications. *Applied Biochemistry and Biotechnology* **90**:155-186.

Camargo, F.A.O., Bento, F.M., Okeke, B.C. and Frankenberger, W.T. (2003A) Chromate reduction by chromium-resistant bacteria isolated from soils contaminated with dichromate. *Journal of Environmental Quality* **32**:1228-1233.

Camargo, F.A.O., Okek, B.C., Bento, F.M. and Frankenberger, W.T. (2003B) In vitro reduction of hexavalent chromium by a cell-free extract of *Bacillus* sp. ES 29 stimulated by Cu^{2+}. *Applied Microbiology and Biotechnology* **62**:569-573.

Campos, J., Martinez–Pacheco, M. and Cervantes, C. (1995) Hexavalent–chromium reduction by a chromate–resistant *Bacillus* sp. strain. *Antonie van Leeuwenhoek* **68**:203–208.

Campos–García, J., Martínez–Cadena, G., Alvarez–González, R., Cervantes C. (1997) Purification and partial characterization of a chromate reductase from *Bacillus*. *Revista Latinoamericana de Microbiologia* **39**:73–81.

Carothers, D.J., Pons, G. and Patel, M.S. (1989) Dihydrolipoamide dehydrogenase: Functional similarities and divergent evolution of the pyridine nucleotide-disulfide oxidoreductases. *Archives of Biochemistry and Biophysics* **268**:409-425.

Cervantes, C. (1991) Bacterial interaction with chromate. *Antonie van Leeuwenhoek* **59**:229-233.

Cervantes, C., Campos–García, J., Devars, S., Gutiérrez–Corona, F., Loza–Tavera, H., Torres–Guzmán, J.C. and Moreno–Sánchez, R. (2001) Interactions of chromium with microorganisms and plants. *FEMS Microbiology Reviews* **25**:335–347.

Cervantes, C. and Ohtake, H. (1988) Plasmid-determined resistance to chromate in *Pseudomonas aeruginosa. FEMS Microbiology Letters* **56**:173-176.

Cervantes, C., Ohtake, H., Chu, L., Misra, T.K. and Silver, S. (1990) Cloning, nucleotide sequence, and expression of the chromate resistance determinants of Pseudomonas aeruginosa plasmid pUM505. *Journal of Bacteriology* **172**:287-291.

Cervantes, C. and Silver, S. (1992) Plasmid chromate resistance and chromate reduction. *Plasmid* **27**:65-71.

Chardin, B., Dolla, A., Chaspoul, F., Fardeau, M.L., Gallice, P. and Bruschi, M. (2002) Bioremediation of chromate: thermodynamic analysis of the effects of Cr(VI) on sulfate-reducing bacteria. *Applied Microbiology and Biotechnology* **60**:352-360.

Chourey, K., Thompson, M.R., Morrell-Falvey, J., VerBerkmoes, N.C., Brown, S.D., Shah, M., Zhou, J., Doktycz, M., Hettich, R.L. and Thompson, D.K. (2006) Global molecular and morphological effects of 24-hour chromium(VI) exposure on *Shewanella oneidensis* MR-1. *Applied and Environmental Microbiology* **72**:6331-6344.

Clark, D.P. (1994) Chromate reductase activity of *Enterobacter aerogenes* is induced by nitrite. *FEMS Microbiology Letters* **122**:233-238.

Clarke, L. and Carbon, J. (1976) A colony bank containing synthetic CoI EI hybrid plasmids representative of the entire *E. coli* genome. *Cell* **9**:91-99.

Codd, R., Dillon, C.T., Levina, T. and Lay, P.A. (2001) Studies on the genotoxicity of chromium: from the test tube to the cell. *Coordination Chemistry Reviews* **216**:537-582.

Cooke, V.M., Hughes, M.N. and Poole, R.K. (1995) Reduction of chromate by bacteria isolated from the cooling water of an electricity generating station. *Journal of Industrial Microbiology* **14**:323-328.

Das, S. and Chandra, A.L. (1990) Chromate reduction in *Streptomyces*. *Experientia* **46**:731–733.

De Grado, M., Castán, P. And Berenguer, J. (1999) A high-transformation-efficiency cloning vector for Thermus thermophilus. *Plasmid* **42**:241-245.

De Kok, A., Hengeveld, A.F., Martin, A. and Westphal, A.H. (1998) The pyruvate dehydrogenase multi-enzyme complex from gram-negative bacteria. *Biochimica et Biophysica Acta* **1385**:353-366.

DeLeo, P.C. and Ehrlich, H.L. (1994) Reduction of hexavalent chromium by *Pseudomonas fluorescens* LB300 in batch and continuous cultures. *Applied Microbiology and Biotechnology* **40**:756-759.

Demirjian, D.C., Morís-Varas, F. and Cassidy, C.S. (2001) Enzymes from extremophiles. *Current Opinion in Chemical Biology* **5**:144-151.

Dua, M., Singh, A., Sethunathan, N. and Johri, A.K. (2002) Biotechnology and bioremediation: successes and limitations. *Applied Microbiology and Biotechnology* **59**:143-152.

Ebbing, D.D. (1996) General Chemistry – Fifth Edition. Houghton Mifflin Company. USA Boston.

Eggink, G., Engel, H., Vriend, G., Terpstra, P. and Witholt, B. (1990) Rubredoxin reductase of *Pseudomonas oleovorans*. Structural relationship to other flavoprotein oxidoreductases based on one NAD and two FAD fingerprints. *The Journal of Molecular Biology* **212**:135-142.

Fitzpatrick, T.B., Amrhein, N. and Macheroux, P. (2003) Characterization of YqjM, and Old Yellow Enzyme homolog from *Bacillus subtilis* involved in the oxidative stress response. *The Journal of Molecular Biology* **278**:19891-19897.

Fredrickson, J.K., Kostandarithes, H.M., Li, S.W., Plymale, A.E. and Daly, M.J. (2000) Reduction of Fe(III), Cr(VI), U(VI), and Tc(VII) by *Deinococcus radiodurans* R1. *Applied and Environmental Microbiology* **66**:2006–2011.

Fredrickson, J.K. and Onstott, T.C. (1996) Microbes deep in side the Earth. *Scientific American* **275**:68-73.

Ganguli, A. and Tripathi, A.K. (1999) Survival and chromate reducing ability of *Pseudomonas aeruginosa* in industrial effluents. *Letters in Applied Microbiology* **28**:76–80.

Ganguli, A. and Tripathi, A.K. (2001) Bioremediation of toxic chromium from electroplating effluent by chromate-reducing *Pseudomonas aeruginosa* A2Chr in two bioreactors. *Applied Microbiology and Biotechnology* **58**:416-420.

Garbisu, C., Alkorta, I., Llama, M.J. and Serra, J.L. (1998) Aerobic chromate reduction by *Bacillus subtilis. Biodegradation* **9**:133–141.

Gardy, J.L., Laird, M.R., Chen, L.F., Rey, S., Walsh, C.J., Ester, M. and Brinkman, F.S.L. (2005) PSORTb v.2.0: expanded prediction of bacterial protein subcellular localization and insights gained from comparative proteome analysis. *Bioinformatics* **21**:617-623.

Gaspard, S., Vazquez, F. and Holliger, C. (1998) Localization and solubilization of the iron(III) reductase of *Geobacter sulfurreducens. Applied and Environmental Microbiology* **64**:3188–3194.

Gonzalez, C.F., Ackerley, D.F., Park, C.H. and Matin, A. (2003) A soluble flavoprotein contributes to chromate reduction and tolerance in *Pseudomonas putida*. *Acta Biotechnologica* **23**:233-239.

Gonzalez, C.F., Ackerley, D.F., Lynch, S.V. and Matin, A. (2005) ChrR, a soluble quinone reductase of *Pseudomonas putida* that defends against H_2O_2. *The Journal of Biological Chemistry* **280**:22590-22595.

Griese, J.J., Jakob, R.P., Schwarzinger, S. and Dobbek, H. (2006) Xenobiotic reductase A in the degradation of quinoline by *Pseudomonas putida* 86: physiological function, structure and mechanism of 8-hydroxycoumarin reduction. *The Journal of Molecular Biology* **361**:140-152.

Gvozdyak, P.I., Mogilevich, N.F., Rylśkii, A.F. and Grishchenko, N.I. (1986) Reduction of hexavalent chromium by collection strains of bacteria. *Mikrobiologiya* **55**:962–965.

Hanahan, D. (1983) Studies on transformation of *E. coli* with plasmid. *Journal of Molecular Biology*. **166**:557-580.

Hawley, D.K. and McClure, W.R. (1983) Compilation and analysis of *Escherichia coli* promoter DNA sequences. *Nucleic Acids Research* **11**:2237-2245.

Henne, A., Brüggemann, H., Raasch, C., Wiezer, A., Hartsch, T., Liesegang, H., Johann, A., Lienard, T., Gohl, O., Martinez-Arias, R., Jacobi, C., Starkuviene, V., Schlenczeck, S., Dencker, S., Huber, R., Klenk, H-P., Kramer, W., Merkl, R., Gottschalk, G. and Fritz, H-J. (2004) The genome sequence of the extreme thermophile *Thermus thermophilus*. *Nature Biotech* **22**:547-553.

Hidalgo, A., Betancor, L., Moreno, R., Zafra, O., Cava, F., Fernández-Lafuente, R., Guisán, J.M. and Berenguer, J. (2004) *Thermus thermophilus* as a cell factory for teh production of a thermophilic Mn-dependent catalase which fails to be synthesized in an active form in *Escherchia coli*. *Applied and Environmental Microbiology* **70**:3839-3844.

Horton, H.R., Moran, L.A., Ochs, R.S., Rawn, J.D. and Scrimgeour, K.G. (1996) Principles of Biochemistry. Second Edition. Prentice–Hall, Upper Saddle River.

Ishibashi, Y., Cervantes, C. and Silver, S. (1990) Chromium reduction in *Pseudomonas putida*. *Applied and Environmental Microbiology* **56**:2268–2270.

Ji, G. and Silver, S. (1995) Bacterial resistance mechanisms for heavy metals of environmental concern. *Journal of Industrial Microbiology* **14**:61-75.

Jiménez-Mejía, R., Campos-García, J. and Cervantes, C. (2006) Membrane topology of the chromate transporter ChrA of *Pseudomonas aeroginosa*. *FEMS Microbiology Letters* **262**:178-184.

Juhnke, S., Peitzsch, N., Hübener, N., Grobe, C. and Nies, D.H. (2002) New genes involved in chromate resistance in *Ralstonia metallidurans* strain CH34. *Archives of Microbiology* **179**:15-25.

Kashefi, K. and Lovley, D.R. (2000) Reduction of Fe(III), Mn(IV), and toxic metals at 100°C by *Pyrobaculum islandicum*. *Applied and Environmental Microbiology* **66**:1050–1056.

Kaufmann, F. and Lovley, D.R. (2001) Isolation and characterization of a soluble NADPH–dependent Fe(III) reductase from *Geobacter sulfurreducens. Journal of Bacteriology* **183**:4468–4476.

Kelley, L.A., MacCallum, R.M. and Sternberg, M.J.E. (2000) Enhanced Genome Annotation using structural profiles in the program 3D-PSSM. *The Journal of Molecular Biology* **299**:499-520.

Kieft, T.L., Fredrickson, J.K., Onstott, T.C., Gorby, Y.A., Kostandarithes, H.M., Bailey, T.J., Kennedy, D.W., Li, S.W., Plymale, A.E., Spadoni, C.M. and Gray, M.S. (1999) Dissimilatory reduction of Fe(III) and other electron acceptors by a *Thermus* isolate. *Applied and Environmental Microbiology* **65**:1214–1221.

Kitzing, K., Fitzpatrick, T.B., Wilken, C., Sawa, J., Bourenkov, G.P., Macheroux, P. and Clausen, T. (2005) The 1.3 Å crystal structure of the flavoprotein YqjM reveals a novel class of Old Yellow Enzymes. *Journal of Biological Chemistry* **280**:27904-27913.

Kohli, R.M., and Massey, V. (1998) The oxidation half-reaction of Old Yellow Enzyme. *Journal of Biological Chemistry* **273**:32763-32770.

Komori, K., Rivas, A., Toda, K. and Ohtake, H. (1990A) Biological removal of toxic chromium using an *Enterobacter cloacae* strain that reduces chromate under anaerobic conditions. *Biotechnology and Bioengineering* **35**:951-954.

Komori, K., Toda, K. and Ohtake, H. (1990B) Effects of oxygen stress on chromate reduction in *Enterobacter cloacae* strain HO1. *Journal of Fermentation and Bioengineering* **69**:67–69.

Komori, K., Wang, P–C., Toda, K. and Ohtake, H. (1989) Factors affecting chromate reduction in *Enterobacter cloacae* strain HO1. *Applied Microbiology and Biotechnology* **31**:567–570.

Kwak, Y.H., Lee, D.S. and Kim, H.B. (2003) *Vibrio harveyi* nitroreductase is also a chromate reductase. *Applied and Environmental Microbiology* **69**:4390–4395.

Laemmli, U.K. (1970) Cleavage of structural proteins during the assembly of the head of bacteriophage T4. *Nature* **227**:680–685.

Lasa, I., De Grado, M., De Pedro, M.A. and Berenguer, J. (1992) Development of *Thermus-Escherichia* shuttle vectors and their use for expression of the *Clostridium thermocellum celA* gene in *Thermus thermophilus*. *Journal of Bacteriology* **174**:6424-6431.

Laxman, R.S. and More, S. (2002) Reduction of hexavalent chromium by *Streptomyces griseus. Minerals Engineering* **15**:831–837.

Lehmacher, A. and Bisswanger, H. (1988) Adaptation of enzymes to high temperatures. Isolation and characterization of the lipoamide dehydrogenase from *Thermus aquaticus*. *Biochemistry (Life Sci Adv)* **7**:29-33.

Liu, K.J., and Shi, X. (2001) *In vivo* reduction of chromium (VI) and its related free radical generation. *Molecular and Cellular Biochemistry* **222**:41-47.

Llovera, S., Bonet, R., Simon–Pujol, M.D. and Congregado, F. (1993A) Chromate reduction by resting cells of *Agrobacterium radiobacter* EPS–916. *Applied and Environmental Microbiology* **59**:3516–3518.

Llovera, S., Bonet, R., Simon–Pujol, M.D. and Congregado F (1993B) Effect of culture medium ions on chromate reduction by resting cells of *Agrobacterium radiobacter. Applied Microbiology and Biotechnology* **39**:424–426.

Losi, M.E., Amrhein, C. and Frankenberger, W.T.S. (1994) Environmental biochemistry of chromium. *Review of Environmental Contaminants and Toxicology* **136**:91–121.

Lovley, D.R. and Coates, J.D. (1997) Bioremediation of metal contamination. *Current Opinion in Biotechnology* **8**:285–289.

Lovley, D.R. (1995) Bioremediation of organic and metal contaminants with dissimilatory metal reduction. *Journal of Industrial Microbiology* **14**:85-93.

Lovley, D.R. and Phillips, E.J.P. (1994) Reduction of chromate by *Desulfovibrio vulgaris* and its c_3 cytochrome. *Applied and Environmental Microbiology* **60**:726–728.

Luli, G.W., Talnagi, J.W., Strohl, W.R. and Pfister, R.M. (1983) Hexavalent chromium-resistant bacteria isolated from river sediments. *Applied and Environmental Microbiology* **46**:846-854.

Mabbett, A.N., Lloyd, J.R. and Macaskie, L.E. (2002) Effect of complexing agents on reduction of Cr(VI) by *Desulfovibrio vulgaris* ATCC 29579. *Biotechnology and Bioengineering* **79**:389–397.

Macaskie, L.E., Clark, P.J., Gilbert, J.D. and Tolley, M.R. (1992) The effect of ageing on the accumulation of uranium deposition in stored biofilm. *Biotechnology Letters* **14**:525–530.

Maseda, H. & Hoshino, T. (1995) Screening and analysis of DNA fragments that show promoter activities in *Thermus thermophilus*. *FEMS Microbiology Letters* **128**:127-134.

Mathews, K.M., van Holde, K.E. and Ahern, K.G. (2000) Biochemistry – 3rd Edition. San Francisco: Addison Wesley Longman, Inc.

Mazoch, J., Tesařík, R., Sedláček, V., Kučera, I. and Turánek, J. (2004) Isolation and biochemical characterization of two soluble iron(III) reductases from *Paracoccus denitrificans*. *European Journal of Biochemistry* **271**:553-562.

McLean, J. and Beveridge, T.J. (2001) Chromate reduction by a Pseudomonad isolate from a site contaminated with chromated copper arsenate. *Applied and Environmental Microbiology* **67**:1076–1084.

Michel, C., Brugna, M., Aubert, C., Bernadac, A. and Bruschi, M. (2001) Enzymatic reduction of chromate: comparative studies using sulfate–reducing bacteria. Key role of polyheme cytochromes *c* and hydrogenases. *Applied Microbiology and Biotechnology* **55**:95–100.

Middleton, S.S., Latmani, R.B., Mackey, M.R., Ellisman, M.H., Tebo, B.M. and Criddle, C.S. (2003) Cometabolism of Cr(VI) by *Shewanella oneidensis* MR-1 produces cell-associated reduced chromium and inhibits growth. *Biotechnology and Bioengineering* **83**:627-637.

Möller, C., and van Heerden, E. (2006) Isolation of a soluble and membrane-associated Fe(III) reductase from the thermophile, *Thermus scotoductus* (SA-01). *FEMS Microbiology Letters* **265**:237-243.

Moreno, R., Haro, A., Castellanos, A. and Berenguer, J. (2005) High-level overproduction of His-tagged *Tth* DNA polymerase in *Thermus thermophilus*. *Applied and Environmental Microbiology* **71**:591-593.

Moreno, R., Zafra, O., Cava, F. and Berenguer, J. (2003) Developement of a gene expression vector for Thermus thermophilus based on the promoter of the respiratory nitrate reductase. *Plasmid* **49**:2-8.

Mulligan, C.N., Yong, R.N. and Gibbs, B.F. (2001) Remediation technologies for metal-contaminated soils and groundwater: an evaluation. *Engineering Geology* **60**:193-207.

Muter, O., Patmalnieks, A. and Rapoport, A. (2001) Interrelations of the yeast *Candida utilis* and Cr(VI): metal reduction and its distribution in the cell and medium. *Process Biochemistry* **36**:963–970.

Myers, C.R., Carstens, B.P., Antholine, W.E. and Myers, J.M. (2000) Chromium(VI) reductase activity is associated with the cytoplasmic membrane of anaerobically grown *Shewanella putrefaciens* MR–1. *Journal of Applied Microbiology* **88**:98–106.

Nagano, N., Orengo, C.A. and Thornton, J.M. (2002) One fold with many functions: the evolutionary relationship between TIM barrel families based on their sequences, structures and functions. *The Journal of Molecular Biology* **321**:741-765.

Nakamura, Y., Gojobori, T. and Ikemura, T. (2000) Codon usage tabulated from international DNA sequence database: status for the year 2000. *Nucleic Acids Research* **28**:292.

Neal, A.L., Lowe, K., Daulton, T.L., Jones–Meehan, J. and Little, B.J. (2002) Oxidation state of chromium associated with cell surfaces of *Shewanella oneidensis* during chromate reduction. *Applied Surface Science* **202**:150–159.

Nepple, B.B., Kessi, J. and Bachofen, R. (2000) Chromate reduction by *Rhodobacter sphaeroides*. *Journal of Industrial Microbiology and Biotechnology* **25**:198–203.

Neveling U, Bringer-Meyer S and Sahm H (1998) Gene and subunit organization of bacterial pyruvate dehydrogenase complexes. *Biochimica et Biophysica Acta* **1385**, 367-372.

Nies, D.H. (1999) Microbial heavy-metal resistance. *Applied Microbiology and Biotechnology* **51**:730-750.

Nies, D.H. (2000) Heavy metal–resistant bacteria as extremophiles: molecular physiology and biotechnological use of *Ralstonia* sp. CH34. *Extremophiles* **4**:77–82.

Nies, D.H., Koch, S., Wachi, S., Peitzsch, N. and Saier JR., M.H. (1998) CHR, a novel family of prokaryotic proton motive force-driven transporters probably containing chromate/sulfate antiporters. *Journal of Bacteriology* **180**:5799-5802.

Nies, A., Nies, D.H. and Silver, S. (1989) Cloning and expression of plasmid genes encoding resistance to chromate and cobalt in *Alcaligenes eutrophus.* *Journal of Bacteriology* **171**:5065-5070.

Nies, A., Nies, D.H. and Silver, S. (1990) Nucleotide sequence and expression of a plasmid-encoded chromate resistance determinant form *Alcaligenes eutrophus*. *The Journal of Biological Chemistry* **265**:5648-5653.

Ohtake, H., Cervantes, C. and Silver, S. (1987) Decreased chromate uptake in *Pseudomonas fluorescens* carrying a chromate resistance plasmid. *Journal of Bacteriology* **169**:3853-3856.

Ohtake, H., Komori, K., Cervantes, C. and Toda, K. (1990) Chromate-resistance in a chromate-reducing strain of *Enterobacter cloacae. FEMS Microbiology Letters* **67**:85-88.

Onstott, T.C., Moser, D.P., Pfiffner, S.M., Fredrickson, J.K., Brockman, F.J., Phelps, T.J., White, D.C., Peacock, A., Balkwill, D., Hoover, R., Krumholz, L.R., Borscik, M., Kieft, T.L. and Wilson, R. (2003) Indigenous and contaminant microbes in ultradeep mines. *Environmental Microbiology* **5**:1168-1191.

Oze, C., Bird, D.K. and Fendorf, S. (2007) Genesis of hexavalent chromium from natural sources in soil and groundwater. *Proceedings of the National Academy of Science USA* **104**:6544-6549.

Park, C.H., Keyhan, M., Wielinga, B., Fendorf, S. and Matin, A. (2000) Purification to homogeneity and characterization of a novel *Pseudomonas putida* chromate reductase. *Applied and Environmental Microbiology* **66**:1788–1795.

Pattanapipitpaisal, P., Brown, N.L. and Macaskie, L.E. (2001) Chromate reduction and 16S rRNA identification of bacteria isolated from a Cr(VI)–contaminated site. *Applied Microbiology and Biotechnology* **57**:257–261.

Petrat, F., Paluch, S., Dogruöz, E., Dörfler, P., Kirsch, M., Korth, H-G., Sustmann, R. and de Groot, H. (2003) Reduction of Fe(III) ions complexed to physiological ligands by lipoyl dehydrogenase and other flavoenzymes in vitro. Implications for an enzymatic reduction of Fe(III) ions of the labile iron pool. *Journal of Biological Chemistry* **278**:46403-46413.

Pimentel. B.E., Moreno–Sánchez, R. and Cervantes, C. (2002) Efflux of chromate by *Pseudomonas aeruginosa* cells expressing the ChrA protein. *FEMS Microbiology Letters* **212**:249–254.

Pourbaix, M. (1966) Atlas of electrochemical equilibria in aqueous solutions. Pergamon, Oxford.

Puzon, G.F., Roberts, A.G., Kramer, D.M. and Xun, L. (2005) Formation of soluble organo-chromium(III) complexes after chromate reduction in the presence of cellular organics. *Environmental Science and Technology* **39**:2811-2817.

QuiIntana, M., Curutchet, G. and Donati, E. (2001) Factors affecting chromium(VI) reduction by *Thiobacillus ferroxidans. Biochemical Engineering Journal* **9**:11–15.

Rabilloud, T., Carpentier, G. and Tarroux P. (1988) Improvement and simplification of low–background silver staining proteins by using sodium dithionite. *Electrophoresis* **9**:288–291.

Rai, D., Sass, B.M. and Moore, D.A. (1987) Chromium (III) hydrolysis constants and solubility of chromium (III) hydroxide. *Inorganic Chemistry* **26**:345–349.

Ramírez-Díaz, M.I., Díaz-Pérez, C., Vargas, E., Riveros-Rosas, H., Campos-García, J. and Cervantes, C. (2007) Mechanisms of bacterial resistance to chromium compounds. *Biometals* DOI:10.1007/s10534-007-9121-8.

Ramírez-Ramírez, R., Calvo-Méndez, C., Ávila-Rodríguez, M., Lappe, P., Ulloa, M., Vázquez-Juárez, R. and Gutiérrez-Corona, J.F. (2004) Cr(VI) reduction in achromate-resistant strain of *Candida maltosa* isolated from the leather industry. *Antonie van Leeuwenhoek* **85**:63-68.

Sani, R.K., Peyton, B.M., Smith, W.A., Apel, W.A. and Petersen, J.N. (2002) Dissimilatory reduction of Cr(VI), Fe(III), and U(VI) by *Cellulomonas* isolates. *Applied Microbiology and Biotechnology* **60**:192-199.

Schieman, E.A., Yonge, D.R., Rege, M.A., Petersen, J.N., Turick, C.E., Johnstone, D.L. and Apel, W.A. (1998) Comparative kinetics of bacterial reduction of chromium. *Journal of Environmental Engineering* **124**:449–455.

Shen, H., Pritchard, P.H. and Sewell, G.W. (1996) Kinetics of chromate reduction during naphthalene degradation in mixed culture. *Biotechnology and Bioengineering* **52**:357–363.

Shen, H. and Wang, Y-T. (1993) Characterization of enzymatic reduction of hexavalent chromium *Escherichia coli* ATCC 33456. *Applied and Environmental Microbiology* **59**:3771-3777.

Shen, H. and Wang, Y-T. (1994) Modeling hexavalent chromium reduction in *Escherichia coli* 33456. *Biotechnology and Bioengineering* **43**:293-300.

Shi, X. and Dalal, N.S. (1989) Chromium(V) and hydroxyl radical formation during the glutathione reductase-catalyzed reduction of chromium(VI). *Biochemical and Biophysical Research Communications* **163**:627-634.

Shi, X. and Dalal, N.S. (1990A) NADPH–dependent flavoenzymes catalyze one electron reduction of metal ions and molecular oxygen and generate hydroxyl radicals. *FEBS Letters* **276**:189–191.

Shi, X. and Dalal, N.S. (1990B) One-electron reduction of chromate by NADPH-dependent glutathione reductase. *Journal of Inorganic Biochemistry* **40**:1-12.

Shi, X. and Dalal, N.S. (1990C) On the hydroxyl radical formation in the reaction between hydrogen peroxide and biologically generated chromium(V) species. *Archives of Biochemistry and Biophysics* **277**:342-350.

Silver, S. and Phung, L.T. (1996) Bacterial heavy metal resistance: new surprises. *Annual Review of Microbiology* **50**:753-789.

Sisti, F., Allegretti, P. and Donati, E. (1996) Reduction of dichromate by *Thiobacillus ferrooxidans. Biotechnology Letters* **18**:1477-1480.

Slilaty, S.N., and Lebel, S. (1998) Accurate insertional inactivation of *lacZα*: construction of pTrueBlue and M13TrueBlue cloning vectors. *Gene* **213**:83-91.

Smith, B.J. (1994) SDS polyacrylamide gel electrophoresis of proteins. *Methods in Molecular Biology* **32**:23–34.

Smith, P.K., Krohn, R.I., Hermanson, G.T., Mallia, A.K., Gartner, F.H., Provenzano, M.D., Fujimoto, E.K., Goeke, N.M., Olson, B.J. and Klenk, D.C. (1985) Measurement of protein using bicinchoninic acid. *Analytical Biochemistry* **150**:76-85.

Stetter, K.O. (1999) Extremophiles and their adaptation to hot environments. *FEBS Letters* **452**:22-25.

Suzuki, T., Miyata, N., Horitsu, H., Kawai, K., Takamizawa, K., Tai, Y. and Okazaki, M. (1992) NAD(P)H–dependent chromium (VI) reductase of *Pseudomonas ambigua* G–1: a Cr(V) intermediate is formed during the reduction of Cr(VI) to Cr(III). *Journal of Bacteriology* **174**:5340–5345.

Takai, K., Moser, D.P., DeFlaun, M., Onstott, T.C. and Fredrickson, J.K. (2001A) Archaeal diversity in waters from deep South African gold mines. *Applied and Environmental Microbiology* **67**:5750-5760.

Takai, K., Moser, D.P., Onstott, T.C., Spoelstra, N., Pfiffner, S.M., Dohnalkova, A. and Fredrickson, J.K. (2001B) *Alkaliphilus transvaalensis* gen. nov., sp. nov., an extremely alkaliphilic bacterium isolated from a deep South African gold mine. *International Journal of Systematic and Evolutionary Microbiology* **51**:1245-1256.

Tebo, B.M. and Obraztsova, A.Y. (1998) Sulfate–reducing bacterium grows with Cr(VI), U(VI), Mn(VI), and Fe(III) as electron acceptors. *FEMS Microbiology Letters* **162**:193–198.

Thomas, J.G., Ayling, A and Baneyx, F. (1997) Molecular chaperones, folding catalysts, and the recovery of active recombinant proteins from *E. coli*. To fold or to refold. *Applied Biochemistry and Biotechnology* **66**:197-238.

Thompson, J.D., Higgens, D.G. and Gibson, T.J. (1994) CLUSTAL W: improving the sensitivity of progressive multiple sequence alignment through sequence weighting, position-specific gap penalties and weight matrix choice. *Nucleic Acids Research* **22**:4673-4680.

Towner, P. (1991) Isolation of DNA by SDS-proteinase K treatment, p.52-53. *In* T.A. Brown (ed.) Essential molecular biology, vol 1. A practical approach. Oxford University Press, UK.

Tucker, M.D., Barton, L.L. and Thomson, B.M. (1998) Reduction of Cr, Mo, Se and U by *Desulfovibrio desulfuricans* immobilized in polyacrylamide gels. *Journal of Industrial Microbiology and Biotechnology* **20**:13–19.

Turick, C.E., Apel, W.A. and Carmiol, N.S. (1996) Isolation of hexavalent chromium–reducing anaerobes from hexavalent–chromium–contaminated and noncontaminated environments. *Applied Microbiology and Biotechnology* **44**:683–688.

Urone, P.F. (1955) Stability of colorimetric reagent for chromium, *s*–diphenylcarbazide, in various solvents. *Analytical Chemistry* **27**:1354–1355.

Vainshtein, M., Kuschk, P., Mattusch, J., Vatsourina, A. and Wiessner, A. (2003) Model experiments on the microbial removal of chromium from contaminated groundwater. *Water Research* **37**:1401–1405.

Valls, M and de Lorenzo, V. (2002) Exploiting the genetic and biochemical capacities of bacteria for the remediation of heavy metal pollution. *FEMS Microbiology Reviews* **26**:327–338.

Van Loosdrecht, M.C.M. and Henze, M. (1999) Maintenance, endogenous respiration, lysis, decay and predation. *Water Science and Technology* **39**:107–117.

Vega, M.C., Lorentzen, E., Linden, A. and Wilmanns, M. (2003) Evolutionary markers in the $(\beta/\alpha)_8$-barrel fold. *Current Opinion in Chemical Biology* **7**:694-701.

Vennit, S. and Levy, L.S. (1974) Mutagenicity of chromates in bacteria and its relevance to chromate carcinogenesis. *Nature* **250**:493–495.

Viamajala, S., Peyton, B.M., Apel, W.A. and Petersen, J.N. (2002A) Chromate/nitrate interactions in *Shewanella oneidensis* MR–1: evidence for multiple hexavalent chromium [Cr(VI)] reduction mechanisms dependent on physiological growth conditions. *Biotechnology and Bioengineering* **78**:770–778.

Viamajala, S., Peyton, B,M., Apel, W.A. and Petersen, J.N. (2002B) Chromate reduction in *Shewanella oneidensis* MR-1 is and inducible process associated with anaerobic growth. *Biotechnology Progress* **18**:290-295.

Viamajala, S., Peyton, B.M., Sani, R.K., Apel, W.A. and Petersen, J.N. (2004) Toxic effects of chromium(VI) on anaerobic and aerobic growth of *Shewanella oneidensis* MR-1. *Biotechnology Progress* **20**:87-95.

Voet, D. and Voet, J.G. (1990) Biochemistry. John Wiley and Sons, Inc., New York, USA.

Wang, P.C., Mori, T., Komori, K., Sasatsu, M., Toda, K. and Ohtake, H. (1989) Isolation and characterization of an *Enterobacter cloacae* strain that reduces hexavalent chromium under anaerobic conditions. *Applied and Environmental Microbiology* **55**:1665-1669.

Wang, P.C., Mori, T., Toda, K. And Ohtake, H. (1990) Membrane-associated chromate reductase activity from *Enterobacter cloacae*. *Journal of Bacteriology* 172:1670-1672.

Wang, Y–T. and Shen, H. (1995) Bacterial reduction of hexavalent chromium. *Journal of Industrial Microbiology* **14**:159-163.

Wang, Y–T. and Shen, H. (1997) Modelling Cr(VI) reduction by pure bacterial cultures. *Water Research* **31**:727–732.

Wang, Y−T. and Xiao, C. (1995) Factors affecting hexavalent chromium reduction in pure cultures of bacteria. *Water Research* **29**:2467−2474.

Warburg, O., and Christian, W. (1933) Über das gelbe Ferment und seine Wirkungen. *Biochemistry Z.* **266**:377-411.

Wierenga, R.K., Terpstra, P. and Hol, W.G.J. (1986) Prediction of the occurrence of the ADP-binding βαβ-fold in proteins, using an amino acid sequence fingerprint. *The Journal of Molecular Biology* **187**:101-107.

Williams, R.E., and Bruce, N.C. (2002) 'New uses for an old enzyme' – the Old Yellow enzyme family of flavoenzymes. *Microbiology* **148**:1607-1614.

Williams, J.W. and Silver, S. (1984) Bacterial resistance and detoxification of heavy metals. *Enzyme and Microbial Technology* **6**:530−537.

Yamamoto, K., Kato, J., Yano, T. and Ohtake, H. (1993) Kinetics and modeling of hexavalent chromium reduction in *Enterobacter cloacae. Biotechnology and Bioengineering* **41**:129-133.

Ye, J., Wang, S., Leonard, S.S., Sun, Y., Butterworth, L., Antonini, J., Ding, M., Rojanasakul, Y., Vallyathan, V., Castranova, V. and Shi, X. (1999) Role of reactive oxygen species and p53 in chromium(VI)−induced apoptosis. *The Journal of Biological Chemistry* **274**:34974−34980.

Zayed, A.M. and Terry, N. (2003) Chromium in the environment: factors affecting biological remediation. *Plant Soil* **249**, 139-156.

Zenno, S., Kobori, T., Tanokura, M. and Saigo, K. (1998) Conversion of NfsA, the major *Escherichia coli* nitroreductase, to a flavin reductase with an activity similar to that of Frp, a flavin reductase in *Vibrio harveyi*, by a single amino acid substitution. *Journal of Bacteriology* **180**:422-425.

Zhang, C., Liu, S., Logan, J., Mazumder, R. and Phelps, T.J. (1996) Enhancement of Fe(III), Co(III), and Cr(VI) reduction at elevated temperatures and by a thermophilic bacterium. *Applied Biochemistry and Biotechnology* **57/58**:923–932.